BEHAVIOUR OF SHORT PILE UNDER MACHINE INDUCED HORIZONTAL VIBRATIONS

A DISSERTATION

Submitted in partial fulfilment of the requirements for the award of the degree
of

MASTER OF TECHNOLOGY
in
EARTHQUAKE ENGINEERING

(*With Specialization in Soil Dynamics*)

By

MAHIMA KHANDELWAL

DEPARTMENT OF EARTHQUAKE ENGINEERING
INDIAN INSTITUTE OF TECHNOLOGY ROORKEE
ROORKEE – 247667, INDIA
MAY, 2016

CANDIDATE'S DECLARATION

It is certified that this work has been carried out in Department of Earthquake Engineering at Indian Institute of Technology under the guidance of Dr. S. Mukerjee, visiting faculty of, Department of Earthquake Engineering, Indian Institute of Technology Roorkee, Roorkee, India.

Date: 2-May-2016 (Mahima Khandelwal)

Place: Roorkee 14525009

CERTIFICATE

This is to certify that the above statement made by the candidate is correct to the best of my knowledge and belief.

Dr. S. Mukerjee

Visiting Faculty

Department of Earthquake Engineering

Indian Institute of Technology, Roorkee,

Roorkee-247667, Uttarakhand, India.

ACKNOWLEDGEMENT

With great pleasure I would like to express my sincere gratitude and thanks to my respected supervisor, Dr. S. Mukerjee, a visiting faculty, of Department of Earthquake Engineering, Indian Institute Of Technology, Roorkee for his valuable guidance and consistent encouragement throughout the work. This work is simply the reflection of their thoughts, ideas, and concepts and all his efforts. I am highly indebted to him for his kind and valuable suggestions and of course his valuable time during the period of the work.

I would acknowledge my gratefulness to my friends who provided valuable suggestion and encouragement whenever I needed. I am also extremely grateful for my family for their support, love, patience and for being a constant source of inspiration.

Date: 2 May 2016 MAHIMA KHANDELWAL

Place: Roorkee (14525009)

ABSTRACT

Short rigid piles are widely used to support structures such as wind turbines, traffic signals, jetties, transmission towers, highway overhead signs and water front structures.

In order to assess the effect of L/D ratio and strain on short piles subjected to horizontal sinusoidal vibrations. Four RCC short piles of diameter 20cm, 30cm, 40cm and 50cm each having a length of 2m were cast The important part of this dynamic analysis is to calculate the stiffness and the damping ratio. For a better understanding of the site geotechnical properties of the site were also evaluated.

To generate horizontal sinusoidal vibrations a motor-oscillator assembly was used. Four foundation bolts were cast into the pile cap to enable the mounting of a motor-oscillator assembly. Three acceleration transducers were suitably mounted on the vertical face of the pile cap to monitor the induced accelerations. These piles have been tested for four different force level i.e. eccentricity setting of motor-oscillator assembly

For each pile and eccentricity setting, acceleration-frequency records were analysed to obtain resonant frequency of the soil-pile system and shear strain at ground level. Using this data, a procedure has been developed to obtain damping ratio and stiffness of the soil-pile system. Conclusions have been drawn relating (i) Exciting force level and resonant frequency, (ii) Soil-pile stiffness and strain level and (iii) System damping and strain level, considering each pile individually. The influence of L/D ratio on the dynamic response of the soil-pile system has also been demonstrated.

Keywords: Dynamic, short pile, machine vibrations, horizontal sinusoidal vibrations

Table of content

List of Figure

List of Table

1 Introduction

Pile foundation is required when the soil bearing capacity is not sufficient for the structure to withstand. A pile foundation consists of two components: Pile cap and single or group of piles. Pile transfers the loads from structures to the hard strata, rocks or soil with high bearing capacity.

Piles may be classified as long and short in accordance with the L/D ratio of the pile and short piles are which have large diameter generally from 2 to 4 m long and from 250mm to 350mm in diameter . They are widely used to support structures such as such as wind turbines, traffic signals, jetties, transmission towers, highway overhead signs and water front structures.

The structure supported on short piles have to withstand significant lateral loads and overturning moments but small vertical loads which in consequence are often neglected.

The failure mechanism of laterally loaded short rigid pile is different from that of the long flexible pile [8]. In short pile failure takes place when the lateral earth pressures reach the ultimate passive lateral resistance of the soil along the pile length, hence its design is primarily governed by the lateral soil failure instead of the yielding of the pile material.

In the short pile the point of inflexion is 1/5 from the base while for long pile it is 3/5 from the base and the pile body tends to rotate about the inflexion point and causes the development of passive resistance in the soil in front of the pile above the inflexion point and back of the pile below the rotation point and produce a small negative deflection close to the pile base [11] the maximum negative deflection occurs exactly in the base of pile.

Necessary condition for considering a pile as a short rigid pile [7] is that the embedment depth of the pile has to be less than 2T, where T is relative stiffness factor

In cohesionless,

$$L_s < 2T \tag{1.1}$$

Where, T : Stiffness Factor

$$T = \left[\frac{\mathrm{E_p\, I_p}}{\eta_h}\right]^{\frac{1}{5}} \tag{1.2}$$

Where,

E_pI_p : bending stiffness of pile

η_h : Coefficient of subgrade reaction

Another condition for considering pile as a short rigid pile is [6],

$$.05\left[\frac{E_e}{G^*}\right]^{\frac{1}{2}} < \text{D/B} < \left[\frac{E_e}{G^*}\right]^{\frac{2}{7}} \tag{1.3}$$

Where,

G* : Equivalent shear modulus

E_e : Effective Young's modulus

D/B : Depth to Diameter ratio

$$G^* = \left[\frac{E_s}{2(1+\mu)}\right]\left[1+\frac{3\mu}{4}\right] \tag{1.4}$$

$$E_e = \frac{EI_p}{\left(\pi\frac{B^4}{64}\right)} \tag{1.5}$$

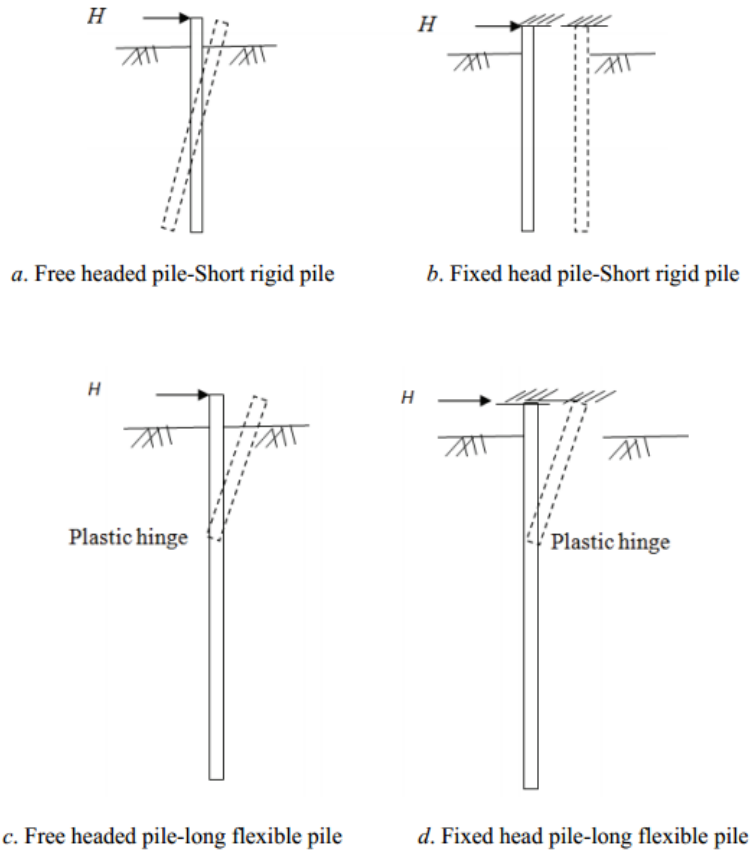

Figure 1-1 Typical failure modes in short rigid piles and long flexible piles [1]

Figure 1-2 Soil reaction and Bending moment distribution of free headed and fixed headed in cohesionless soil [6]

1.1 Design Consideration:

The minimum area of longitudinal reinforcement of any type or grade within the pile shaft shall be 0.4 percent of the cross-sectional area of the pile shaft.

The minimum reinforcement shall be provided throughout the length of the shaft.

Clear cover to all main reinforcement in pile shaft shall be not less than 50 mm.

Minimum 6 numbers of vertical bars shall be used for a circular pile and minimum diameter of vertical bar shall be 12 mm.

The clear overhang of the pile cap beyond the outermost pile in the group shall be a minimum of 150 mm.

The embedment of pile into cap should be 75 mm.

Concrete:

The minimum grade of concrete to be used for bored piling shall be M 25. For sub aqueous concrete, the requirements specified in IS 456 shall be followed. The minimum cement content shall be 400 kg/m3. However, with proper mix design and use of proper admixture the cement content may be reduced but in no case the cement content shall be less than 350 kg/m3.

1.2 Scope of Work:

Short rigid piles are widely used in situations where moment-carrying capacity is the dominant design requirement. Structures such as wind turbines, traffic signals, jetties, transmission towers, highway overhead signs and water front structures are often supported by large diameter piers with high stiffness, which behave as short rigid piles. A short rigid pile fails by rotation, mobilizing passive resistance on the opposite pile faces above and below the point of rotation. The moment carrying capacity of short rigid piles is found to be logically dependent on the geometry of the foundation, slope and soil properties.

The majority of the experimental studies were focused on the response of specific pile groups and compared with the response of a single pile. However no laboratory or field test data is available on the response of short rigid piles subjected to dynamic loading. Hence, it is needed to perform dynamic tests on short rigid piles.

2 Review of Literature

Short rigid piles are widely used to support structures such as such as wind turbines, traffic signals, jetties, transmission towers, highway overhead signs and water front structures. Hence short piles have to withstand significant lateral loads and overturning moments. Various analytical process are available for evaluating the behavior of piles under the lateral and vertical loads such as elastic continuum approach, winkler's method and finite element method [14]-

Elastic continuum approach : this elastic continuum approach considers the continuous nature of soil. While elastic modulus is an idealized representation of the soil, it is possible to consider the soil yield and this method can also give approximate solution for varying modulus with depth and layered soil. The major drawback of this model is that the accuracy of the model depends on the accurate evaluation of the soil modulus.

FEM : Finite Element Method (FEM) is one of the most conscientious numerical modeling methods which encounter realistic 3D effects of soil stresses and deformations around the piles. In this approach discretization of finite soil domain is done with FE elements and approximate boundary conditions are imposed. This approach is usually preferred for large projects due to its cost and specialized software.

Winkler's method : the analytical subgrade reaction model, typically known as the winklers model, can be used for the analysis of pile under lateral loading.in this model the soil medium is represented by a number of identical but mutually independent, closely spaced, discrete, linearly elastic spring.

Limitation of the method - In this continuous nature of the soil medium is ignored and assume that these springs are uncoupled, that is the stiffness of one spring does not affect another.

Advantage- method is relatively simple and been used in practice for a long time. This method can incorporate factors such as non linearity, variation of subgrade reaction with depth and also can account for various soil layer.

It considers that there is a linear relationship between the deflection (y) and the contact pressure (p) at any point of the soil in contact with the pile. Nonlinear behavior of soil can also be simulate by using p-y curves.

For the case of dynamic loads, stiffness and damping contributions of soil are considered by a series of unconnected lumped springs and dashpots. Novak proposed to use dynamic stiffness but it is difficult to implement because of the complex and frequency dependent expressions for the dynamic stiffness. Frequency domain analysis can only be used to implement this approach. It cannot be applied for nonlinear cases as it is based on the superposition principle.

Novak's Dynamic stiffness of soils:

The assumption made by Novak (1974) is that the soil is composed of a set of independent, infinitesimally thin horizontal layers, plain strain state which experience small displacements and can extend laterally to infinity. The soil layers are considered homogeneous, isotropic and linear-elastic. The pile is assumed to be vertical, cylindrical and moving as a rigid body. For dynamic stiffness of piles the approximate analytical expression presented by Novak is based on linear elasticity. It is considered that a harmonic vibration is experienced by the massless rigid circular disc that represents the pile cross-section.

The solution for various modes of vibration given by Novak to obtain damping and stiffness constants are -

Horizontal translation stiffness and damping ratio:

$$k_{xp} = \frac{E_p I_p}{r_o^3} \times f_{x1} \tag{2.1}$$

$$C_{xp} = \frac{E_p I_p}{r_o^2 v_s} \times f_{x2} \tag{2.2}$$

Rotational stiffness and damping ratio:

$$K_{\emptyset p} = \frac{E_p I_p}{r_o^3} \times f_{\emptyset 1} \tag{2.3}$$

$$C_{\emptyset p} = \frac{E_p I_p}{v_s} \times f_{\emptyset 2} \tag{2.4}$$

Coupled vibration stiffness and damping ratio:

$$K_{x\emptyset p} = \frac{E_p I_p}{r_o^2} \times f_{x\emptyset 1} \tag{2.5}$$

$$C_{x\emptyset p} = \frac{E_p I_p}{r_o v_s} \times f_{x\emptyset 2} \tag{2.6}$$

Where,

K_{xp} = stiffness of the pile

I_p = moment of inertia of pile

r_o = equivalent radius of pile

E_p = modulus of elasticity of Pile material

v_s = shear wave velocity

C_{xp} = damping constant for the pile

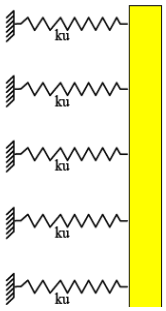

Figure 2-1 Novak's pile-soil model

3 Site Characteristics

Before we determine the dynamic behavior of short piles, various soil properties and pile dimensions and specification are required . Here are some field tests carried out on the site to determine the index properties of the field.

3.1 Site Description :

The experimental setup to record the dynamic response of the short piles is located in front of the Soil Dynamics lab, Department of Earthquake Engineering, IIT Roorkee. Various geotechnical properties like moisture content, specific gravity, grain size distribution and SPT values were determined for the site.

3.2 Standard Penetration Test :

The SPT test results upto a depth of 5.6m were studied to find the angle of internal friction and the soil profile for the site.

According to IS: 2131-1981

This method describes the standard penetration test using split spoon sampler to obtain the resistance of soil to penetration (N- value), using a 63.5 kg hammer falling freely 75 cm and to obtain representative samples for identification and laboratory tests.

For conducting Standard Penetration Test, the split spoon sampler resting on the bottom of borehole should be allowed to sink under its own weight, then the sampler shall be seated 15cm. with the blows of hammer falling through 75cm. Thereafter, the sampler shall be further driven by 30cm or 50 blows. The number of blows required to effect each 15 cm (N1) of drive may be considered to be seating drive. The total blows required for the second and third 15 cm of penetration shall be termed the penetration resistance N (N2+N3).

Figure 3-1 Performing Standard Penetration Test at the site

3.2.1 Corrections :

1) **Due to Overburden**- The N value for cohesionless soil shall be corrected for overburden as

$$N' = C_N N \tag{3.1}$$

N' = corrected value of observed N

C_N = correction factor for overburden pressure

The correction proposed by Peck, Hansen and Thornburn (1974) is given as

$$C_N = 0.77 \log_{10}\left(\frac{20}{p'}\right) \tag{3.2}$$

Where, p' = effective overburden pressure at the depth at which N value is measured, in kg/cm^2

2) **Due to Dilatancy**- The value obtained in 1 shall be corrected for dilatancy if the stratum consists of fine sand and silt below water table for values of N' greater than 15, as

$$N'' = 15 + 0.5(N' - 15) \quad (3.3)$$

If,

$$N' \leq 15, N'' = N' \quad (3.4)$$

The field N values after correction for overburden pressure and dilatancy are mentioned in the Table below:

Table 3-1 Field N-values corrected for overburden pressure and dilatancy

N	length of sample (cm)	wt. of sample (gm)	volume (cm)	density (gm/cm^3)	overburden pressure p' (kg/cm^2)	Cn	N'	N''
4	15	328	170.031	1.92906	0.1446795	1.64828	6.593119	7
4	15	328	170.031	1.92906	0.289358999	1.416487	5.665946	6
6	15	314	170.031	1.846722	0.427863154	1.285688	7.71413	8
7	15	326	170.031	1.917297	0.571660462	1.188797	8.321577	8
9	6.5	147	73.6801	1.995111	0.771171592	1.088687	9.798181	10
7	15	326	170.031	1.917297	1.087525668	0.973735	6.816143	7

Average N = 8

The angle of internal friction can be obtained from the correlation between SPT N-value and angle of shearing resistance as given by Peck et al (1974). The angle of internal friction from the chart was found to be 30^0.

3.3 Moisture Content :

IS : 2720 (Part 2) – 1973

The moisture content for the soil at different depths is determined, the ratio expressed as percentage of weight of water in a given soil mass the weight of dry solid particles in natured condition.

The percent of water content

$$W = \frac{(W2 - W3)}{(W3 - W1)} \times 100 \qquad (3.5)$$

W2 - Wt. of container with wet soil

W3 - Wt. of container with dry soil

W1 - Wt. of container only

Table 3-2 Moisture content of soil adjacent to the piles

Depth (m)	Wt. of container only W1 (gm)	Wt. of container with wet soil W2 (gm)	Wt. of container with dry soil W3	wt.of water (gm)	dry soil (gm)	water content % W
0.5	19	51	49	2	30	6.67
0.75	19	51	48	3	29	10.34
1.5	19	52	49	3	30	10.00
2.25	20	50	47	3	27	11.11
3	19	61	57	4	38	10.53
3.5	19	59	54	5	35	14.29
4	19	52	46	6	27	22.22
4.5	20	56	49	7	29	24.14
5	19	56	48	8	29	27.59
5.65	19	54	46	8	27	29.63

3.4 Grain size Distribution:

IS: 2720 (part4)

Grain size distribution curve is an important tool for identifying the soil type. Coarse–grained soils are analyzed by carrying out sieve analysis, whereas fine grained soils require sedimentation analysis. A set of sieves with square openings are placed in decreasing order of their sieve screen size, and a soil sample of predetermined weight is sieved through it. The soil retained on each sieve is weighed.

Figure3-2 Performing Grain size analysis

Table 3-3 Sieve analysis results for soil at depth = .5m

s.no.	sieve size (mm)	wt. retained(gm)	%wt. retained	cumulative %retained	% N
1	4.75	0	0	0	100
2	4	0	0	0	100
3	2.36	0	0	0	100
4	2	0	0	0	100
5	1.18	0	0	0	100
6	0.6	0	0	0	100
7	0.425	9	1.8	1.8	98.2
8	0.3	33	6.6	8.4	91.6
9	0.15	259	51.8	60.2	39.8
10	0.075	137	27.4	87.6	12.4
11	0	62	12.4	100	0

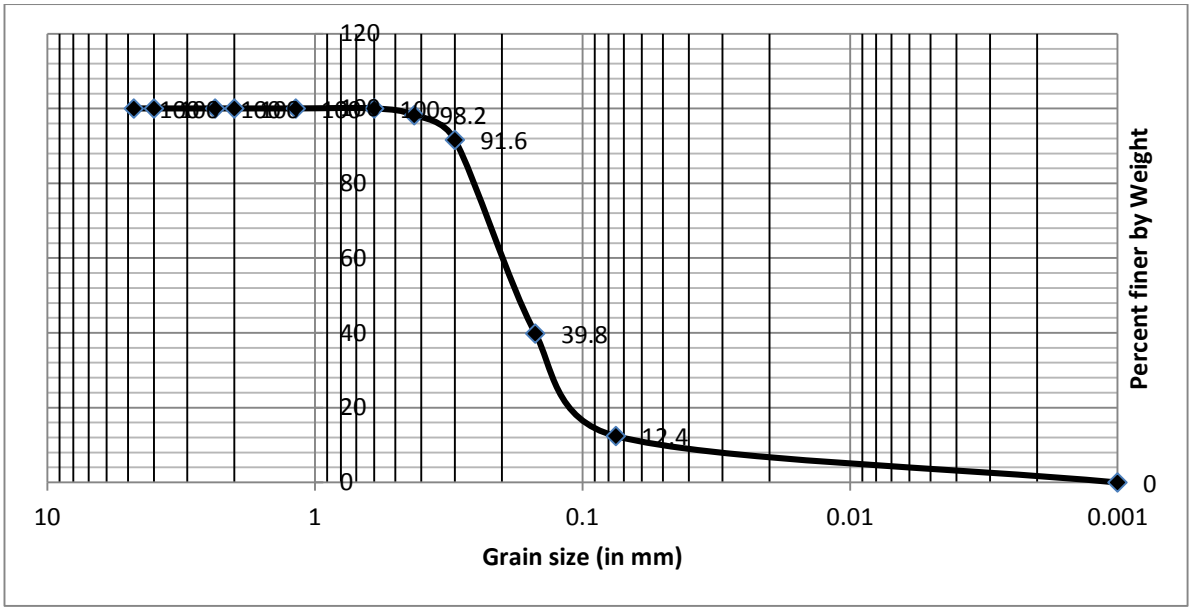

Figure 3-3 Grain size distribution curve for soil at depth of .5m

The coefficient of uniformity C_u is a shape parameter and is defined as:

$$C_u = \frac{D_{60}}{D_{10}} \tag{3.6}$$

D_{10} corresponds to 10% of the sample finer in weight on the Grain size distribution curve. It is also called the effective size.

D_{60} is grain diameter (mm) corresponding to 60% finer than.

$D_{10} = 0.065$

$D_{60} = 0.21$

$C_u = 3.23$

Another shape parameter coefficient of curvature C_c is defined as:

$$C_c = \frac{D_{30}^2}{(D_{10} \times D_{60})} \quad (3.7)$$

D_{30} is grain diameter (mm) corresponding to 30% finer than.

$D_{30} = 0.14$

$C_c = 1.43$

For a soil to be well graded, $C_u > 6$ and $1 < C_c < 3$. These criteria are not satisfied, hence it is poorly graded and is classified as SM.

Table 3-4 Sieve analysis results for soil at depth = .75m

s.no.	sieve size (mm)	wt. retained(gm)	%wt. retained	cumulative %retained	% N
1	4.75	0	0	0	100
2	4	0	0	0	100
3	2.36	0	0	0	100
4	2	0	0	0	100
5	1.18	0	0	0	100
6	0.6	0	0	0	100
7	0.425	11	2.2	2.2	97.8
8	0.3	16	3.2	5.4	94.6
9	0.15	235	47	52.4	47.6
10	0.075	161	32.2	84.6	15.4
11	0	77	15.4	100	0

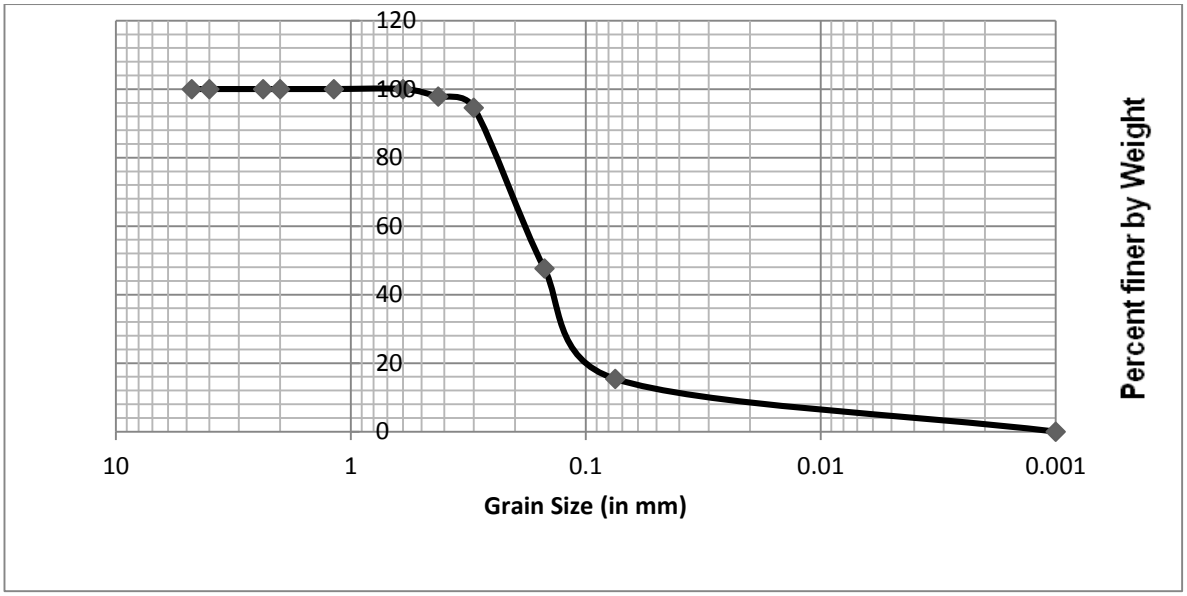

Figure 3-4 Grain size distribution curve for soil at depth of .75m

D_{60} =0.18

D_{10} = 0.055

D_{30} = 0.12

C_u = 3.27

C_c = 1.45

Table 3-5 Sieve analysis results for soil at depth = 1.5m

s.no.	sieve size (mm)	wt. retained(gm)	%wt. retained	cumulative %retained	% N
1	4.75	0	0	0	100
2	4	0	0	0	100
3	2.36	0	0	0	100
4	2	0	0	0	100
5	1.18	0	0	0	100
6	0.6	0	0	0	100
7	0.425	9	1.8	1.8	98.2
8	0.3	22	4.4	6.2	93.8
9	0.15	236	47.2	53.4	46.6
10	0.075	152	30.4	83.8	16.2
11	0	81	16.2	100	0

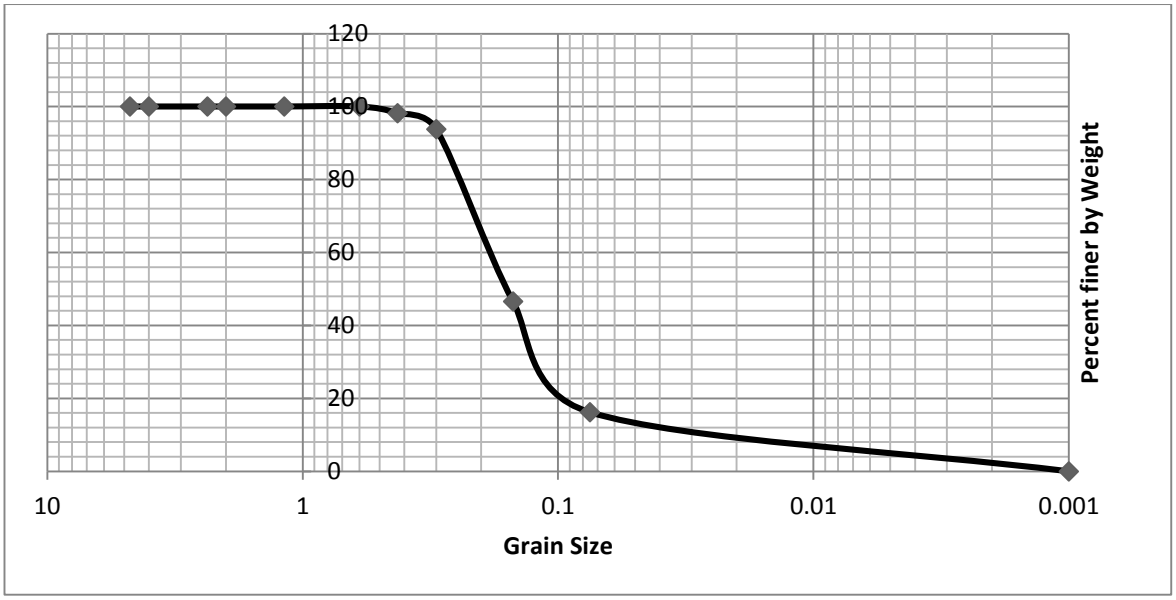

Figure 3-5 Grain size distribution curve for soil at depth of 1.5m

D_{60} =0.18

D_{10} = 0.045

D_{30} = 0.12

C_u = 4

C_c = 1.77

Table 3-6 Sieve analysis results for soil at depth = 3m

s.no.	sieve size(mm)	wt. retained(gm)	%wt. retained	cumulative %retained	% N
1	4.75	0	0	0	100
2	4	0	0	0	100
3	2.36	0	0	0	100
4	2	0	0	0	100
5	1.18	0	0	0	100
6	0.6	0	0	0	100
7	0.425	7	1.4	1.4	98.6
8	0.3	5	1	2.4	97.6
9	0.15	243	48.6	51	49
10	0.075	183	36.6	87.6	12.4
11	0	62	12.4	100	0

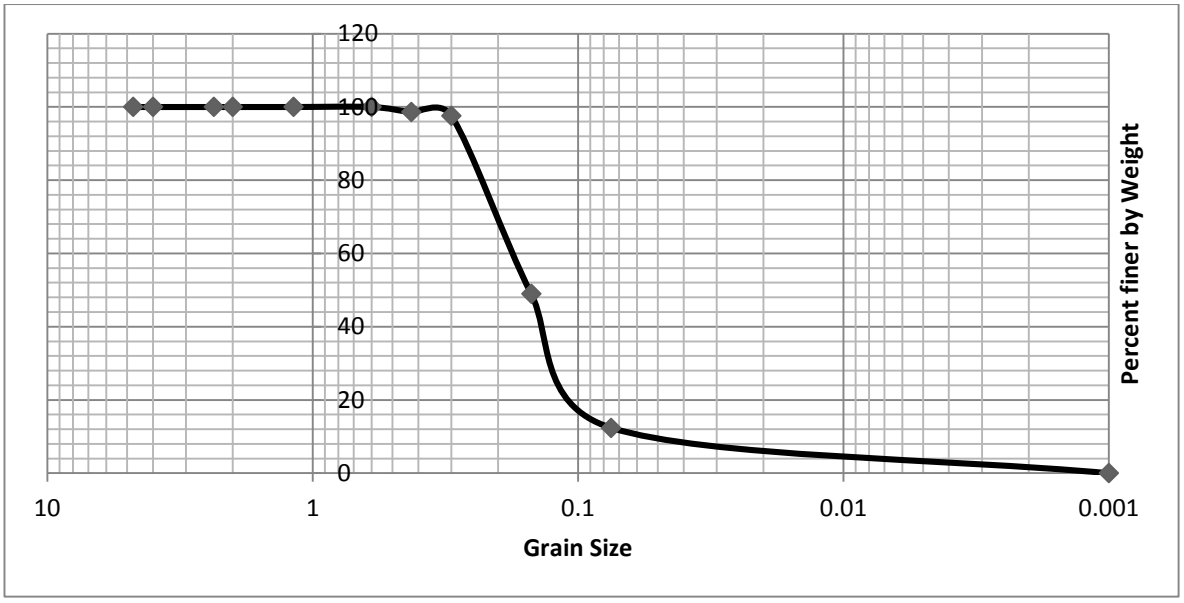

Figure 3-6 Grain size distribution curve for soil at depth of 3m

D_{60} =0.18

D_{10} = 0.66

D_{30} = 0.125

C_u = 2.72

C_c = 1.31

3.5 Specific Gravity:

IS : 2720 (Part 3) -1980

The specific gravity of the soil is computed using pycnometer. Ratio of the weight of dry soil in air of given volume to the weight in air of equal volume of distilled water at same temperature.

Specific gravity of soil

$$G = \frac{W2-W1}{(W4-W1)-(W3-W2)} \quad (3.8)$$

Where,

W1= Weight of specific gravity bottle in gm

W2= Weight of bottle + dry soil in gm

W3= Weight of bottle + soil + water in gm

W4= Weight of bottle full of water only in gm

Table 3-7 Specific Gravity at different depth

Depth (m)	W1 (gm)	W2 (gm)	W3 (gm)	W4 (gm)	sp. Gravity
0.5	652	852	1554	1429	2.67
0.75	652	852	1553	1429	2.63
1.5	652	852	1555	1429	2.70
2.25	652	852	1553	1429	2.63
3	652	852	1552	1429	2.60

Figure 3-7 Performing pycnometer test

Table 3-8 Summary of soil properties :

S. No.	Soil Property	Quantity
1	Soil Classification	SM
2	Coefficient of uniformity C_u	3.3
3	Coefficient of curvature C_c	1.49
4	Specific Gravity (G)	2.64
5	Angle of internal friction	30^0

3.6 Pile and Pile Cap Dimensions and Specification :

Pile Diameter- 20, 30, 40 and 50 cm

Length of Piles- 2m

Grade of Concrete- M25

3.6.1 Reinforcement Detailing:

As per recommendation of IS : 2911 (part 1) (sec2)- 2010 Code of Practice for Design and Construction of Pile Foundations (Bored Cast In-situ Concrete Piles)

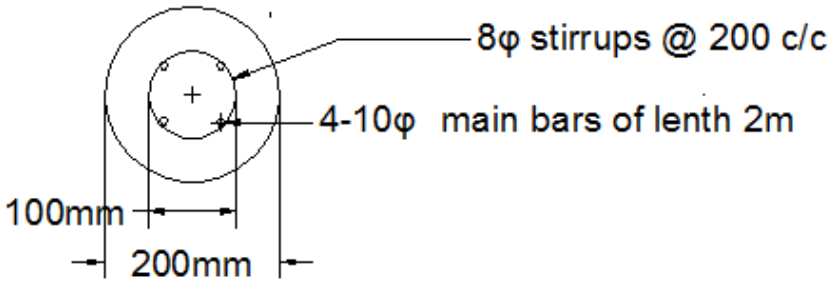

Figure 3-8 Cross sectional view of pile having diameter 20cm

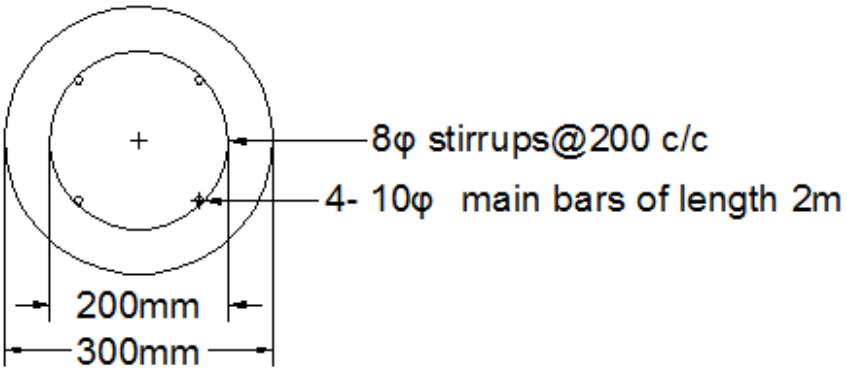

Figure 3-9 Cross sectional view of pile having diameter 30cm

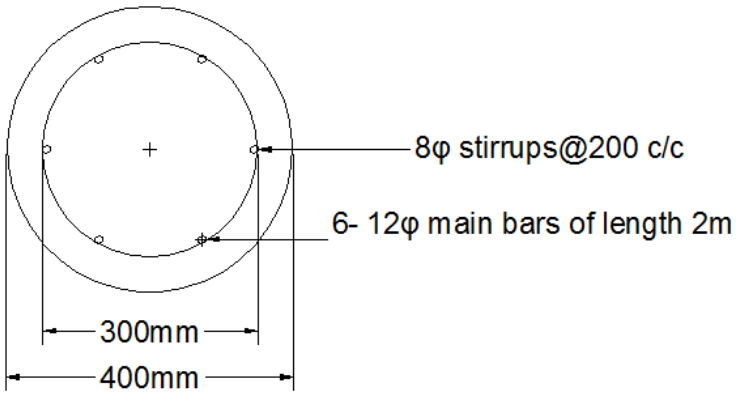

Figure 3-10 Cross – sectional view of pile having diameter 40 cm

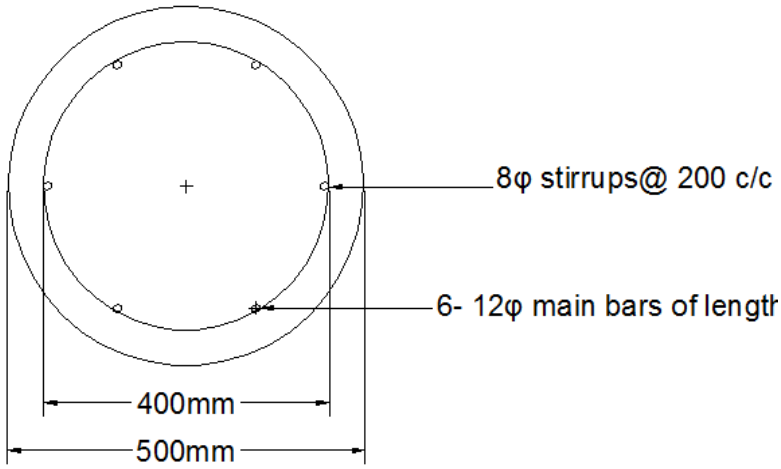

Figure 3-11 Cross – sectional view of pile having diameter 50cm

3.6.2 Pile Cap:

Grade of concrete: M25

Grade of steel: HSDB (Fe 415)

Wt. of oscillator and motor assembly = 3.67 KN

Wt. of Pile Cap = 0.7 x 0.7 x 0.3 x 24 = 3.528 KN

Total Load = 3.67 + 3.528 = 7.198 KN

The pile cap has been provided 4 bars of 10mm diameter at 200 mm center to center spacing in both directions.

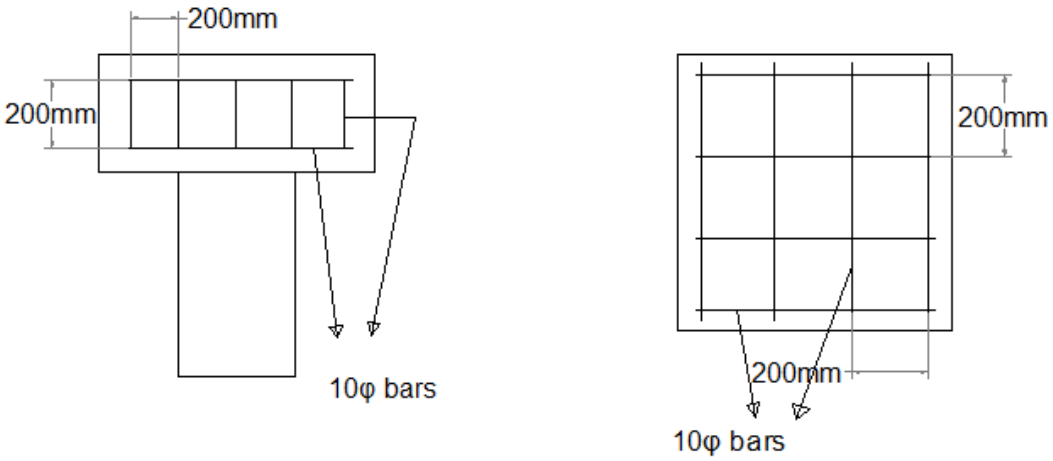

Figure 3-12 Pile cap reinforcement detail

3.7 Check :

Before we start experiment first step is to check that the piles constructed are short piles .

So, first condition as defined earlier in introduction is,

$L_s < 2T$

Where, T : Stiffness Factor

$$T = \left[\frac{E_p I_p}{\eta_h}\right]^{\frac{1}{5}}$$

Where,

E_pI_p: bending stiffness of pile

η_h :Coefficient of subgrade reaction

Now for silty sand typical value for modulus of subgrade reaction is 24000-48000KN/m^3[4]

So,

$$\eta_h = \frac{K_s}{L_s}$$

= 12-24 MN/m^3

E_p = 25 GPa

Table 3-9 Calculation of T for all pile diameters

diameter (m)	I	EI	T	2T
0.2	0.0000785	1962500	0.99435	1.9887
0.3	0.000397406	9935156.25	1.044279958	2.08855992
0.4	0.001256	31400000	1.314522222	2.62904444
0.5	0.003066406	76660156.25	1.571433266	3.14286653

So, length = 2m is ok for short pile.

Another condition is

$$.05\left[\frac{E_e}{G^*}\right]^{\frac{1}{2}} < \text{D/B} < \left[\frac{E_e}{G^*}\right]^{\frac{2}{7}}$$

Where,

G* : Equivalent shear modulus

E_e : Effective Young's modulus

D/B : Depth to Diameter ratio

$$G^* = \left[\frac{E_s}{2(1+\mu)}\right]\left[1+\frac{3\mu}{4}\right]$$

$$E_e = \frac{EI_p}{\left(\pi\frac{B^4}{64}\right)}$$

Now, poisson's ratio, μ = .35

E_s = 20 MPa (Kezdi 1974 and Prat et al. 1995)

E_e = 25 GPa

$$G^* = \left[\frac{20\times10^6}{2(1+\mu)}\right]\left[1+\frac{3\mu}{4}\right]$$

= 9351851.9 N/m^2

. 05 $\left[\frac{E_e}{G^*}\right]^{\frac{1}{2}}$ < D/B <$\left[\frac{E_e}{G^*}\right]^{\frac{2}{7}}$

2.58 < D/B < 9.89

D/B = 4, 5, 6.67, 10 all seems almost ok.

Hence all the piles are short piles as they fulfill both the criteria.

4 Experimental Setup

A comprehensive study of the measured dynamic response of the individual pile under lateral excitation is carried out. The in-situ tests on piles subjected to lateral vibration is performed to obtain the natural frequency, stiffness and damping ratio of the soil- pile system. The dynamic response of the pile depends on the subsoil, fixity of the head of the pile and the loads acting on the pile. The piles are subjected to forced vibration and the corresponding displacement is measured.

4.1 Equipment used:

The various components required for carrying out the test are enlisted below:

Mechanical Oscillator: A Lazan type mechanical oscillator with two counter rotating eccentric masses is used to produce sinusoidal excitation force. The magnitude of exciting force is regulated by adjusting the angle of eccentric masses. The oscillator used for testing has mass of 8.4 kg each with a radius of 0.063m. The oscillator will have to be mounted in such a way so that the horizontal vibrations occur along the longitudinal axis of the pile cap. The force level can be regulated by adjusting the angle of the eccentric masses.

DC motor: Motor of suitable power rating to run the mechanical oscillator in required frequency range at full load.

Speed Control Unit: Device to control the speed compatible with the dc motor is used.

Figure 4-1 Lateral Forced Vibration Setup

Acceleration pickups: Three piezoelectric acceleration pickups of same response characterstics are used to register the acceleration. These pickups are places at 50mm, 150mm and 250mm from the top, on the transverse face of the cap for lateral excitation. The accelerometers having different sensitivity are calibrated before recording is started.

Recording Device: With the help of Lab- View software the data for acceleration is recorded and saved at different frequencies.

For mounting the oscillator-motor assembly, a pile cap of dimension 0.7 x 0.7 x 0.3m was casted with provision of four bolts to ease the fixation. The pile cap was made of the same grade of concrete as used in the pile shaft i.e. M25. The center to center spacing of the piles is 10d, where d is the diameter of piles.

The motor-oscillator assembly will have to be firmly mounted on the pile-cap so that the entire system acts as a single unit. The oscillator will be set at a particular eccentricity, and will connect to a direct current motor and its speed will be regulated by the speed control unit. The operating frequency will be measured by a tachometer. The acceleration at the particular frequency will register through the software. The speed has to be increased gradually, and at each increment acceleration records will be taken.

4.2 Aspects of study:

The test was carried out on different sets of piles with varying dimensions and condition to study the following broad areas:

Effect of L/D ratio: Four piles with L/D ratio of 10, 6.67, 5 and 4 were tested. Pile have circular cross section with diameter of 200, 300, 400 and 500mm respectively and each having a length of 2m. Hence, the effect of variation of L/D ratio of the pile on the dynamic response of the pile can be assessed by comparing the results. The test was performed at four different eccentricity.

Effect of strain: These piles were tested at four different eccentricity setting of oscilattor with the objective of study the effect of strain on the response of the pile under lateral excitation.

Construction of piles of depth 2m and having diameter of 20, 30, 40 and50cm .

Following are some pictures of site during the construction.

Figure 4-2 Vertical and Transverse reinforcement in Pile stem

Figure 4-3 Showing the reinforcement in the pile cap

Figure 4-4 Showing construction process

Figure 4-5 Constructed Pile

5 Results and Discussion

Steps involved in the analysis:

1) From the raw data for acceleration v/s time at different frequencies, plot the graph for frequency against displacement in mm using the formula:

$$A_x = \frac{a_x}{4\pi^2 f^2} \tag{5.1}$$

Where,

A_x = displacement in mm

a_x = acceleration in mm/sec2

f = frequency in Hz

2) From the graph obtained above, find the damped natural frequency (ω_{ndz}).

3) Assume a specific value of the damping ratio (ξ).

4) Now find the undamped natural frequency using the relation

$$\omega_{nz} = \omega_{ndz}\sqrt{1 - 2\xi^2} \tag{5.2}$$

5) Find the magnification factor (μ) for each frequency using the relation

$$\mu = \frac{1}{\sqrt{\left\{1-\left(\frac{\omega}{\omega_n}\right)^2\right\}^2 + \left(2\xi\frac{\omega}{\omega_n}\right)^2}} \tag{5.3}$$

6) Compute the static rotation (θst) for each displacement

$$\delta^{st} = \frac{A_\theta}{\mu} \tag{5.4}$$

7) From the horizontal displacements A_x, find out A_θ , the angular displacement corresponding to each horizontal displacement.

8) Find out the moment corresponding to each frequency:

$$M_d = 2m_e r \sin\frac{\theta}{2} h\omega^2 \quad (5.5)$$

Where,

M_d = Moment acting due to horizontal dynamic loads on the top of the pile cap

M_e = Rotating mass in the oscillator (= 16.8 kg)

r = Eccentricity of the rotating mass with respect to oscillator shaft (= 0.063m)

ω = Frequency (rad/sec)

θ = Angle of eccentricity at which the oscillator is set

h = moment arm i.e. the distance between point of application of force and top of the pile cap (= 0.235)

9) A plot of static displacement versus moment at each frequency is plotted. The slope of the curve gives the stiffness of the soil-pile system in the lateral direction (K_θ).

10) Using this value of K_θ and the maximum rotational amplitude $(A_\theta)_{max}$ the damping ratio is recalculated from the following formula

$$\xi^2 = \frac{+b \pm \sqrt{b^2 - 4a^2 b}}{2b} \quad (5.6)$$

where,

$$\alpha = \frac{\omega_{nz}^2 . 2m_e . r . \sin\left(\frac{\theta}{2}\right) . h}{k_\theta (A_\theta)_{max}} \quad (5.7)$$

$(A_\theta)_{max}$ is dynamic rotational amplitude at resonant frequency

$$b = 4(\alpha^2 + 1) \quad (5.8)$$

11) The damping obtained in the step 10 should match the assumed damping ratio. The process is repeated till the two values converged. This converged value is the damping for the soil- pile system.

12) The stiffness for the damping obtained in the above step is the stiffness of the soil- pile system under horizontal dynamic loads.

5.1 Effect of Strain:

To study the effect of strain four cast in-situ RCC short piles of diameters 20cm, 30cm, 40cm and 50cm and having a same length of 2m were cast. Individual pile was excited to four different eccentricity settings of the oscillator. The driving frequency was varied from 2Hz to 45Hz.

Table 5-1 Representing pile diameters and corresponding eccentricity setting of oscillator

Pile Diameter (cm)	Eccentricity (°)
20	20,30,40
30	20,30,40,50
40	20,30,40,50
50	30,40,50,60

A sample curve for short pile of 40cm diameter excited to eccentricity 30° is given:

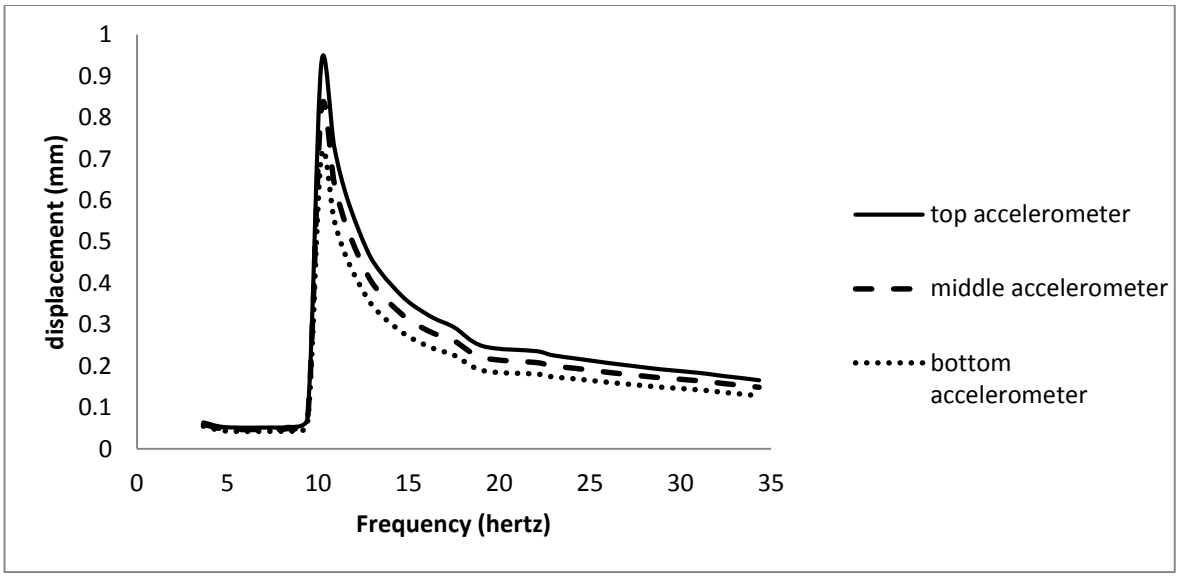

Figure 5-1 Horizontal displacement v/s Frequency plot for 40cm diameter short pile excited to e=30°

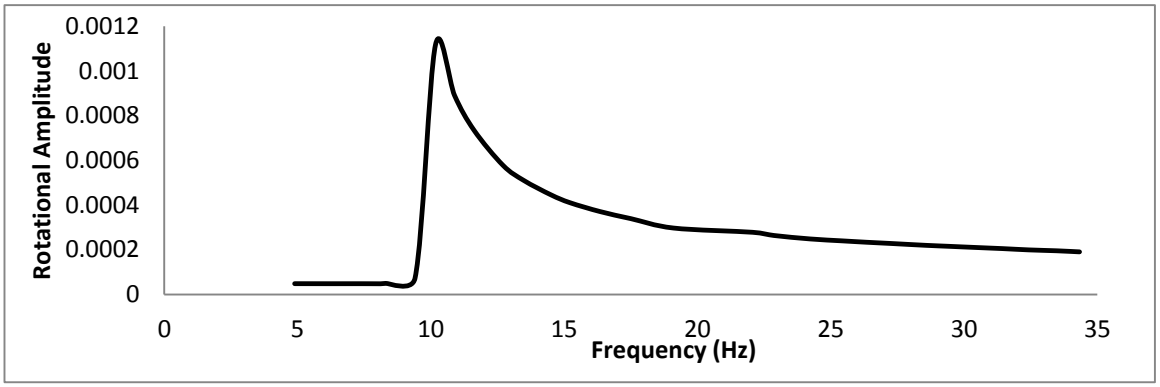

Figure 5-2 Rotational amplitude versus Frequency curve for 40cm diameter short pile excited to e=30°

Table 5-2 Representing Frequency and Calculations for Displacements and Rotational Amplitude for 40cm diameter short pile excited to e=30°

rms	f (Hz)	top accel.	middle accel.	bottom accel.	top displ. (mm)	middle displ.	bottom displ.	ω	Aθ
220	3.666666667	3.47E-03	3.20E-03	2.95E-03	0.064173745	0.05920076	0.054543571	23.03835	4.81509E-05
293	4.883333333	5.05E-03	4.55E-03	4.11E-03	0.052592287	0.047460979	0.042826402	30.68289	4.88294E-05
443	7.383333333	1.13E-02	1.03E-02	9.21E-03	0.051716908	0.046735992	0.041970734	46.39085	4.87309E-05
498	8.3	1.48E-02	1.35E-02	1.20E-02	0.053421029	0.048718147	0.04338605	52.15044	5.01749E-05
564	9.4	2.59E-02	2.34E-02	2.07E-02	0.07296309	0.065834943	0.058288698	59.06194	7.3372E-05
610	10.16666667	3.86E-01	3.40E-01	2.93E-01	0.927000575	0.81758288	0.70363923	63.87905	0.001116807
653	10.88333333	3.48E-01	3.06E-01	2.63E-01	0.730143469	0.642440633	0.552079125	68.382	0.000890322
697	11.61666667	3.27E-01	2.88E-01	2.48E-01	0.602844621	0.530278315	0.455938748	72.98967	0.000734529
762	12.7	3.11E-01	2.74E-01	2.36E-01	0.479740156	0.42168829	0.364102623	79.79645	0.000578188
809	13.48333333	3.11E-01	2.73E-01	2.36E-01	0.424582587	0.372484878	0.322508763	84.71828	0.000510369
870	14.5	3.17E-01	2.79E-01	2.41E-01	0.374640967	0.329237995	0.285406215	91.10619	0.000446174
913	15.21666667	3.24E-01	2.84E-01	2.47E-01	0.347321341	0.305014669	0.265148716	95.60914	0.000410863
981	16.35	3.40E-01	3.00E-01	2.61E-01	0.316393057	0.279030824	0.242178637	102.7301	0.000371072
1050	17.5	3.62E-01	3.21E-01	2.78E-01	0.293660326	0.260453353	0.225739535	109.9557	0.000339604
1146	19.1	3.64E-01	3.23E-01	2.77E-01	0.247999843	0.219927146	0.188471383	120.0088	0.000297642
1324	22.06666667	4.62E-01	4.08E-01	3.53E-01	0.23595297	0.20798134	0.180239349	138.649	0.000278568
1372	22.86666667	4.77E-01	4.22E-01	3.66E-01	0.226711166	0.200405208	0.173843671	143.6755	0.000264337
1454	24.23333333	5.16E-01	4.58E-01	3.98E-01	0.218201393	0.193887917	0.168442797	152.2625	0.000248793
1524	25.4	5.48E-01	4.87E-01	4.23E-01	0.211167719	0.187671267	0.1630721	159.5929	0.000240478
1580	26.33333333	5.74E-01	5.10E-01	4.43E-01	0.205688361	0.182754443	0.158856084	165.4572	0.000234161
1636	27.26666667	6.01E-01	5.34E-01	4.64E-01	0.200848749	0.178644092	0.155158499	171.3215	0.000228451
1714	28.56666667	6.37E-01	5.67E-01	4.92E-01	0.193880254	0.172669894	0.14981501	179.4897	0.000220326
1766	29.43333333	6.63E-01	5.91E-01	5.12E-01	0.190154997	0.169634904	0.146983694	184.9351	0.000215857
1830	30.5	6.96E-01	6.21E-01	5.38E-01	0.185815751	0.165906724	0.143748904	191.6372	0.000210334
1886	31.43333333	7.22E-01	6.45E-01	5.58E-01	0.181530752	0.162248321	0.140395214	197.5015	0.000205678
1946	32.43333333	7.44E-01	6.65E-01	5.75E-01	0.175687386	0.157177919	0.135712354	203.7846	0.000199875
2008	33.46666667	7.69E-01	6.88E-01	5.93E-01	0.170645453	0.152676968	0.131468954	210.2773	0.000195882
2060	34.33333333	7.87E-01	7.04E-01	6.05E-01	0.165814264	0.148350647	0.127606256	215.7227	0.00019104

From experimental curve:

Resonant Frequency, f_{ndz} = 10.16666667 Hz

Resonant Frequency (circular), $\omega_{ndz} = 2 \times \pi \times f_{ndz}$ = 2x3.14x10.1667 = 63.87905062 rad/sec

Assuming damping, ξ = 7.5%

Undamped natural frequency, $\omega_{nz} = \omega_{ndz}\sqrt{1-2\xi^2}$ = 63.51871465 rad/sec

Let us consider a frequency of 9.4Hz

From the table, corresponding to frequency of 9.4Hz,

ω = 2x3.14x9.4 = 59.06194189 rad/sec

ω/ω_{nz} = 0.929835

Now magnification factor,

$$\mu = \frac{1}{\sqrt{\left\{1-\left(\frac{\omega}{\omega_n}\right)^2\right\}^2+\left(2\xi\frac{\omega}{\omega_n}\right)^2}}$$

μ = 5.144245

Dynamic rotational amplitude, (A_θ) =.000073372 radian

Static Displacement, $\delta_{st} = \frac{A_\theta}{\mu}$ = .0000142629 rad

Moment, $M_d = 2m_e r \sin\frac{\theta}{2} h\omega^2$

Where m_e = 16.8

r = 0.063

h = 0.235

M_d = 224.5584324 N-m/rad

Similarly, ω, ω/ω_{nz}, μ, A_θ, δ_{st}, M_d are calculated for each frequency.

Stiffness (K_θ) of the soil-pile system is the slope of the curve between moment and static displacement, for the assumed damping ratio.

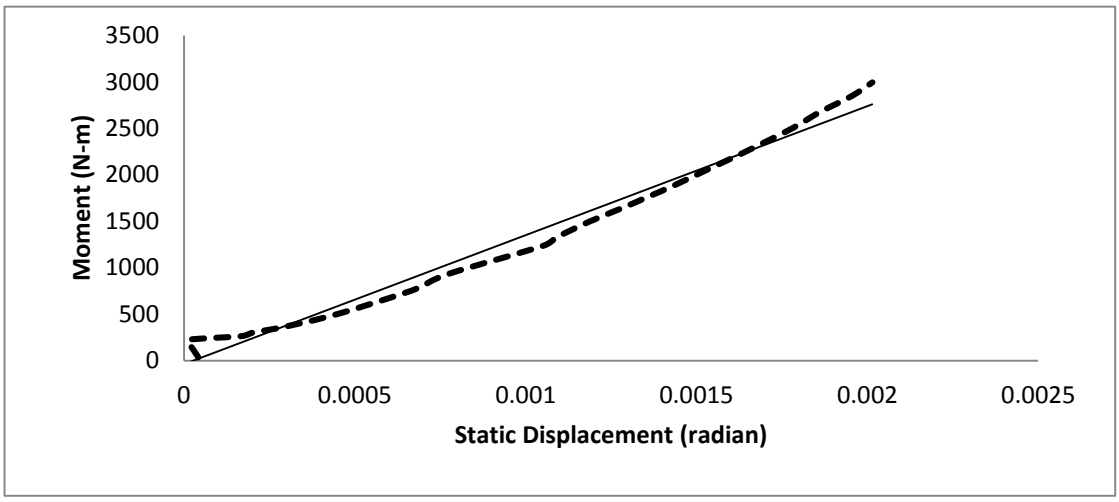

Figure 5-3 Moment versus Static Displacement for 40cm diameter short pile excited to e=30°

For assumed damping ratio of 7.5%, K_θ obtained from the curve is,

K_θ = 1387795.045 N-m/rad

Now, damping is recalculated by substituting this value in the following equations:

$\xi^2 = \frac{+b \pm \sqrt{b^2 - 4a^2 b}}{2b}$

where,

$\alpha = \frac{\omega_{nz}^2 . 2m_e . r . \sin\left(\frac{\theta}{2}\right) . h}{k_\theta (A_\theta)_{max}}$ = 0.16948352

where,

$(A_\theta)_{max}$ is dynamic rotational amplitude at resonant frequency

b = $4(\alpha^2 + 1)$ = 4.114898655

ξ^2 = 0.007030071

ξ = 8.38%

So, here assumed damping ratio and calculated damping ratio are not same. Iteration is applied till the assumed and calculated value converge. This final value is the damping ratio of soil-pile system. The stiffness (K_θ) corresponding to that value is the stiffness of the soil-pile system.

Now, for 40cm diameter short pile excited to eccentricity of 30° :

The converged damping ratio ξ = 8.39%

Corresponding stiffness K_θ = 1386801.214 N-m/rad

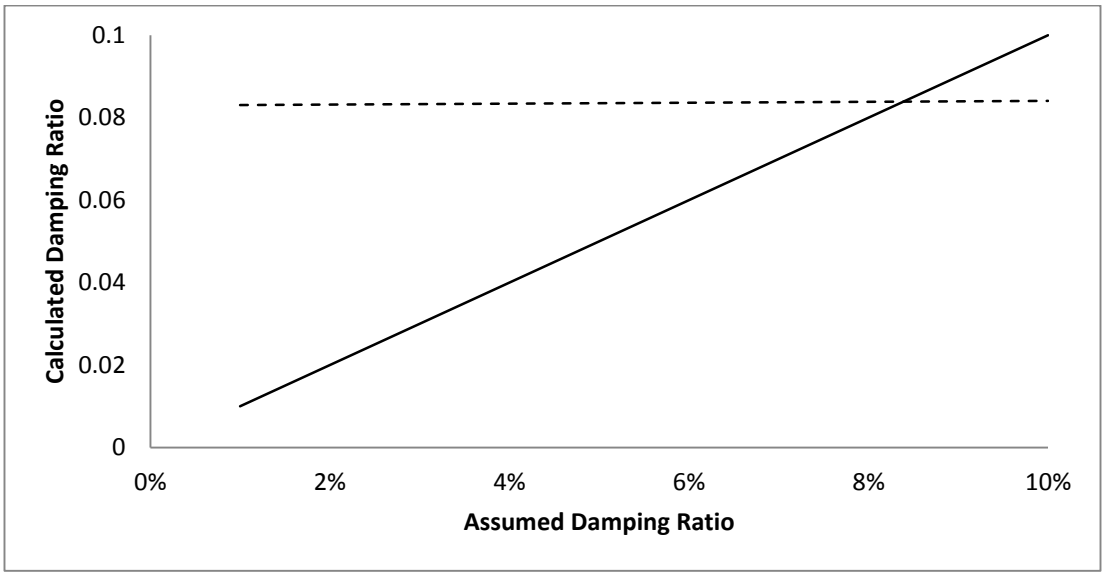

Figure 5-4 Co-relation between calculated and assumed damping ratio for 40cm diameter short pile excited to e=30°

For the same short pile of 40 diameter Damping ratio, Stiffness, Resonant frequency and Shear strain are calculated for various eccentricity i.e. e = 20°, e = 30°, e = 40° and e = 50°. With the force level the variation of Damping ratio, Stiffness, Resonant frequency and Shear strain ratio is shown below:

Table 5-3 Test results of 40cm diameter short pile at e=30°

Eccentricity	Stiffness (N-m/rad)	Damping	Resonant Frequency
20.00	3174086.84	0.12	16.63
30.00	1386801.21	0.08	10.17
40.00	1217849.81	0.08	8.82
50.00	631934.18	0.05	7.90

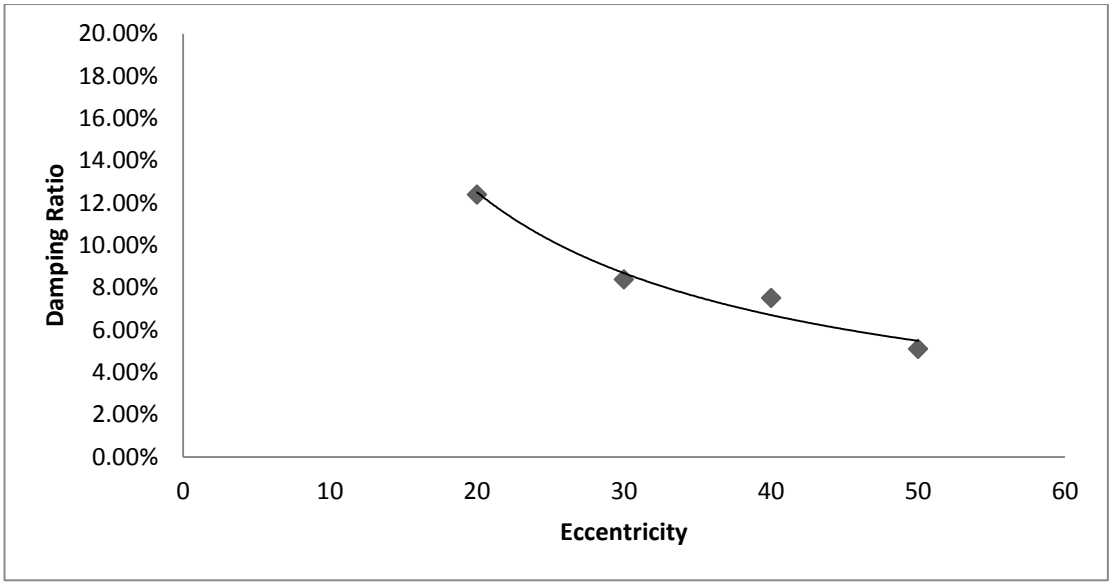

Figure 5-5 Variation of Damping Ratio with Eccentricity setting of oscillator for short pile of diameter 40cm

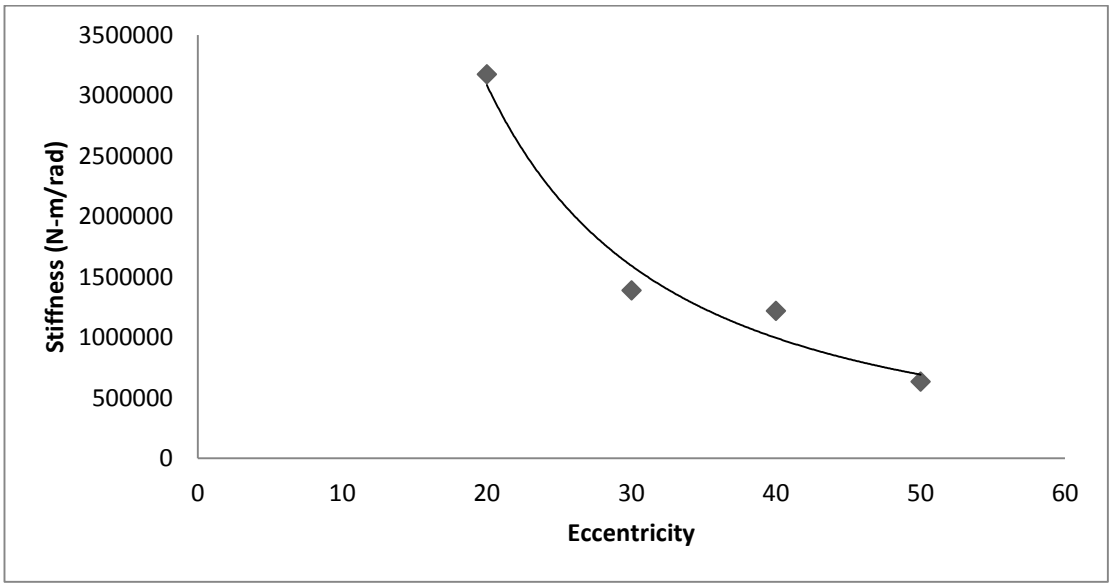

Figure 5-6 Variation of Stiffness with Eccentricity setting of oscillator for short pile of diameter 40cm

5.1.1 Evaluation of strain level:

For each eccentricity setting of motor-oscillator assembly the contra-flexure depth is obtained. Contra-flexure depth is the depth measured from the top of the pile cap to the point where horizontal displacement is zero. The pile depth below this contra-flexure point does not contribute in calculating the stiffness of the soil-pile system as there is no displacement of pile below contra-flexure point. Shear strain is the ratio

of horizontal displacement at ground level to the vertical distance between ground level and contra-flexure point i.e. shear strain is equal to (A/h) as shown in the fig below:

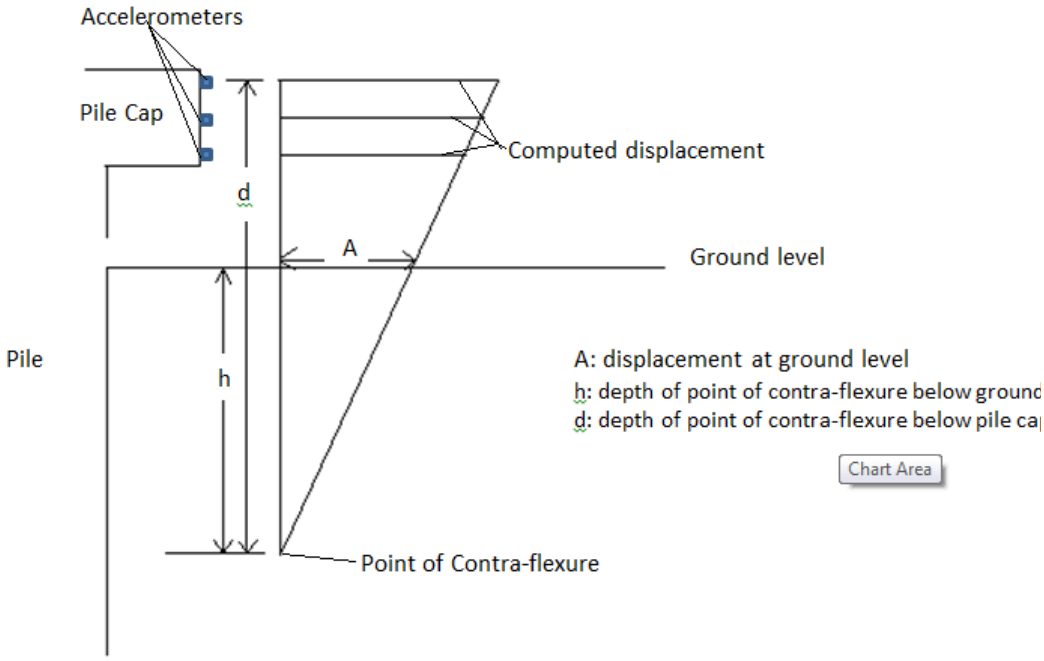

Figure 5-7 Locating Contra-flexure point

So, Contra-flexure depth, horizontal displacement at the ground level and shear strain is calculated for each eccentricity setting of motor-oscillator assembly. With the increase in force level variation of shear strain for short pile of diameter 40cm is given below.

Table 5-4 Shear Strain at Ground Level For Short pile of 40cm diameter

Eccentricity	Max Displacement at gound level (mm)	Contra-Flexure Depth (mm)	shear strain($x10^{-4}$)
20.00	0.18	731.43	5.85
30.00	0.51	880.05	11.17
40.00	1.01	921.82	20.40
50.00	0.96	664.26	39.95

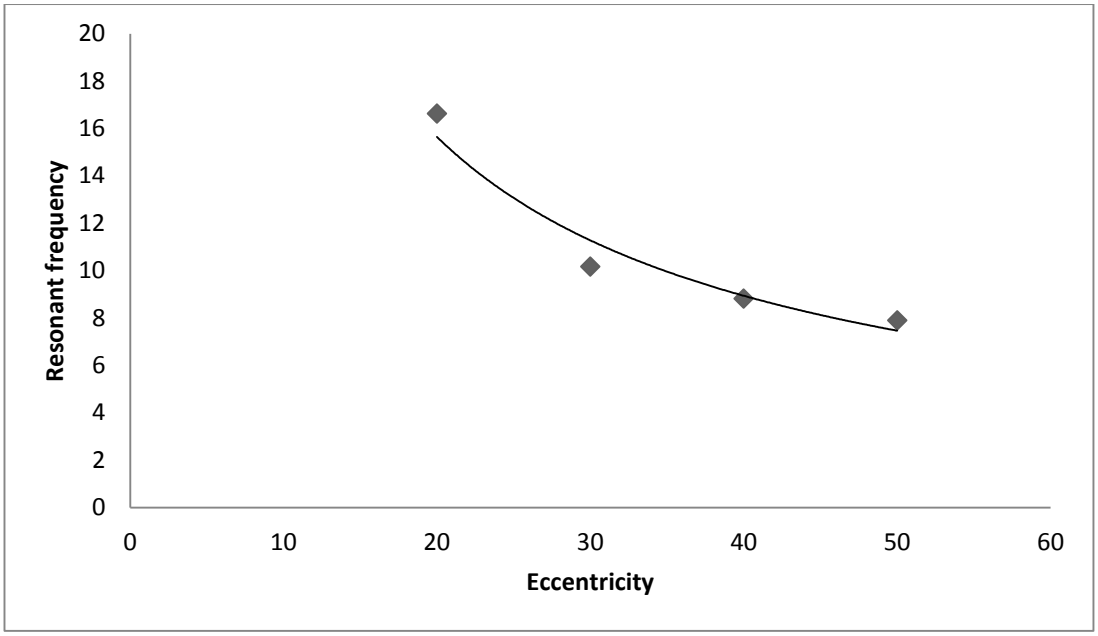

Figure 5-8 Variation of Resonant frequency with eccentricity setting of motor- oscillator assembly for 40 diameter short pile

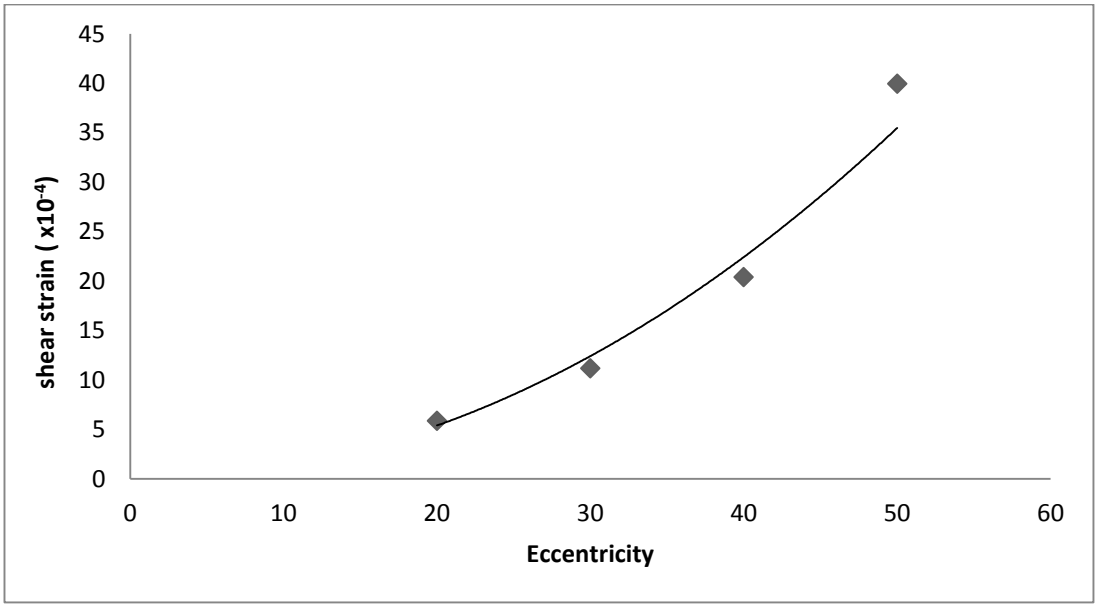

Figure 5-9 Variation of Shear strain with eccentricity setting of motor- oscillator assembly for 40 diameter short pile

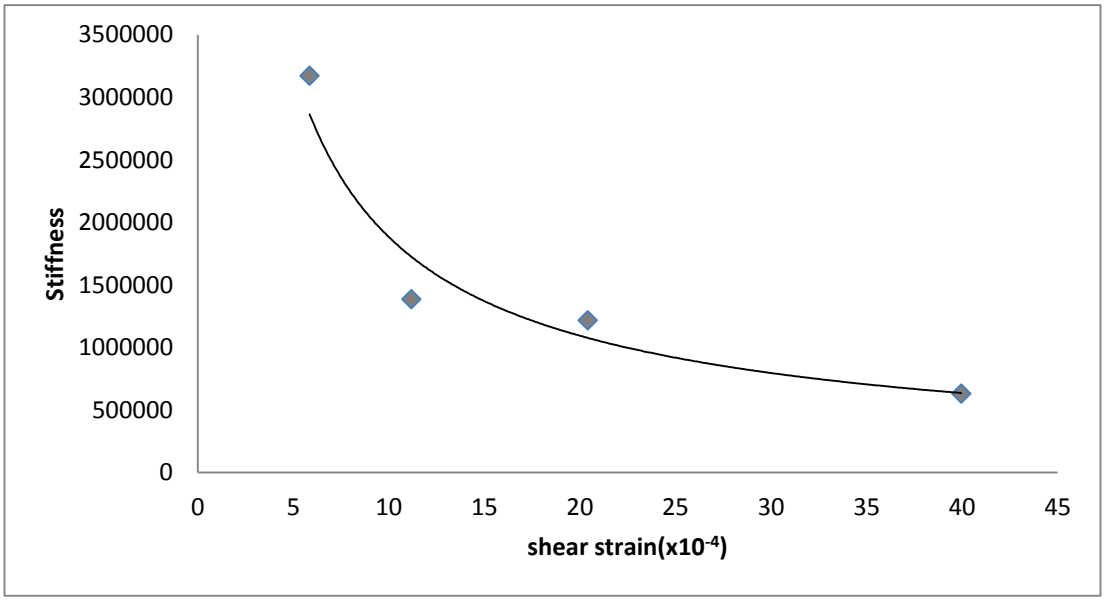

Figure 5-10 Variation of Stiffness with Shear Strain for 40 diameter short pile

Similar procedure is adopted for all the short piles, Damping ratio, Stiffness, Resonant Frequency and Shear strain are calculated for different eccentricity setting of motor-oscillator assembly. And similar trend is obtained for 20cm and 30cm diameter of pile the results are as below:

Table 5-5 Test results for short pile of 20cm diameter

Eccentricity	Stiffness (N-m/rad)	Damping	Resonant Frequency	shear strain ($x10^{-4}$)
20.00	706521.58	0.08	8.33	8.59
30.00	262862.39	0.07	5.00	17.63
40.00	197546.09	0.05	4.00	30.83

Table 5-6 Test results for short pile of 30cm diameter

Eccentricity	Stiffness (N-m/rad)	Damping	Resonant Frequency	shear strain ($x10^{-4}$)
20.00	2671360.77	0.09	13.50	6.57
30.00	941965.22	0.08	9.40	14.92
40.00	930548.59	0.06	7.18	23.77
50.00	457382.27	0.05	6.40	49.36

Table 5-7 Test results for short pile of 50cm diameter

Eccentricity	Stiffness (N-m/rad)	Damping	Resonant Frequency	shear strain
30.00	13498614.97	0.11	21.50	3.78
40.00	11008134.02	0.13	21.40	5.04
50.00	7719487.08	0.16	21.20	7.25
60.00	4309749.43	0.19	18.27	9.64

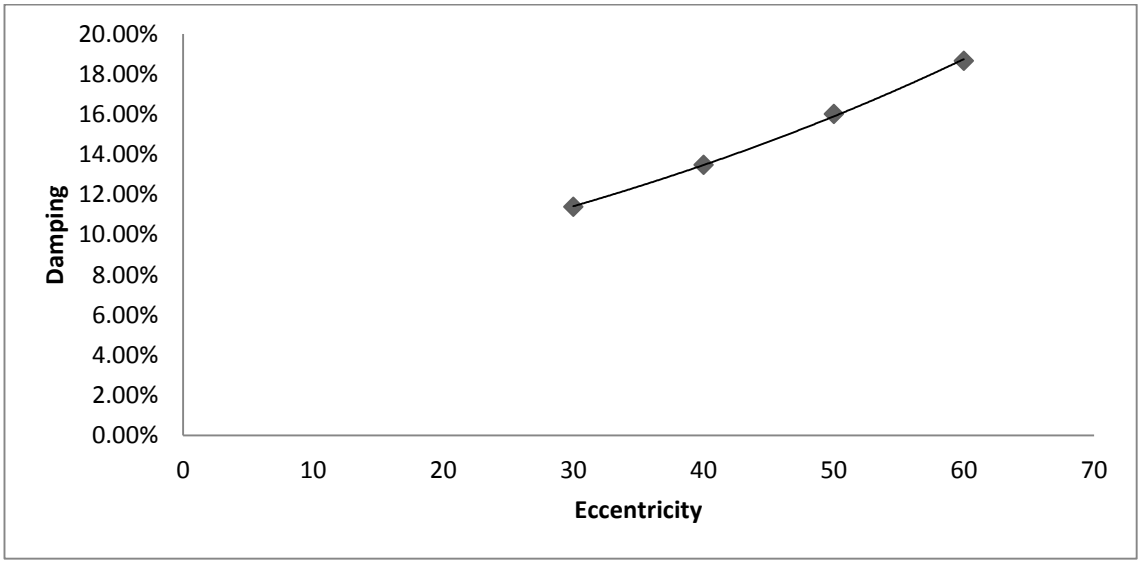

Figure 5-11 Variation of Damping with Eccentricity setting of oscillator for short pile of diameter 50cm

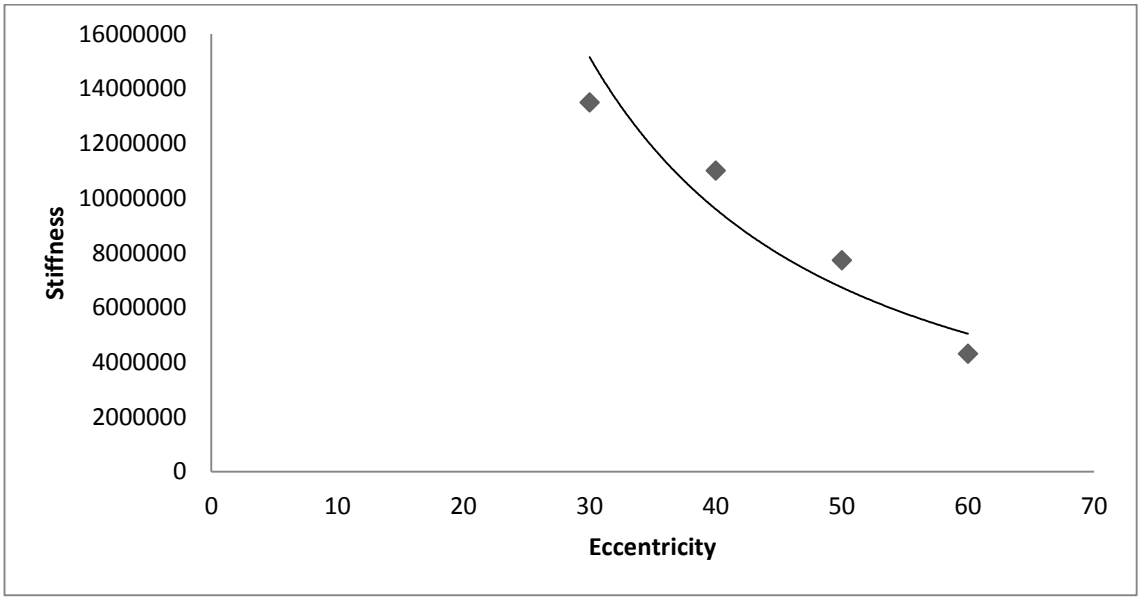

Figure 5-12 Variation of Stiffness with Eccentricity setting of oscillator for short pile of diameter 50cm

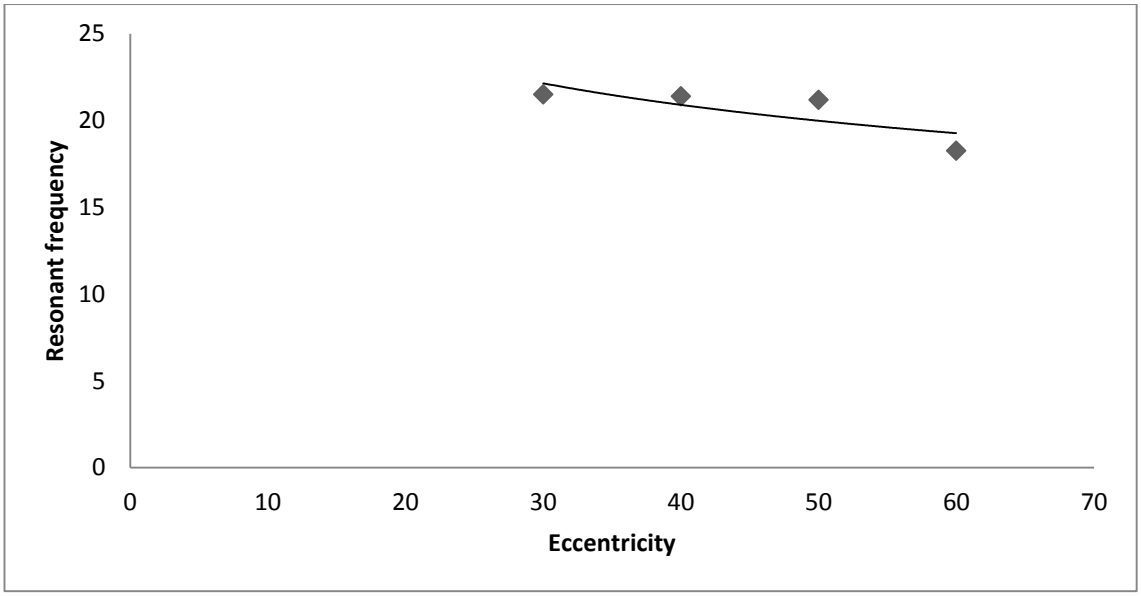

Figure 5-13 Variation of Resonant frequency with Eccentricity setting of oscillator for short pile of diameter 50cm

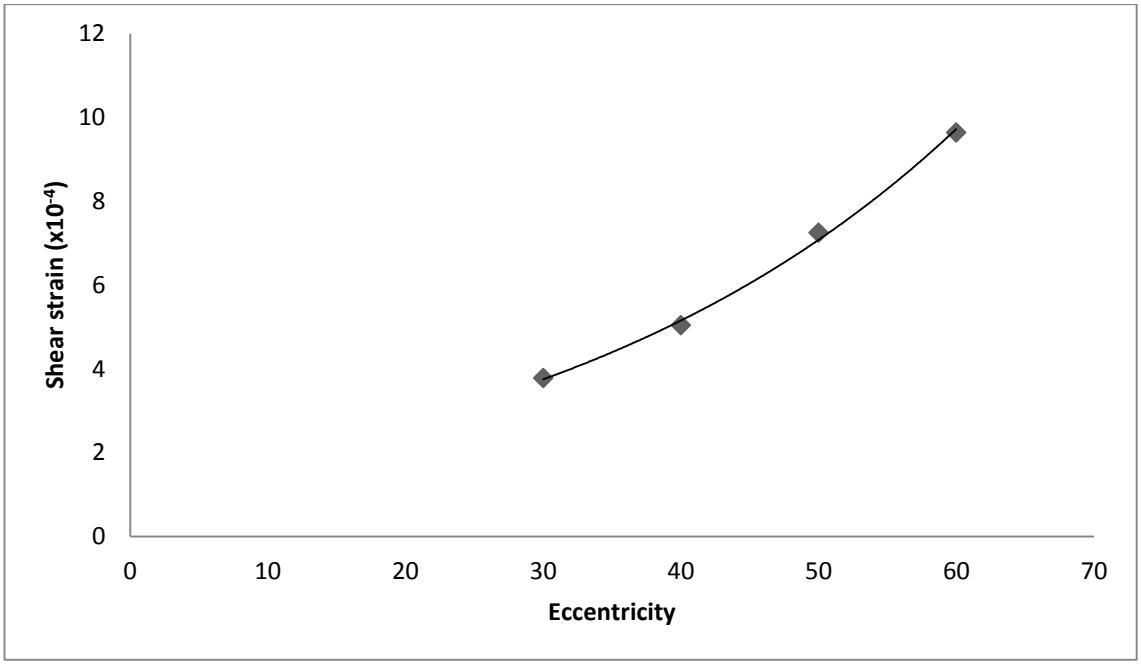

Figure 5-14 Variation of Shear strain with Eccentricity setting of oscillator for short pile of diameter 50cm

From the family of curve we concluded that for a particular pile diameter the results are:

Strain increases with an increase in the eccentricity setting of oscillator as force level is increasing this is expected trend.

Stiffness decreases with an increase in the eccentricity setting of oscillator, the result is as reported in Kramer [16] because with the increase in eccentricity of oscillator strain increases, shear modulus decreases hence stiffness decreases.

Damping ratio decreases with eccentricity of oscillator for pile diameter 20cm, 30cm and 40cm this may be because of separation of soil and pile as with increase in force level, strain increases and hence soil-pile separation increases, the same trend was obtained by Sonal Singh [17] for under-reamed piles. But for 50 cm diameter the trend is opposite this is because the strain values are comparatively lower and soil-pile separation is insignificant.

Resonant frequency is decreasing with eccentricity as stiffness is decreasing.

5.2 Effect of L/D ratio:

To study the effect of L/D ratio four cast in-situ RCC short piles of diameters 20cm, 30cm, 40cm and 50cm and having a same length of 2m were cast. That is a L/D ratio of 10, 6.67, 5 and 4. Individual pile was excited to four different eccentricity settings of the oscillator. The driving frequency was varied from 2Hz to 45Hz. The effect of L/D is calculated by comparing the results of same eccentricity for different L/D ratio.

L/D	Eccentricity (°)
4	30,40,50,60
5	20,30,40,50
6.67	20,30,40,50
10	20,30,40

A sample curve for short pile of 30cm diameter excited to eccentricity 30° is given below:

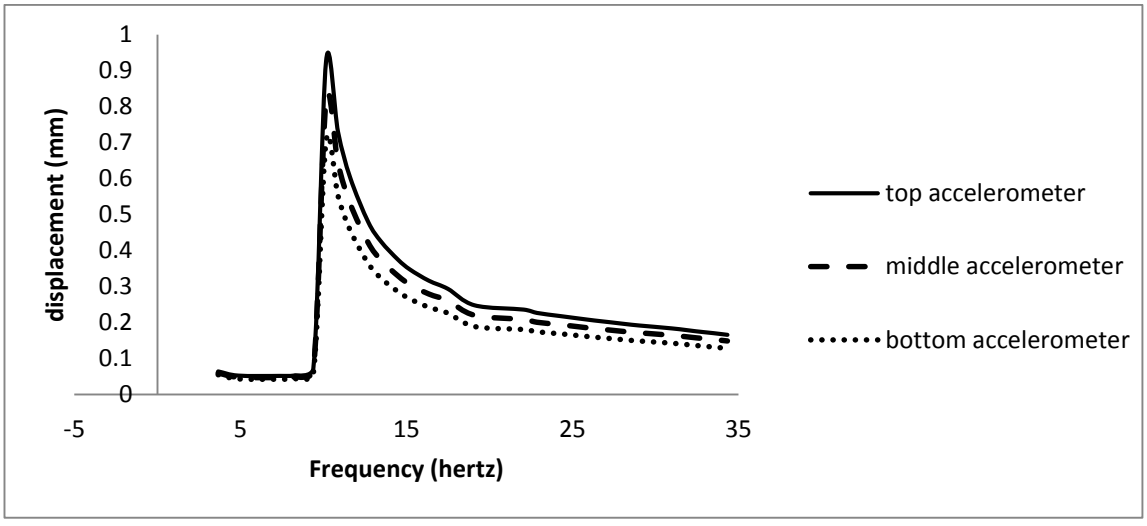

Figure 5-15 Horizontal displacement v/s Frequency plot for 30cm diameter short pile excited to e=30°

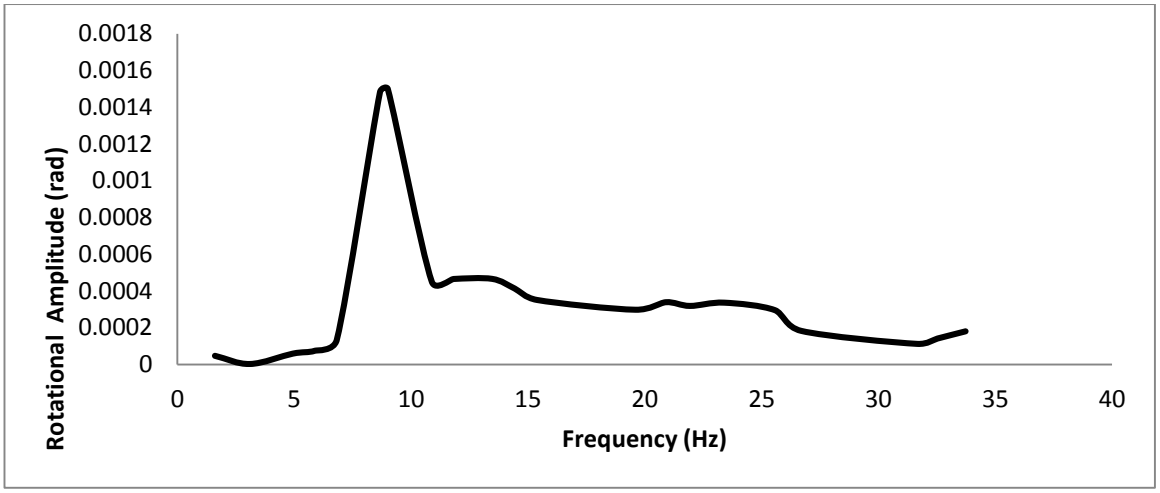

Figure 5-16 Rotational amplitude versus Frequency curve for 30cm diameter short pile excited to e=30°

Table 5-8 Representing Frequency and Calculations for Displacements and Rotational Amplitude for 30cm diameter short pile excited to e=30°

rms	Frequency (Hz)	top accel.	middle accel.	bottom accel.	top displ.(mm)	middle displ.	bottom displ.	ω	Aθ
96	1.6	2.53E-03	2.36E-03	2.43E-03	0.245175965	0.228808711	0.235780706	10.0531	4.69763E-05
186	3.1	2.97E-03	2.99E-03	2.99E-03	0.076805581	0.077343649	0.077275437	19.47787	2.34928E-06
296	4.933333333	5.26E-03	4.73E-03	4.10E-03	0.053684227	0.048242856	0.041910862	30.99705	5.88668E-05
353	5.883333333	8.10E-03	7.42E-03	6.01E-03	0.058122909	0.053258702	0.043179438	36.96607	7.47174E-05
409	6.816666667	1.55E-02	1.40E-02	1.05E-02	0.082815674	0.074801325	0.055976807	42.83038	0.000134194
520	8.666666667	3.09E-01	2.83E-01	2.19E-01	1.02171963	0.934730488	0.725092023	54.45427	0.001483138
546	9.1	4.12E-01	3.85E-01	3.14E-01	1.237366883	1.156735848	0.941667442	57.17699	0.001478497
564	9.4	5.32E-01	5.02E-01	4.26E-01	1.496871123	1.412410608	1.198402498	59.06194	0.001492343
579	9.65	5.33E-01	5.00E-01	4.21E-01	1.421184109	1.334206867	1.123447896	60.63274	0.001488681
653	10.88333333	1.34E-01	1.24E-01	9.10E-02	0.280972991	0.259530954	0.190894846	68.382	0.000450391
709	11.81666667	1.51E-01	1.34E-01	9.87E-02	0.268728718	0.238598881	0.175659149	74.24631	0.000465348
752	12.53333333	1.57E-01	1.37E-01	9.82E-02	0.249039523	0.21709485	0.155321392	78.74926	0.000468591
808	13.46666667	1.70E-01	1.43E-01	1.02E-01	0.233151304	0.196362236	0.139969762	84.61356	0.000465908
866	14.43333333	1.85E-01	1.57E-01	1.16E-01	0.221141503	0.186925734	0.138513345	90.68731	0.000413141
923	15.38333333	2.02E-01	1.71E-01	1.35E-01	0.211893214	0.180060541	0.141649435	96.65633	0.000351219
994	16.56666667	2.17E-01	1.86E-01	1.53E-01	0.196451299	0.168723609	0.138586387	104.0914	0.000289325
1034	17.23333333	2.38E-01	2.10E-01	1.87E-01	0.199367376	0.175697668	0.156829123	108.2802	0.000212691
1102	18.36666667	2.52E-01	2.23E-01	1.92E-01	0.185814935	0.164335876	0.141311591	115.4012	0.000222517
1176	19.6	2.54E-01	2.19E-01	1.62E-01	0.164555936	0.141783338	0.104987952	123.1504	0.00029784
1254	20.9	2.59E-01	2.17E-01	1.40E-01	0.147481305	0.123381322	0.079728373	131.3186	0.000338765
1316	21.93333333	2.66E-01	2.17E-01	1.43E-01	0.137611301	0.112067857	0.07389812	137.8112	0.000318566
1404	23.4	2.72E-01	2.15E-01	1.24E-01	0.123536608	0.097789989	0.056264316	147.0265	0.000336361
1472	24.53333333	2.67E-01	2.07E-01	1.06E-01	0.110393439	0.08536307	0.043688465	154.1475	0.000333525
1534	25.56666667	2.61E-01	1.97E-01	1.05E-01	0.099051137	0.074935301	0.03989517	160.6401	0.00029578
1602	26.7	2.59E-01	1.99E-01	1.55E-01	0.090408655	0.069303841	0.053875133	167.761	0.000182668
1674	27.9	2.98E-01	2.51E-01	2.52E-01	0.095027351	0.080178752	0.080318478	175.3009	7.35444E-05
1736	28.93333333	3.47E-01	3.12E-01	3.39E-01	0.102866443	0.092659599	0.100607068	181.7935	1.12969E-05
1832	30.53333333	4.14E-01	3.95E-01	4.53E-01	0.11043115	0.105285534	0.120722542	191.8466	5.1457E-05
1900	31.66666667	4.75E-01	4.77E-01	5.66E-01	0.117752794	0.118102022	0.140151803	198.9675	0.000111995
1952	32.53333333	5.05E-01	5.15E-01	6.26E-01	0.118628531	0.120873756	0.146866583	204.413	0.00014119
2024	33.73333333	5.66E-01	5.85E-01	7.31E-01	0.123596439	0.127722323	0.159679408	211.9528	0.000180415

From experimental curve:

Resonant Frequency, f_{ndz} = 9.4 Hz

Resonant Frequency (circular), $\omega_{ndz} = 2 \times \pi \times f_{ndz}$ = 2x3.14x9.14= 59.06194189 rad/sec

Assuming damping, ξ = 6.0%

Undamped natural frequency, $\omega_{nz} = \omega_{ndz}\sqrt{1-2\xi^2}$ = 58.84893479 rad/sec

Let us consider a frequency of 9.65 Hz

From the table, corresponding to frequency of 9.65 Hz,

ω = 2x3.14x9.65 = 60.63273821 rad/sec

ω/ω_{nz} = 1.030312

Now magnification factor,

$$\mu = \frac{1}{\sqrt{\left\{1-\left(\frac{\omega}{\omega_n}\right)^2\right\}^2+\left(2\xi\frac{\omega}{\omega_n}\right)^2}}$$

μ = 7.24075

Dynamic rotational amplitude, (A_θ) = 0.001488681 radian

Static Displacement, $\delta_{st} = \frac{A_\theta}{\mu}$ = 0.000205598 rad

Moment, $M_d = 2m_e r \sin\frac{\theta}{2} h\omega^2$

Where,

m_e = 16.8

r = 0.063

h = 0.235

M_d = 236.6618676 N-m/rad

Similarly, ω, ω/ω_{nz}, μ, A_θ, δ_{st}, M_d are calculated for each frequency.

Stiffness (k_θ) of the soil-pile system is the slope of the curve between moment and static displacement, for the assumed damping ratio.

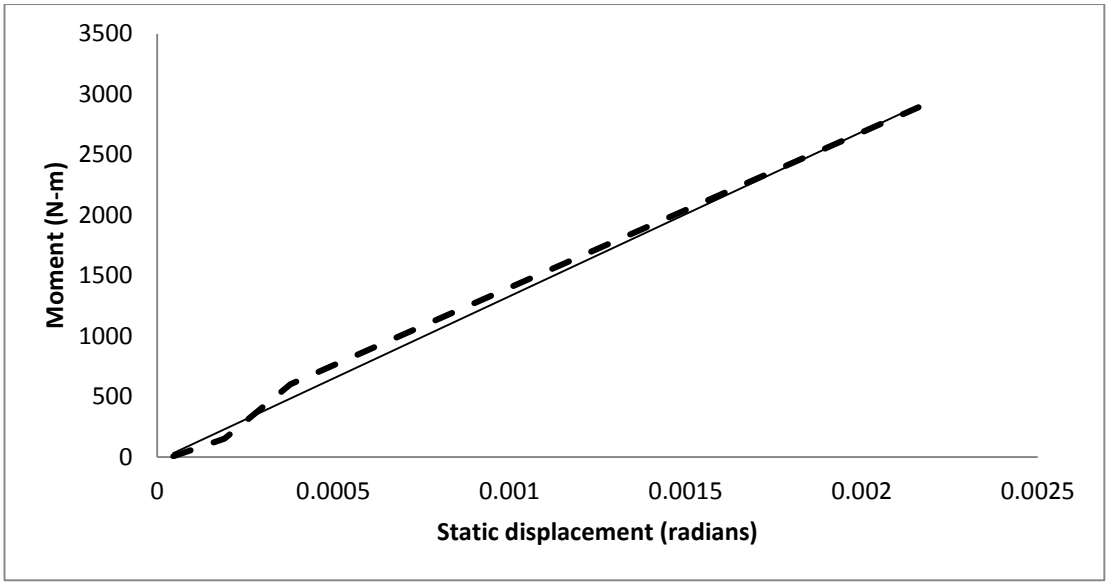

Figure 5-17 Moment versus Static Displacement for 30cm diameter short pile excited to e=30°

For assumed damping ratio of 6.0%, K_θ obtained from the curve is,

K_θ = 946552.5855 N-m/rad

Now, damping is recalculated by substituting this value in the following equations:

$$\xi^2 = \frac{+b \pm \sqrt{b^2} - 4a^2 b}{2b}$$

where,

$$\alpha = \frac{\omega_{nz}^2 . 2m_e . r . \sin\left(\frac{\theta}{2}\right) . h}{k_\theta (A_\theta)_{max}} = 0.158970278$$

where,

$(A_\theta)_{max}$ is dynamic rotational amplitude at resonant frequency

b = $4(\alpha^2 + 1)$ = 4.101086197

ξ^2 = 0.006200608

ξ = 7.87%

So, here assumed damping ratio and calculated damping ratio are not same. Iteration is applied till the assumed and calculated value converge. This final value is the damping ratio of soil-pile system. The stiffness (K_θ) corresponding to that value is the stiffness of the soil-pile system.

Now, for 30cm diameter short pile excited to eccentricity of 30° :

The converged damping ratio ξ = 7.91%

Corresponding stiffness K_θ = 941965.2185 N-m/rad

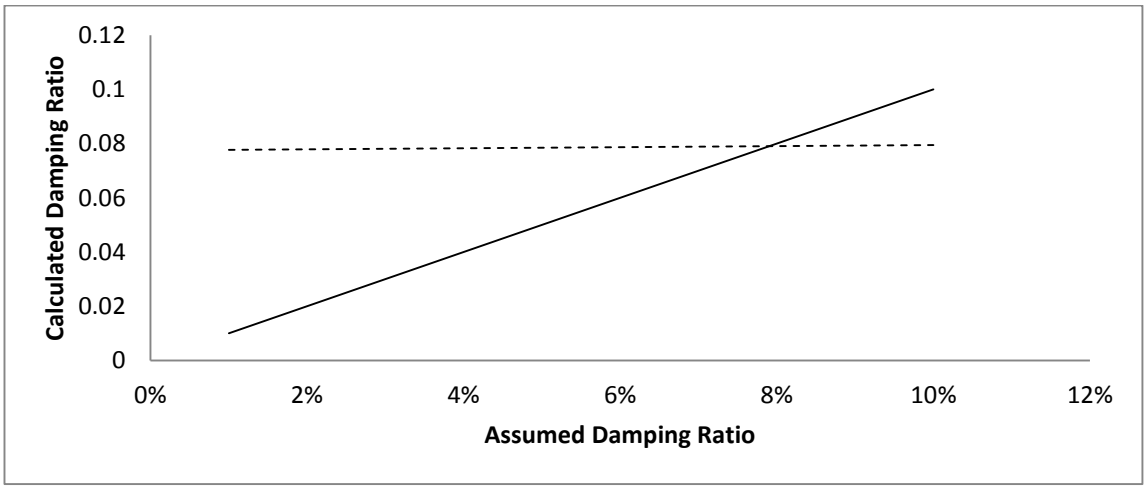

Figure 5-18 Co-relation between calculated and assumed damping ratio for 30cm diameter short pile excited to e=30°

To study the effect of L/D ratio, Damping ratio, Stiffness, Resonant frequency and Shear strain is calculated for various L/D ratio i.e. L/D= 4, L/D = 5, L/D = 6.667, L/D = 10 of short pile excited to same eccentricity setting of motor-oscillator assembly. With the L/D ratio the variation of Damping ratio, Stiffness, Resonant frequency and Shear strain for eccentricity e = 30° is shown below :

Table 5-9 Test results for eccentricity e= 30°

L/D	Stiffness (N-m/rad)	Damping	Resonant Frequency	shear strain ($x10^{-4}$)
4.00	13498614.97	0.11	21.50	3.78
5.00	1386801.21	0.08	10.17	11.17
6.67	941965.22	0.08	9.40	14.92
10.00	262862.39	0.07	5.00	17.63

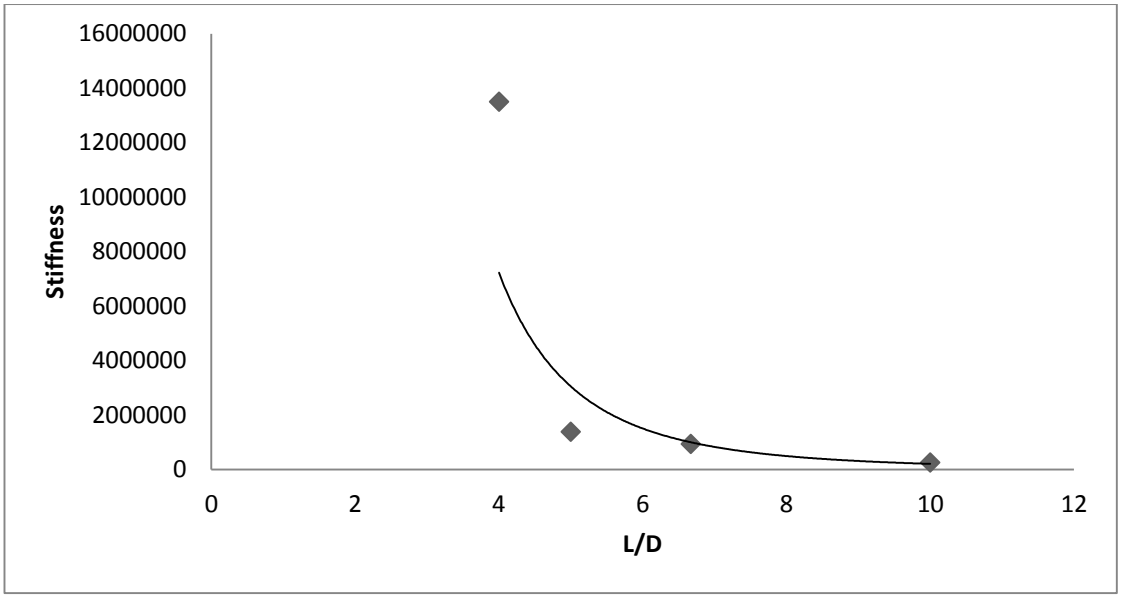

Figure 5-19 Variation of Stiffness with L/D ratio for eccentricity e= 30° setting of motor-oscillator assembly

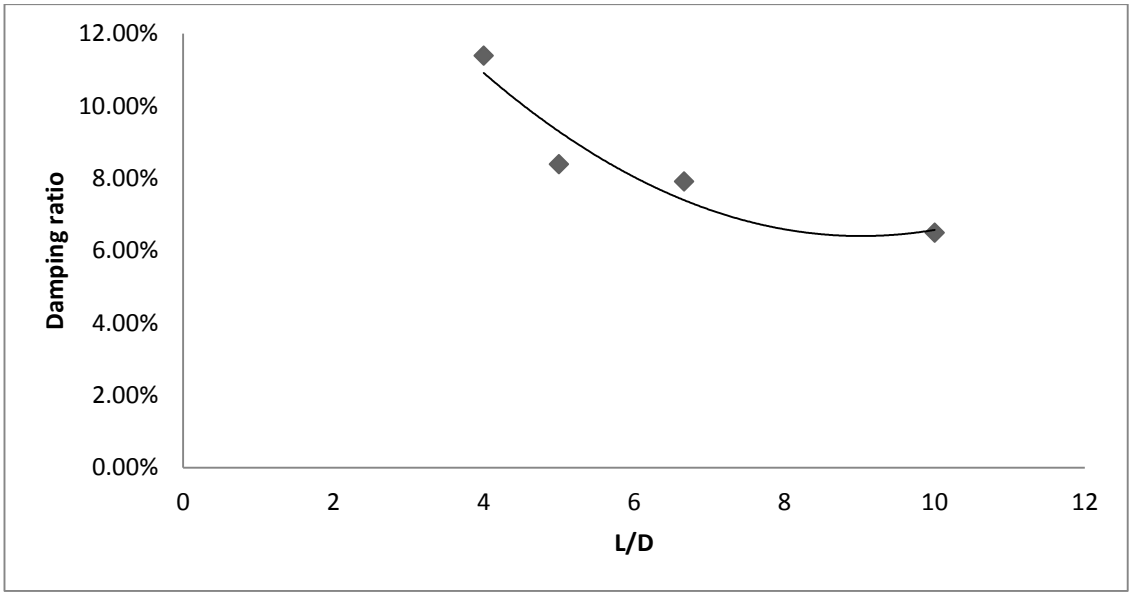

Figure 5-20 Variation of Damping with L/D ratio for eccentricity e= 30° setting of motor-oscillator assembly

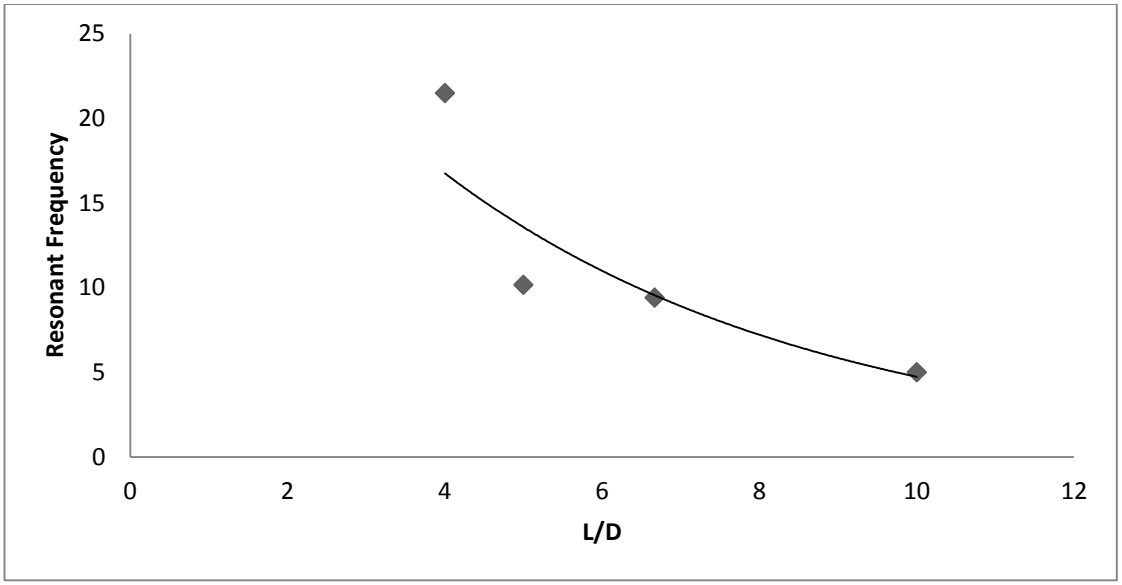

Figure 5-21 Variation of Resonant frequency with L/D ratio for eccentricity e= 30° setting of motor-oscillator assembly

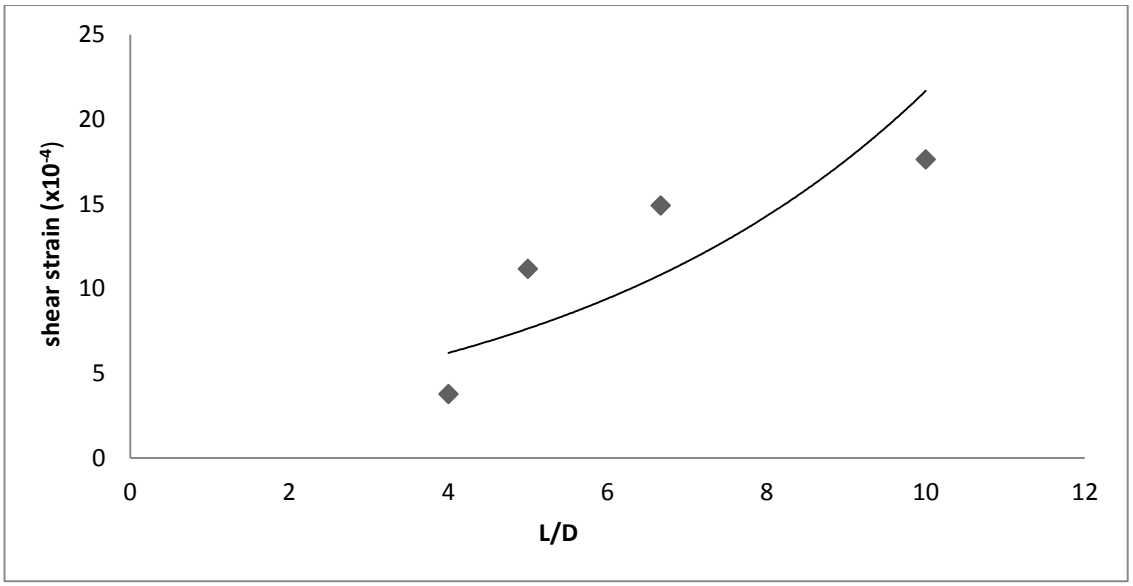

Figure 5-22 Variation of Shear strain with L/D ratio for eccentricity e= 30° setting of motor-oscillator assembly

Similar procedure is adopted for all the eccentricity setting of motor-oscillator assembly , Damping ratio, Stiffness, Resonant Frequency and Shear strain are calculated for different L/D ratio and similar trends are obtained for all eccentricity setting of oscillator the results are as below:

Table 5-10 Test results for eccentricity e= 20°

L/D	Stiffness (N-m/rad)	Damping	Resonant Frequency	shear strain ($x10^{-4}$)
5.00	3174086.84	0.12	16.63	5.85
6.67	2671360.77	0.09	13.50	6.57
10.00	706521.58	0.08	8.33	8.59

Table 5-11 Test results for eccentricity e= 40°

L/D	Stiffness (N-m/rad)	Damping	Resonant Frequency	shear strain ($x10^{-4}$)
4.00	11008134.02	0.13	21.40	5.04
5.00	1217849.81	0.08	8.82	20.40
6.67	930548.59	0.06	7.18	23.77
10.00	197546.09	0.05	4.00	30.83

Table 5-12 Test results for eccentricity e= 50°

L/D	Stiffness (N-m/rad)	Damping	Resonant Frequency	shear strain ($x10^{-4}$)
4.00	7719487.08	0.16	21.20	7.25
5.00	631934.18	0.05	7.90	39.95
6.67	457382.27	0.05	6.40	49.36

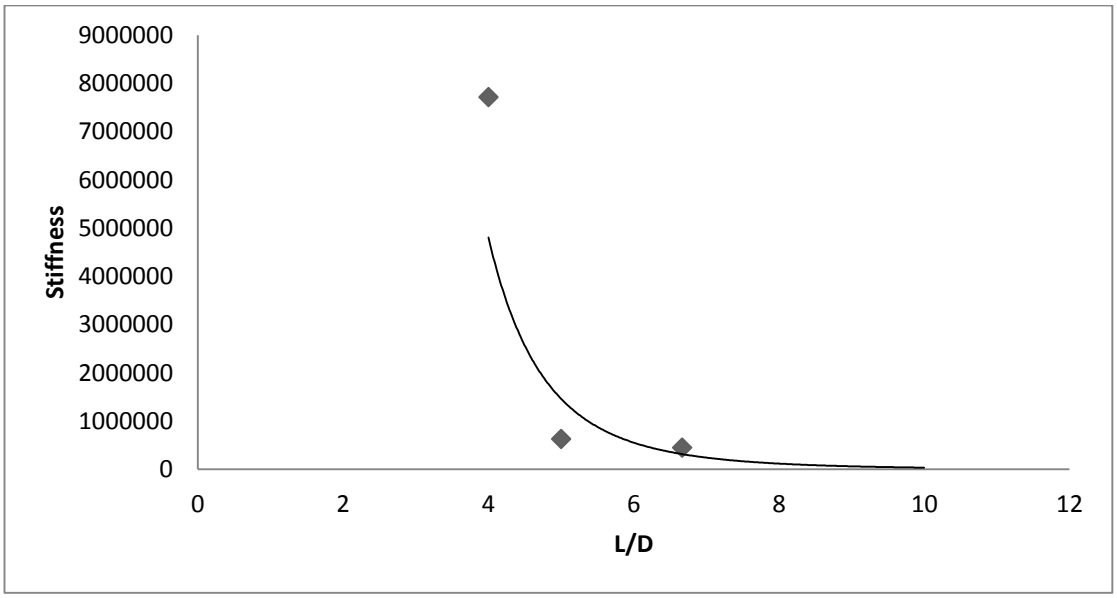

Figure 5-23 Variation of Stiffness with L/D ratio for eccentricity e= 50° setting of motor-oscillator assembly

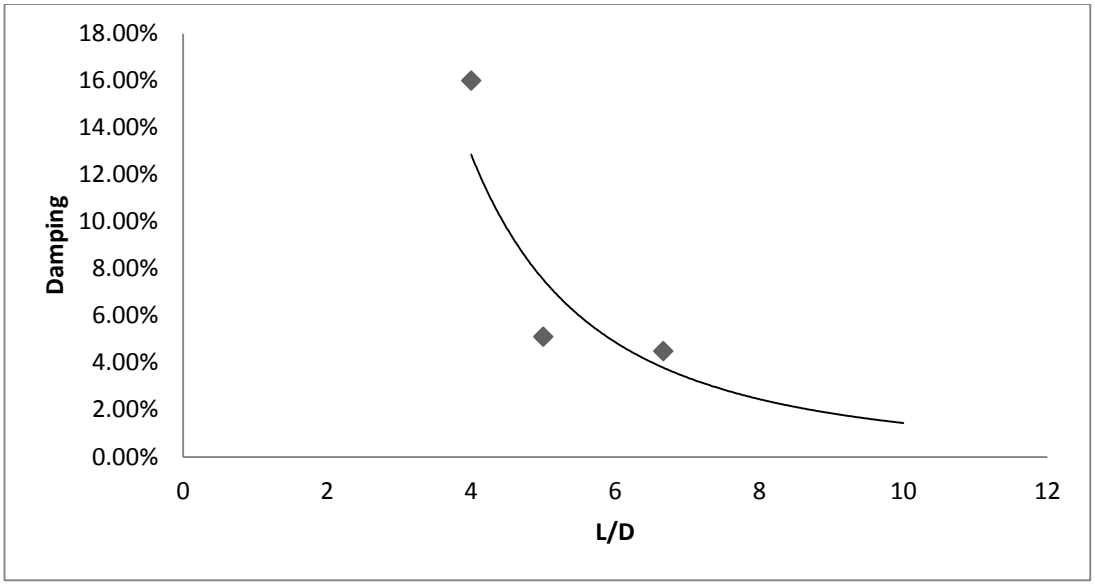

Figure 5-24 Variation of Damping ratio with L/D ratio for eccentricity e= 50° setting of motor-oscillator assembly

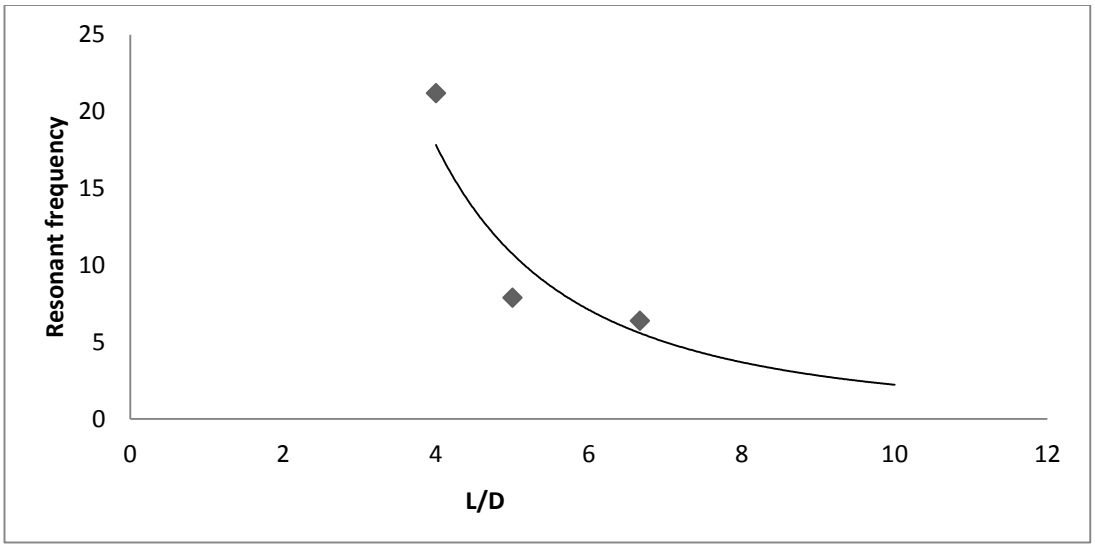

Figure 5-25 Variation of Resonant frequency with L/D ratio for eccentricity e= 50° setting of motor-oscillator assembly

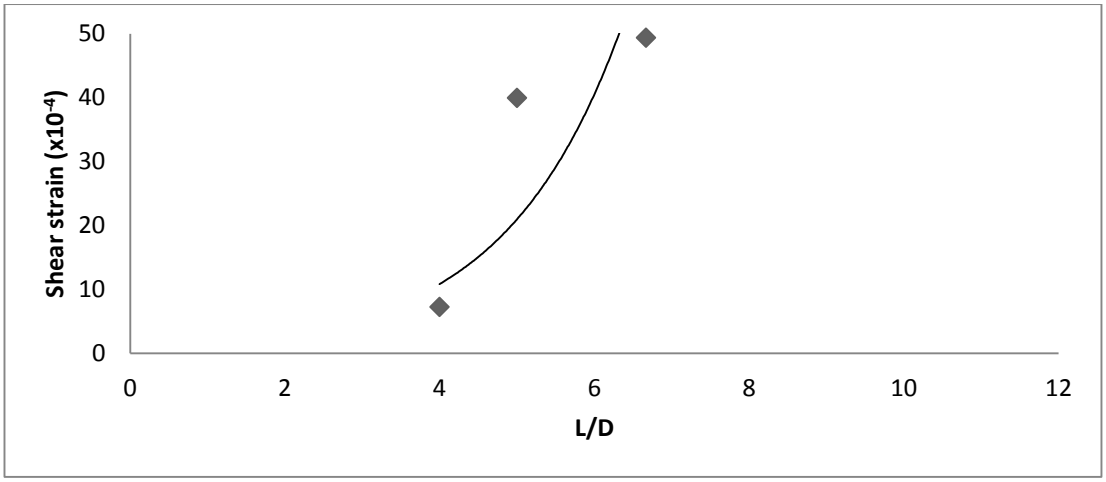

Figure 5-26 Variation of Shear strain with L/D ratio for eccentricity e= 50° setting of motor-oscillator assembly

From the family of curves we concluded that for a particular eccentricity setting of the oscillator results are:

Shear strain increases with an increase in L/D ratio because with L/D, diameter decreases and for same force level, displacement is higher for smaller diameter.

Stiffness is decreasing with an increase in L/D ratio as with L/D ratio, strain value increases, shear modulus decreases and therefore, stiffness decreases.

Damping decreases with an increase in L/D ratio because separation between soil and pile increases.

Resonant frequency decreases with an increase in L/D ratio as stiffness is decreasing.

5.3 Influence of effect of strain for different piles diameters:

The effect of strain on Damping ratio, Stiffness, Resonant frequency and shear strain for all the short piles can be compared by a plotting curves for all diameter in a single curve. These curves are given below:

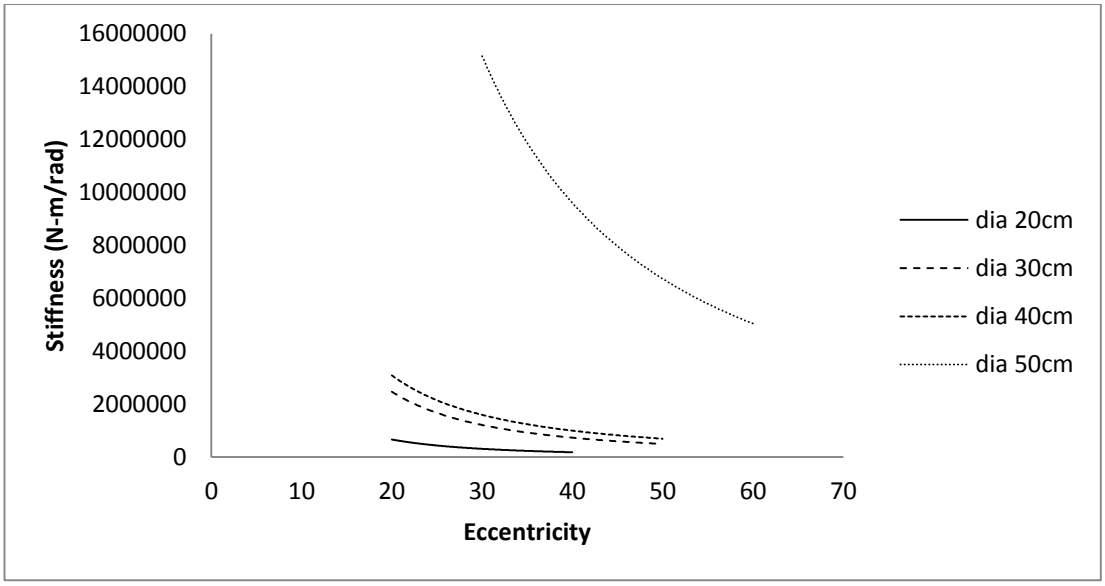

Figure 5-27 Variation of Stiffness with Eccentricity setting of oscillator

This graph shows that the stiffness is decreasing with increasing force level i.e. eccentricity setting of oscillator. From the plot it is clear that the decrease in stiffness is more in the case of pile with diameter of 50cm. This is because the strain is decreasing with increasing diameter of pile.

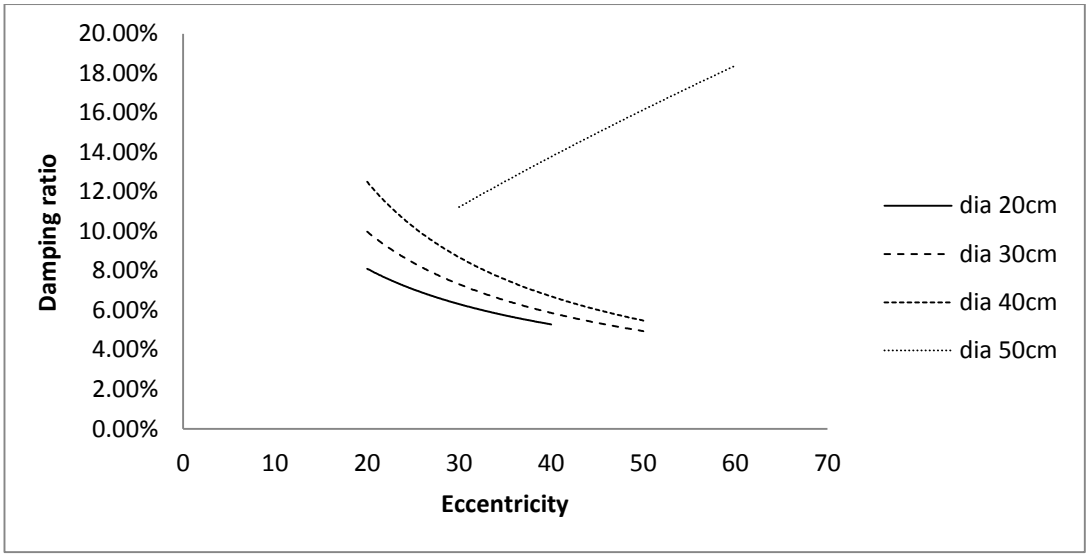

Figure 5-28 Variation of damping ratio with Eccentricity setting of oscillator

This graph shows damping ratio decreases with an increase in the eccentricity setting of the oscillator. This may be attributed to soil-pile separation, but in the case of 50cm diameter pile the damping ratio is found to increase probably because the strain is comparatively less and the soil pile separation is also much smaller. Similar trend has been observed by. Teerawut Juirnarongrit and Scott A. Ashford [15]

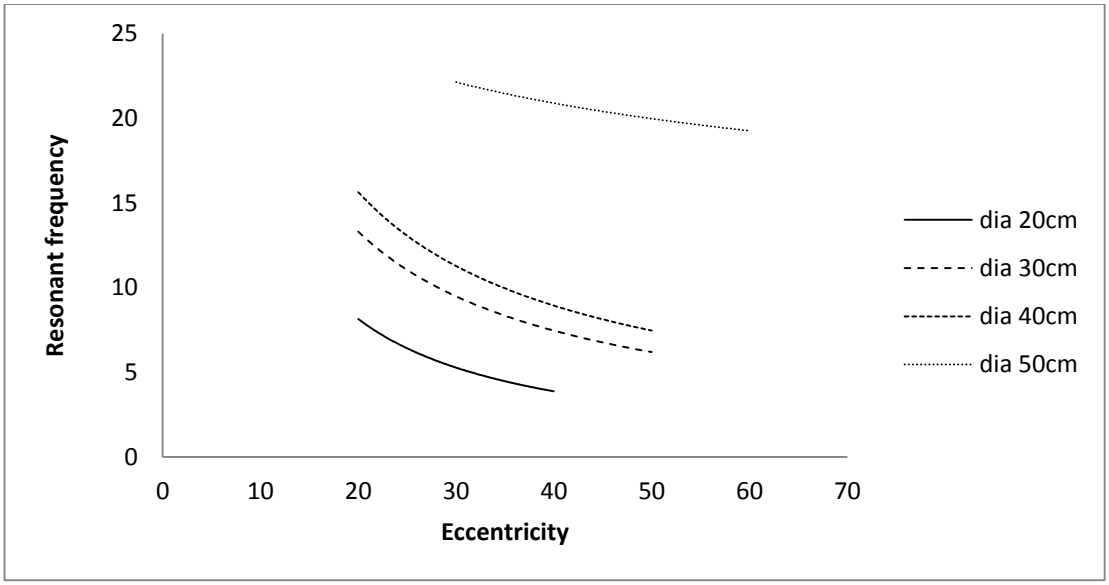

Figure 5-29 Variation of Resonant frequency with Eccentricity setting of oscillator

This graph shows the resonant frequency is decreasing with eccentricity setting of the oscillator. This is due to the fact that stiffness is decreasing with eccentricity setting of oscillator .i.e. force level.

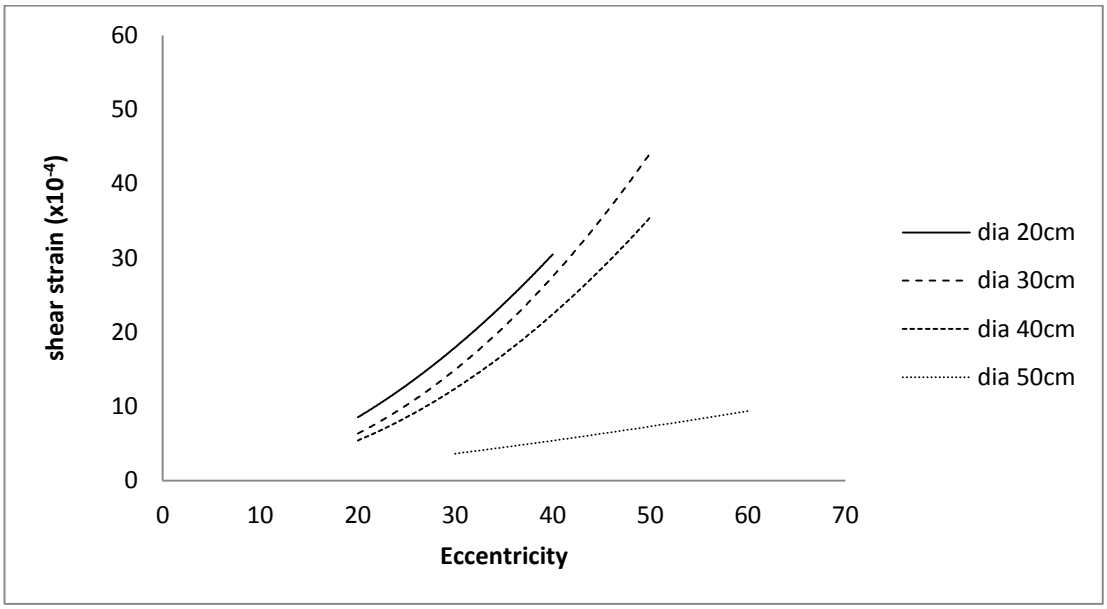

Figure 5-30 Variation of Shear strain with Eccentricity setting of oscillator

This graph shows that the shear strain is increasing with eccentricity setting of the oscillator. This variation is more pronounced for 20cm dia pile when compared to a 50cm dia pile. This may be attributed to the fact that for a small diameter pile a small change in force level creates a larger change in the strain

5.4 Influence of effect of L/D ratio for different eccentricity setting of oscillator:

The effect of L/D ratio on Damping ratio, Stiffness, Resonant frequency and shear strain for all the eccentricity setting of oscillator can be compared by a plotting curves for all eccentricity setting of oscillator in a single curve. These curves are given below:

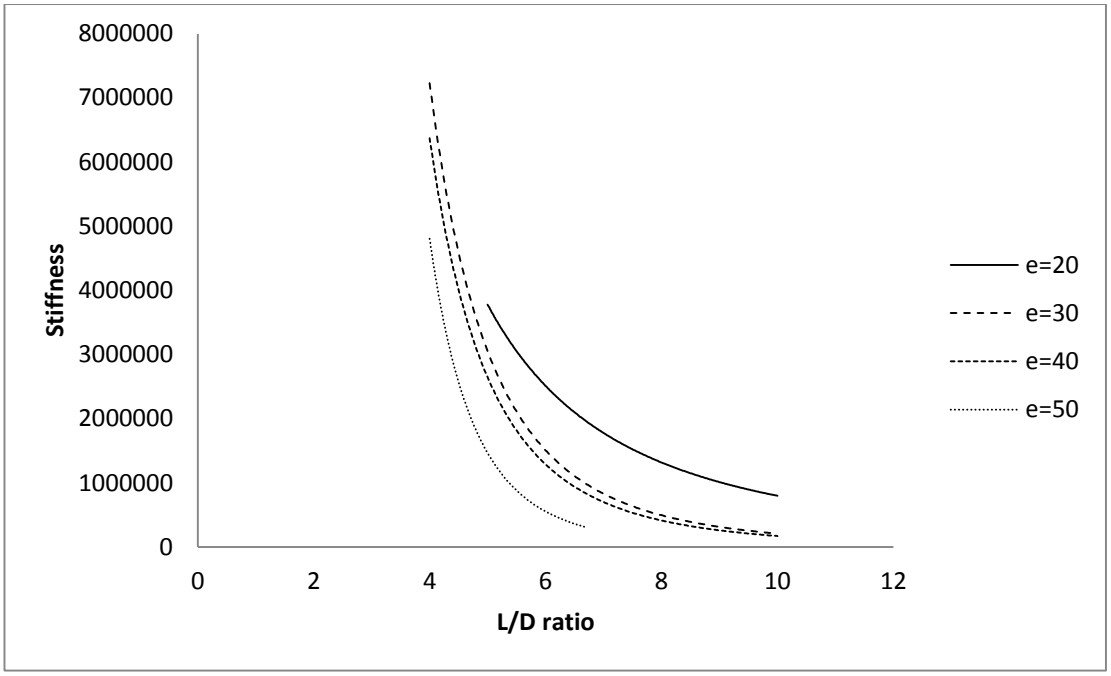

Figure 5-31 Variation of Stiffness with L/D ratio

This curve shows that stiffness is decreasing with L/D ratio. This trend is steeper for larger eccentricity value and with an increase in the force level stiffness is reducing

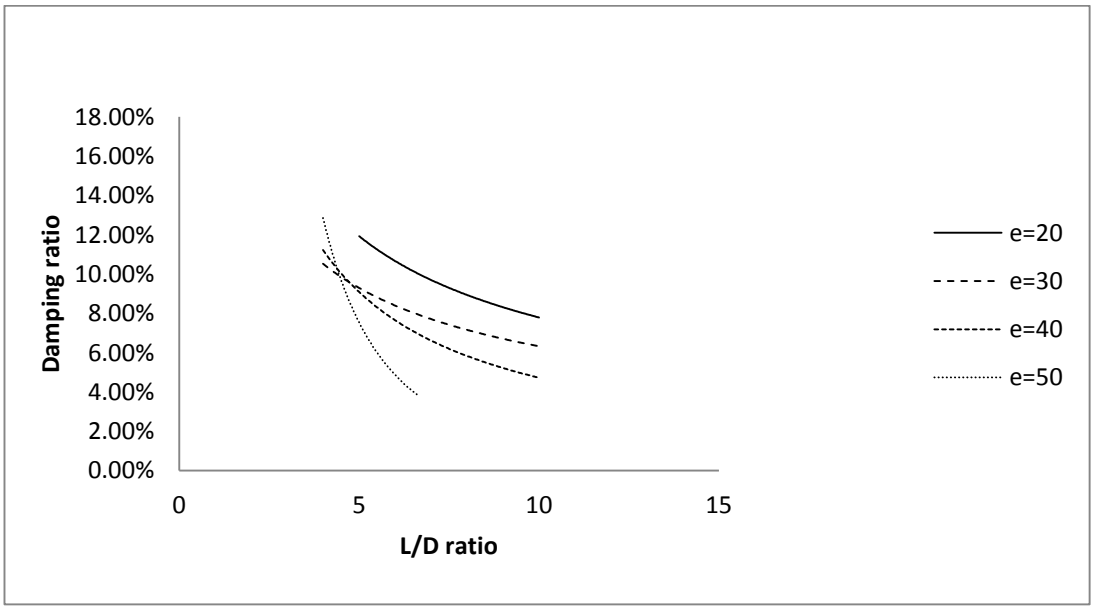

Figure 5-32 Variation of Damping ratio with L/D ratio

This graph shows that the damping ratio is decreasing with L/D ratio. This may be attributed to greater separation between the soil and pile. However at L/D = 4, the

strain is comparatively lower and the soil pile separation is insignificant. Hence damping was observed to increase.

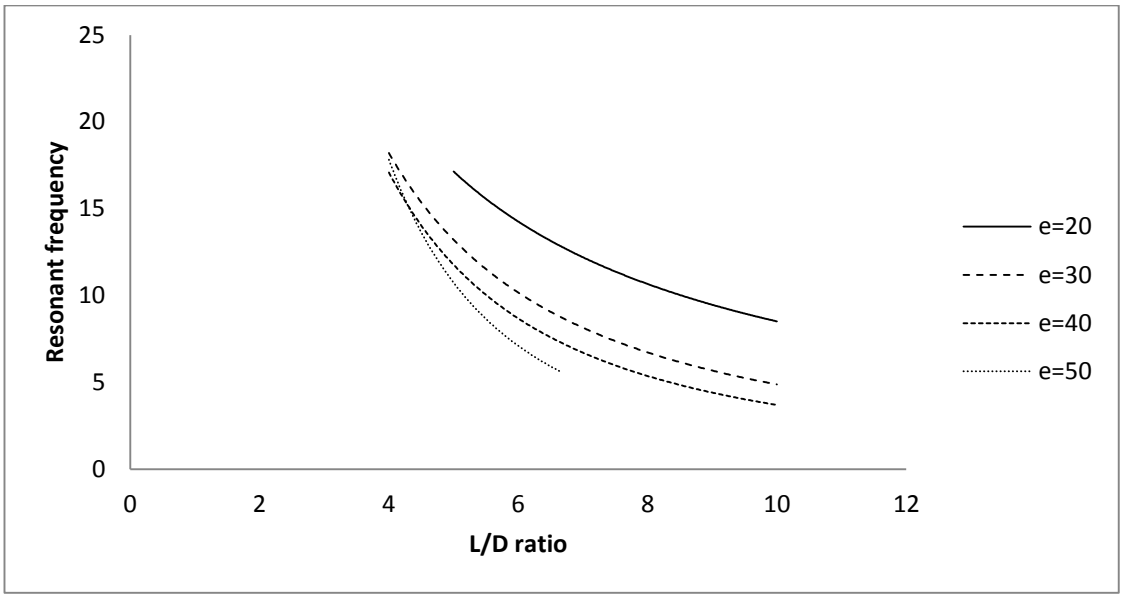

Figure 5-33 Variation of Resonant frequency with L/D ratio

This graph shows that the resonant frequency is decreasing with an increase in L/D ratio, this is expected as stiffness decreases with L/D.

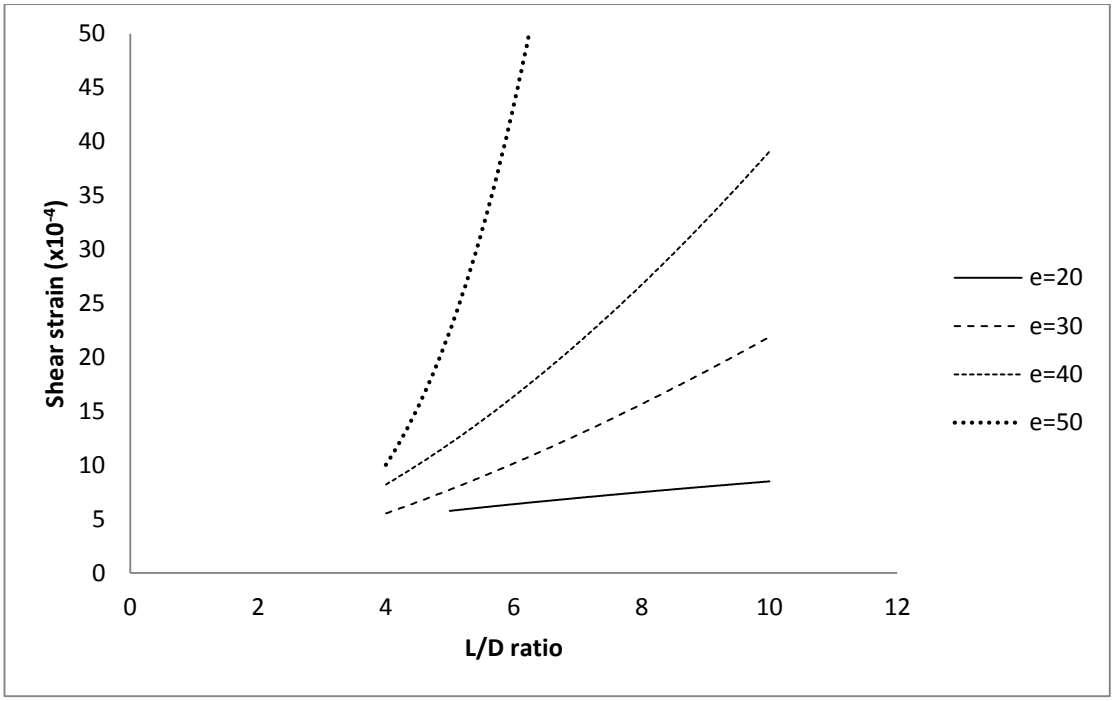

Figure 5-34 Variation of Shear strain with L/D ratio

This graph shows that the shear strain is increasing with L/D ratio. The change is steeper for higher eccentricity settings of oscillator, this may be attributed to higher strain leads at higher force level.

6 Conclusion

Effect of strain :

1) For a single short pile

Stiffness, Damping and Resonant frequency decreases with increase in force level i.e. eccentricity setting of oscillator

Strain level increases with increase in force level i.e. eccentricity setting of oscillator

2) Comparative study for short pile of different diameters.

Stiffness decreases with an increase in force level i.e. eccentricity setting of the oscillator. The decrease in stiffness is more for larger pile diameter. This is because the strain is decreases with an increase diameter of pile

Damping ratio decreases with an increase in the eccentricity setting of the oscillator. This may be attributed to soil-pile separation, but in the case of 50cm diameter pile the damping ratio is found to increase probably because the strain is comparatively less and the soil pile separation is also much smaller.

Resonant frequency decreases with eccentricity setting of the oscillator. This is due to the fact that stiffness decreases with eccentricity setting of oscillator .i.e. force level

Shear strain increases with eccentricity setting of the oscillator. This variation is more pronounced for 20cm dia pile when compared to a 50cm dia pile. This may be attributed to the fact that for a small diameter pile a small change in force level creates a larger change in the strain

Effect of L/D ratio:

1) For single eccentricity setting of the oscillator:

Stiffness, Damping and Resonant frequency decreases with an increase in the L/D ratio.

Strain level increases with an increase in L/D ratio.

2) Comparative study for different eccentricity settings of the oscillator:

Stiffness decreases with L/D ratio. This trend is steeper for larger eccentricity value and with an increase in the force level stiffness is reducing

Damping ratio decreases with L/D ratio. This may be attributed to greater separation between the soil and pile. However at L/D = 4, the strain is comparatively lower and the soil pile separation is insignificant. Hence damping was observed to increase.

Resonant frequency decreases with an increase in L/D ratio, this is expected as stiffness decreases with L/D.

Shear strain increases with L/D ratio. The change is steeper for higher eccentricity settings of oscillator, this may be attributed to higher strain leads at higher force level.

References

[1] Phanikanth, V. S., Deepankar Choudhury, and G. Rami Reddy. "Response of single pile under lateral loads in cohesionless soils." *Electronic Journal of Geotechnical Engineering* 15.10 (2010): 813-830.

[2] Novak, Milos. "Dynamic stiffness and damping of piles." *Canadian Geotechnical Journal* 11.4 (1974): 574-598.

[3] Peck, Ralph Brazelton, Walter Edmund Hanson, and Thomas Hampton Thornburn. *Foundation engineering*. Vol. 10. New York: Wiley, 1974.

[4] Terzaghi, Karl. "Evalution of conefficients of subgrade reaction." *Geotechnique*5.4 (1955): 297-326

[5] Novak, M., and Sheta, M. (1980).Approximate approach to contact effects of piles,Dynamic Response of Pile Foundations: Analytical Aspects, ASCE, New York, N.Y., 53-79..

[6] Carter, John P., and Fred H. Kulhawy. "Analysis of laterally loaded shafts in rock." *Journal of Geotechnical Engineering* 118.6 (1992): 839-855.

[7] Chae, K. S., K. Ugai, and A. Wakai. "Lateral resistance of short single piles and pile groups located near slopes." *International Journal of Geomechanics* 4.2 (2004): 93-103.

[8] Uncuoğlu, Erdal, and Mustafa Laman. "Numerical modelling of short pile behaviour subjected to lateral load." *European Journal of Environmental and Civil Engineering* 16.2 (2012): 204-235.

[9] Deepika, Y., S. Mukerjee, and S. Saran. "INFLUENCE OF PILE LENGTH ON THE DYNAMIC RESPONSE OF UNDER-REAMED PILES SUBJECTED TO VERTICAL VIBRATION."

[10] Chowdhury, Indrajit, and Shambhu P. Dasgupta. "Estimation of lateral load capacity of short piles under earthquake force." *5th international conference in recent advances in earthquake engineering and soil dynamics, San Diego, USA*. 2010.

[11] Guo, Wei Dong. "Laterally loaded rigid piles in cohesionless soil." *Canadian Geotechnical Journal* 45.5 (2008): 676-697.

[12] Mohamedzein, Yahia EA, Muzamil G. Mohamed, and Ahmed M. El Sharief. "Finite element analysis of short piles in expansive soils." *Computers and Geotechnics* 24.3 (1999): 231-243.

[13] Abbas, Jasim M., Qassun S. Mohammed Shafiqu, and Mohd R. Taha. "Effect of shape and slenderness ratio on the behaviour of laterally loaded piles." *The first regional conference of Eng. Sc. NUCE spatial issue*. Vol. 11. No. 200.

[14] Pacheco, Gustavo, Luis E. Suárez, and Miguel Pando. "Dynamic lateral response of single piles considering soil inertia contributions." *The 14th World Conference on Earthquake Engineering*. Vol. 11. 2008.

[15] Juirnarongrit, Teerawut, and Scott A. Ashford. "Effect of Pile Diameter on the Modulus of Sub-grade Reaction." *SSRP* (2001): 22.

[16] Kramer, Steven L. *Geotechnical earthquake engineering*. Pearson Education India, 1996.

[17] Sonal Singh “Response of free standing under-reamed pile subjected to horizontal dynamic loads” Dept.of Earthquake Engg.IIT, Roorkee, India 2014

]

Appendix for Results

A) Pile diameter = 20cm

For e=20°

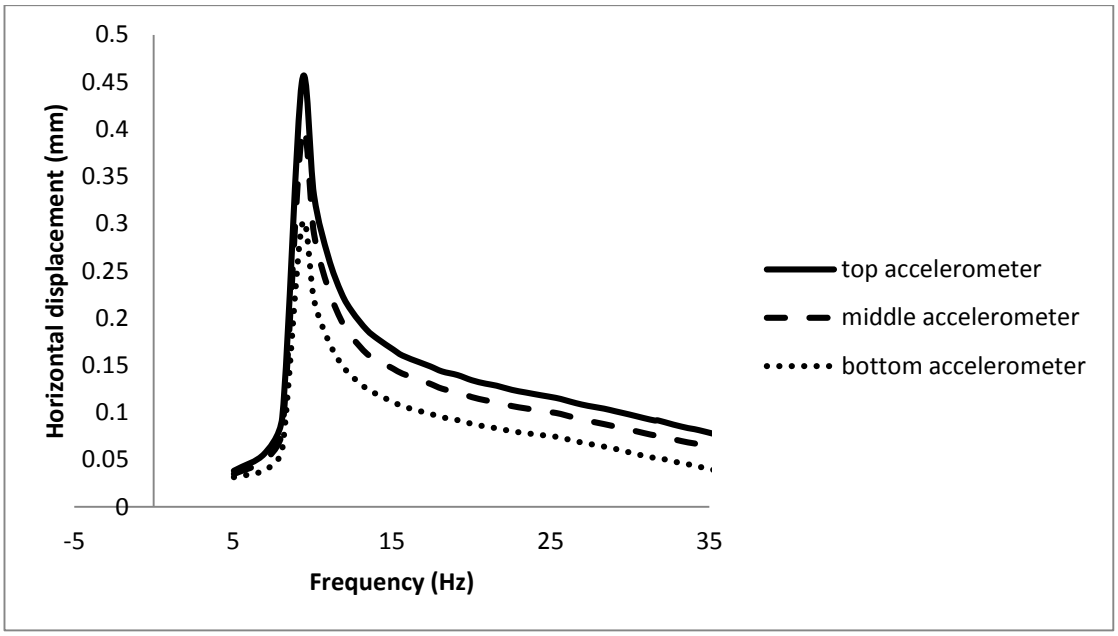

Figure-1: Horizontal displacement v/s Frequency curve for pile diameter 20cm at e= 20°

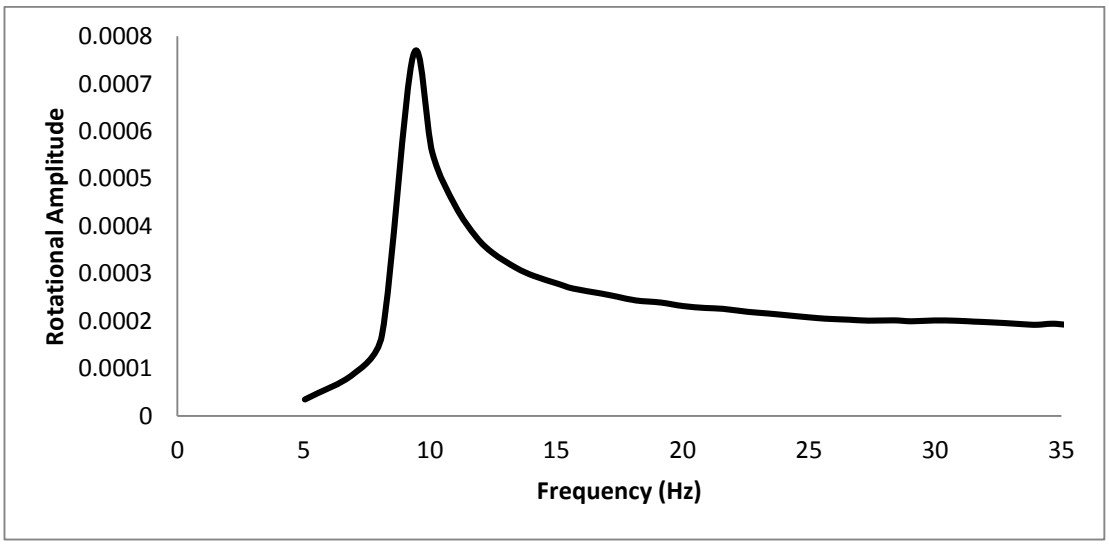

Figure-2: Rotational Amplitude v/s Frequency curve for pile diameter 20cm at e= 20°

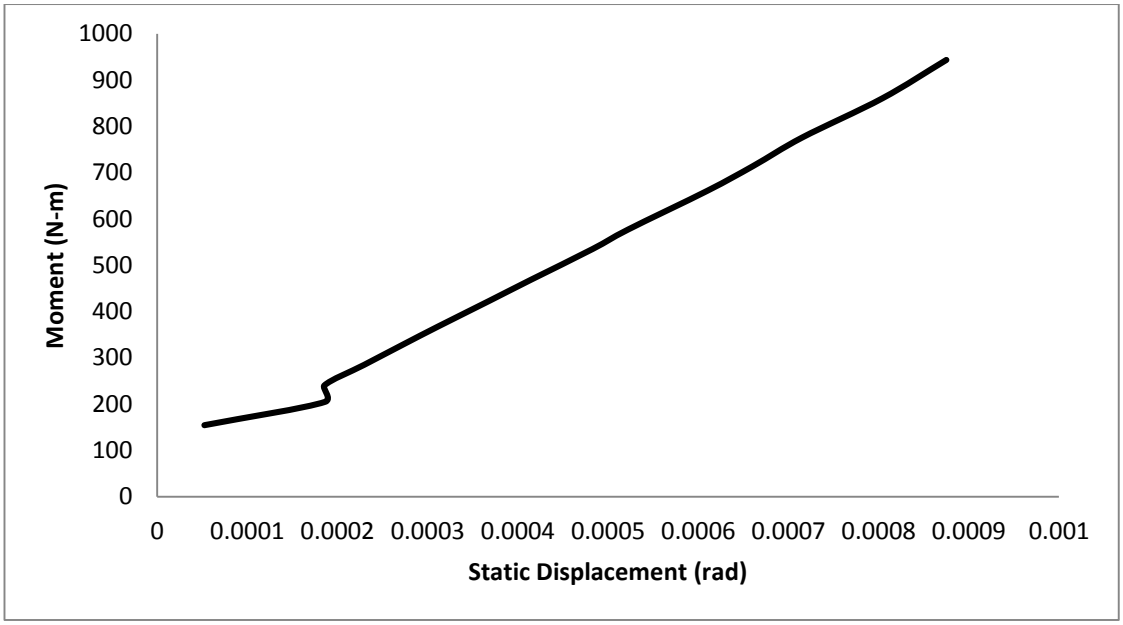

Figure-3: Moment v/s Static Displacement curve for pile diameter 20cm at e= 20°

For e=30°

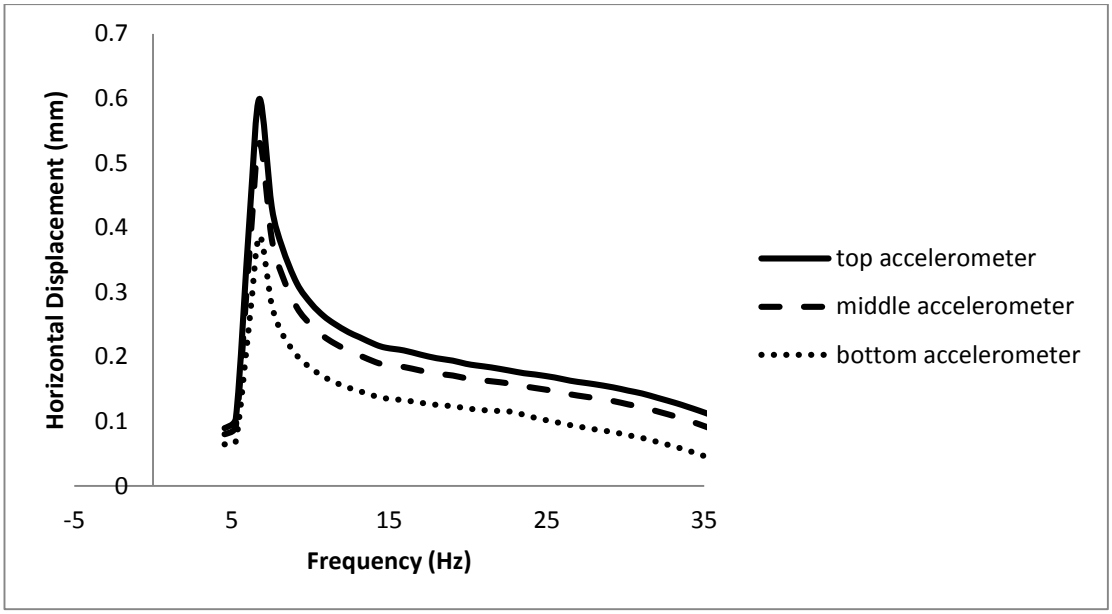

Figure-4: Horizontal displacement v/s Frequency curve for pile diameter 20cm at e= 30°

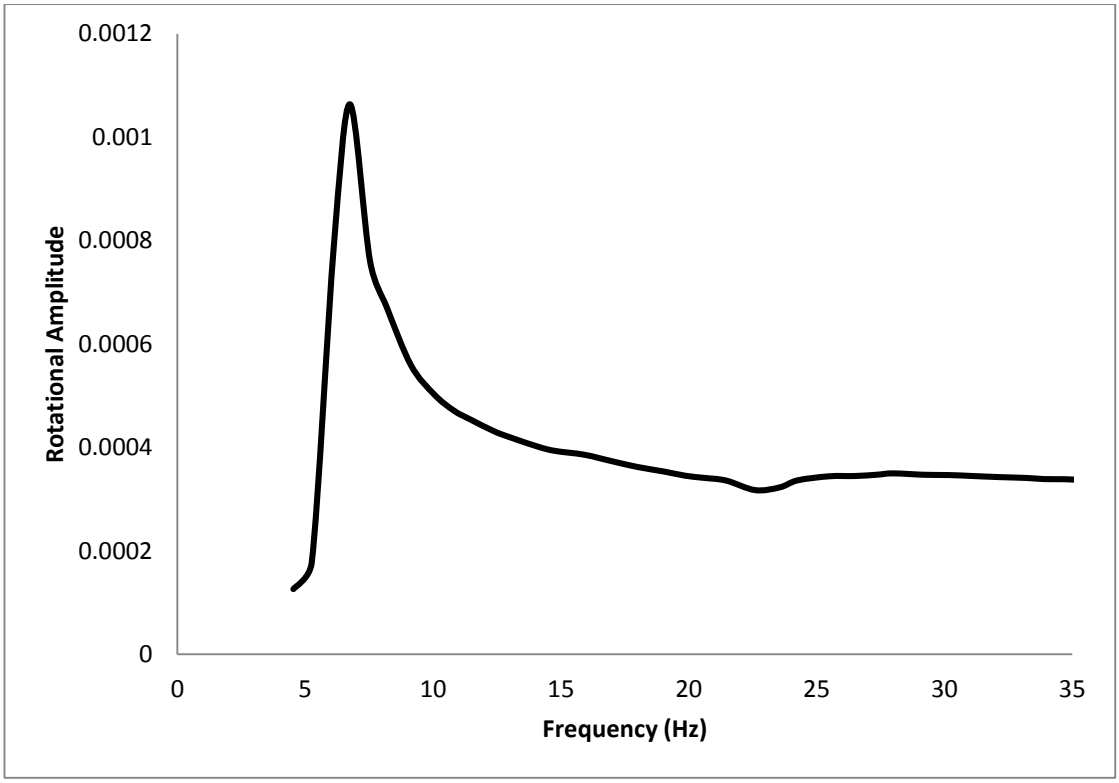

Figure-5: Rotational Amplitude v/s Frequency curve for pile diameter 20cm at e= 30°

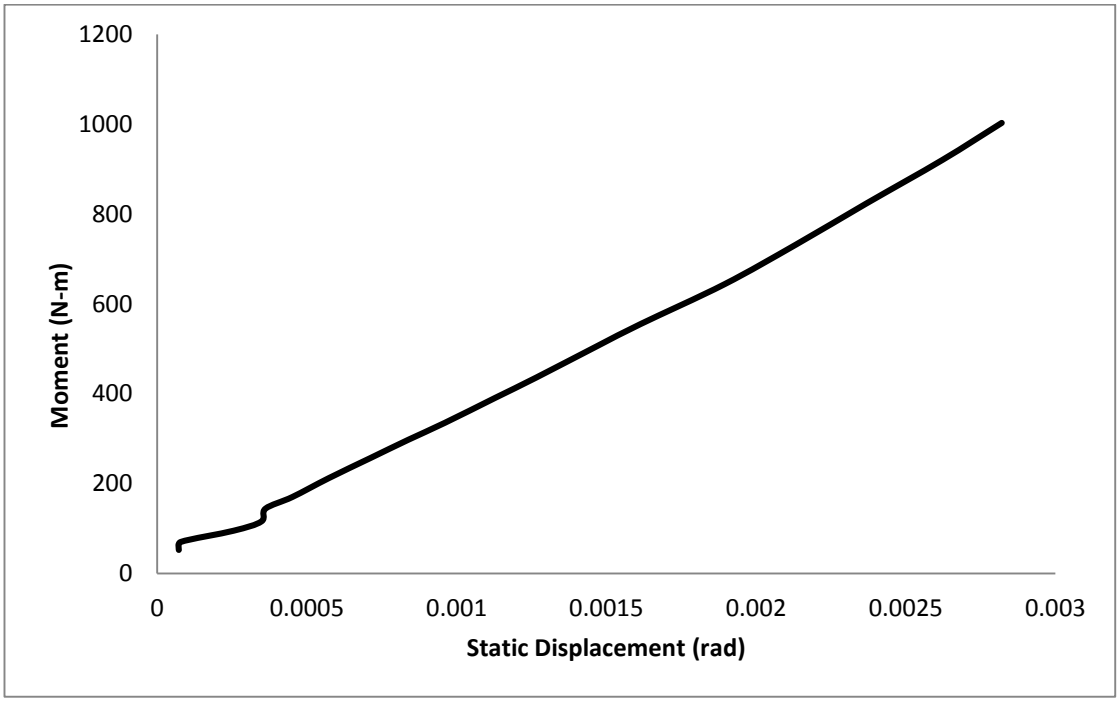

Figure-6: Moment v/s Static Displacement curve for pile diameter 20cm at e= 30°

For e=40°

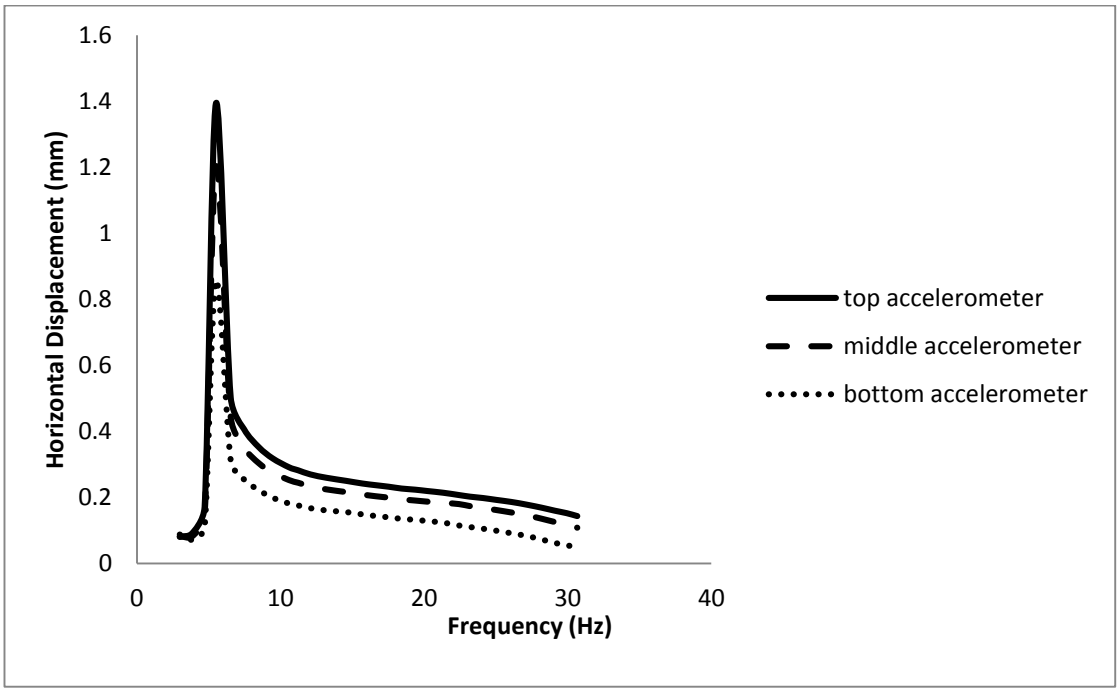

Figure-7: Horizontal displacement v/s Frequency curve for pile diameter 20cm at e= 40°

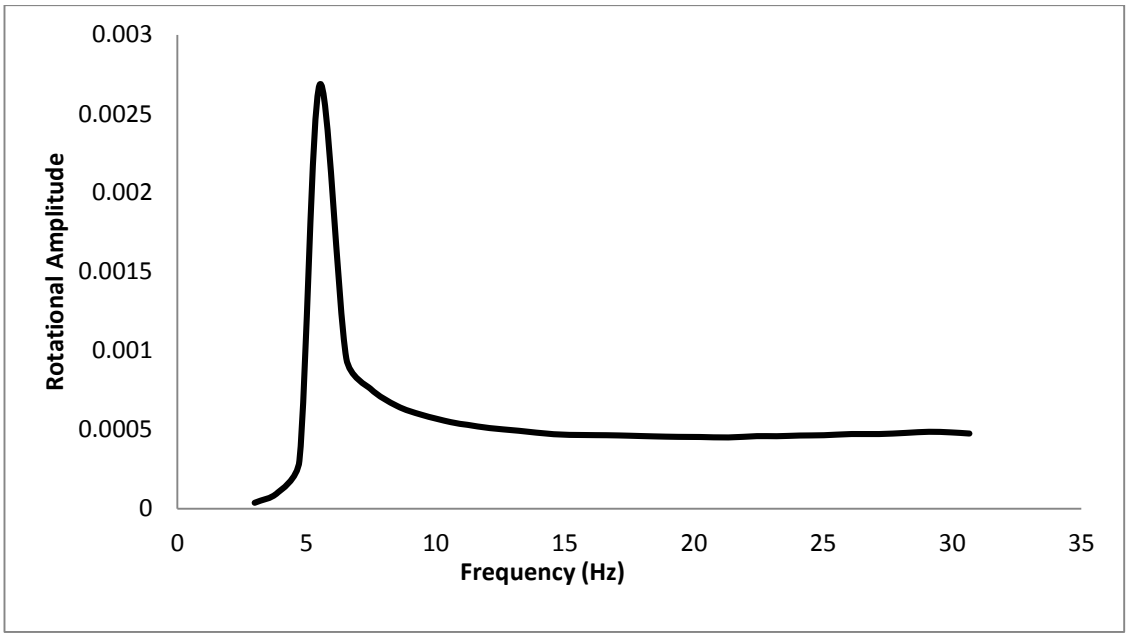

Figure-8: Rotational Amplitude v/s Frequency curve for pile diameter 20cm at e= 40°

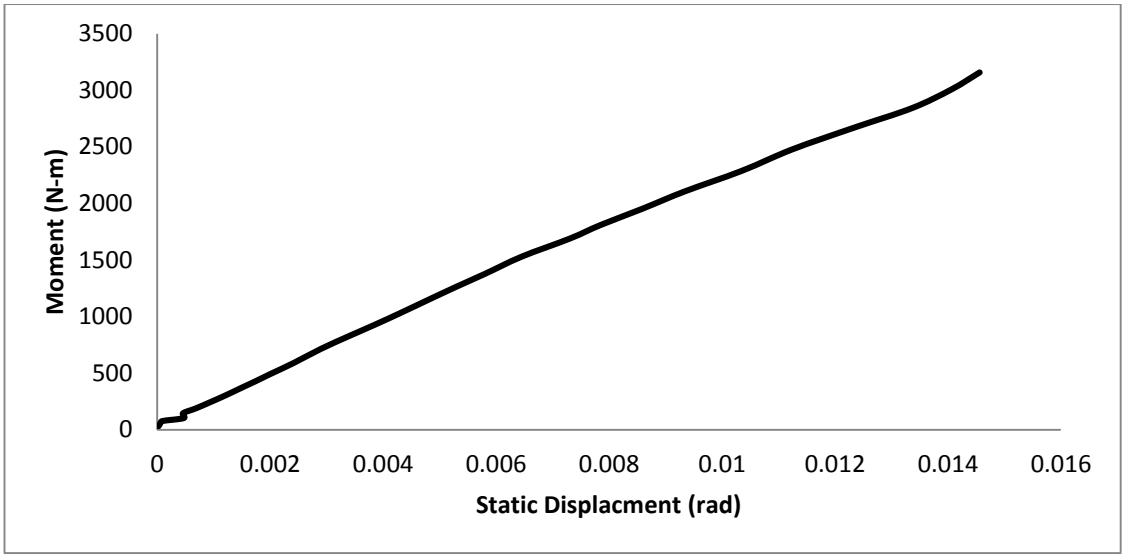

Figure-9: Moment v/s Static Displacement curve for pile diameter 20cm at e= 40°

B) Pile diameter = 30cm

For e=20°

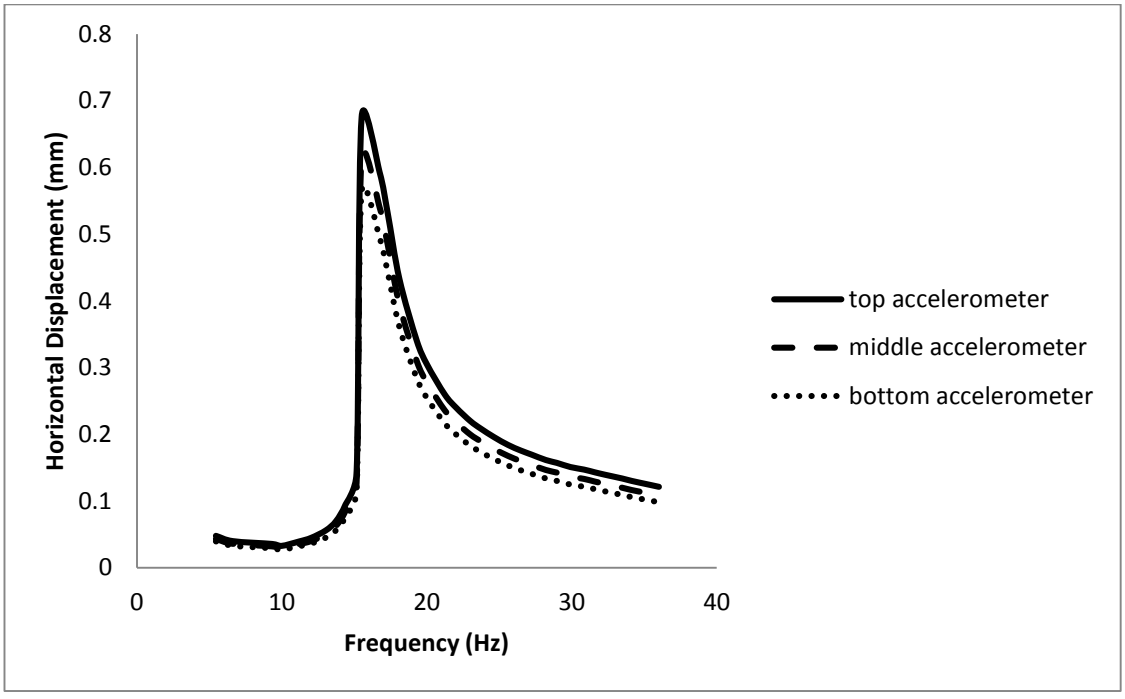

Figure-10: Horizontal displacement v/s Frequency curve for pile diameter 30cm at e= 20°

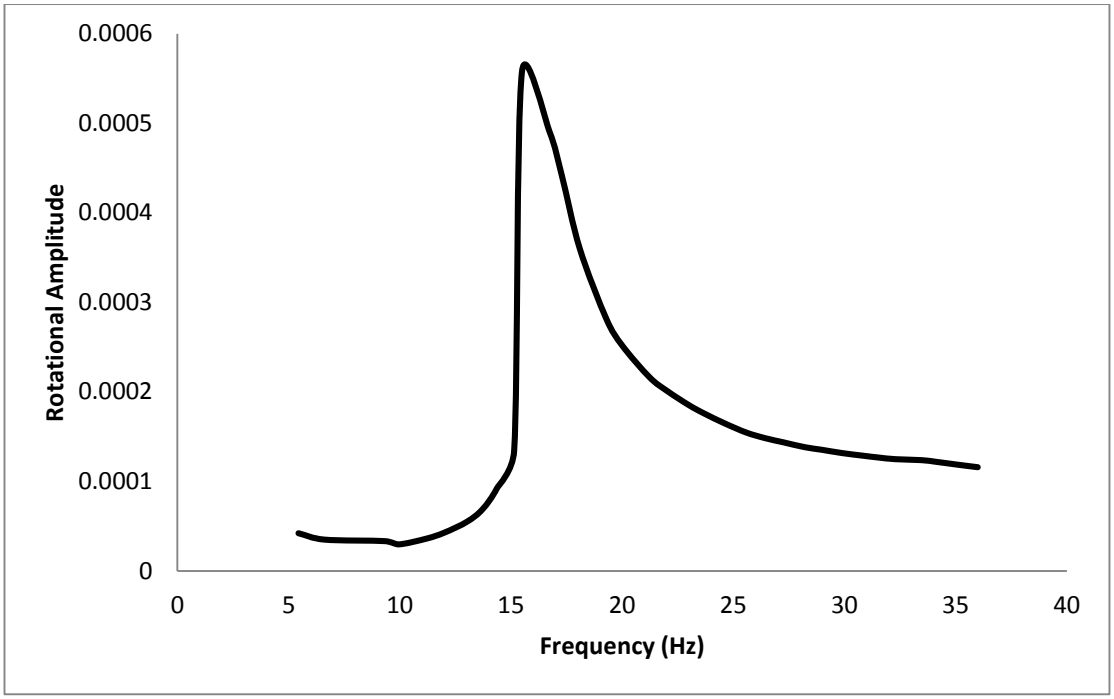

Figure-11: Rotational Amplitude v/s Frequency curve for pile diameter 30cm at e= 20°

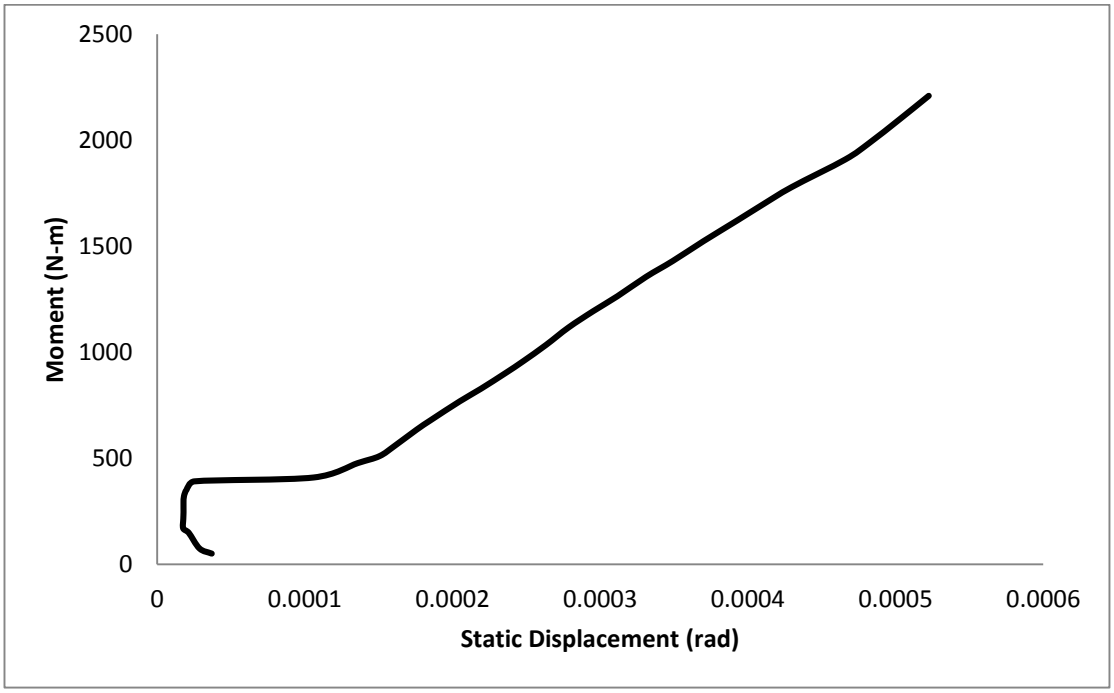

Figure-12: Moment v/s Static Displacement curve for pile diameter 30cm at e= 20°

For e=40°

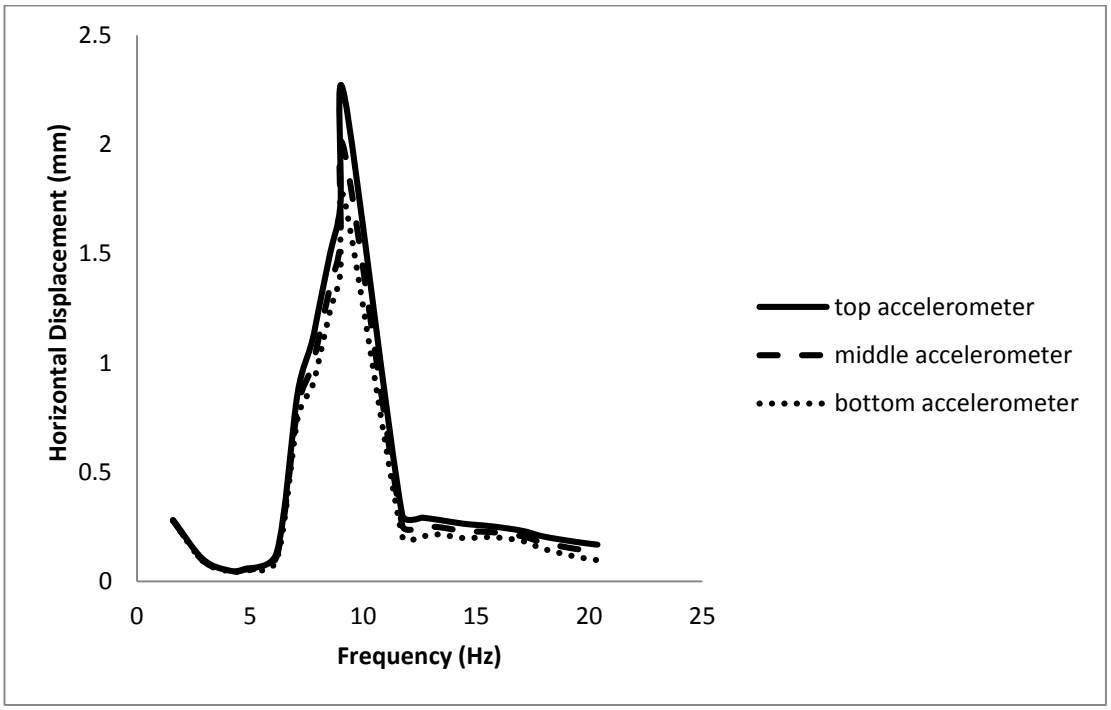

Figure-13: Horizontal displacement v/s Frequency curve for pile diameter 30cm at e= 40°

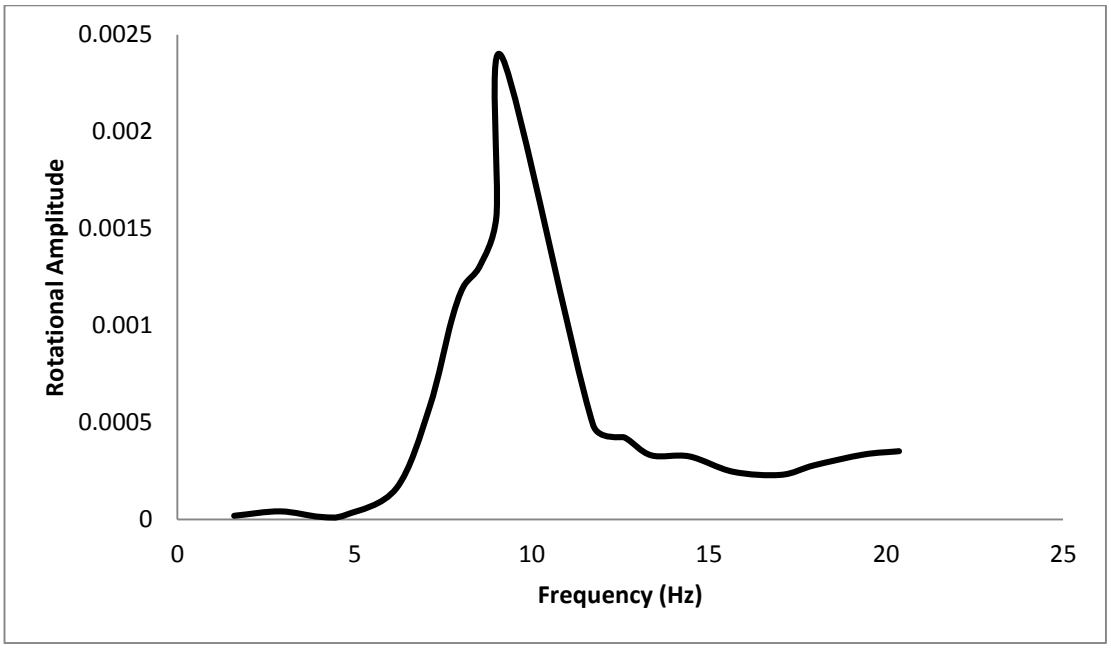

Figure-14: Rotational Amplitude v/s Frequency curve for pile diameter 30cm at e= 40°

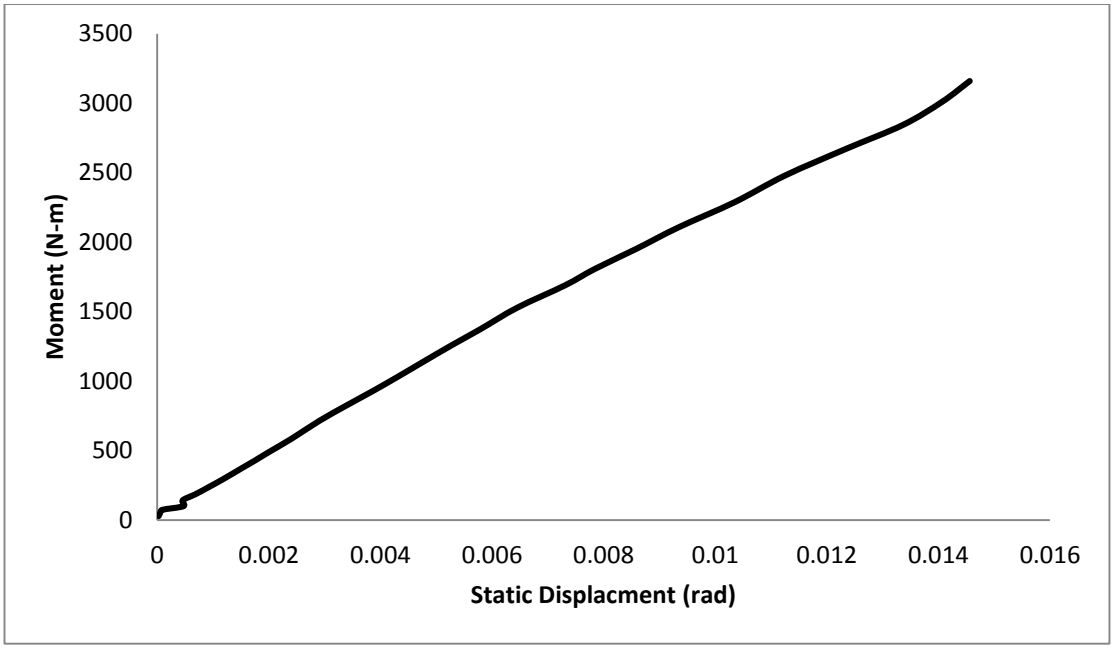

Figure-15: Moment v/s Static Displacement curve for pile diameter 30cm at e= 40°

For e=50°

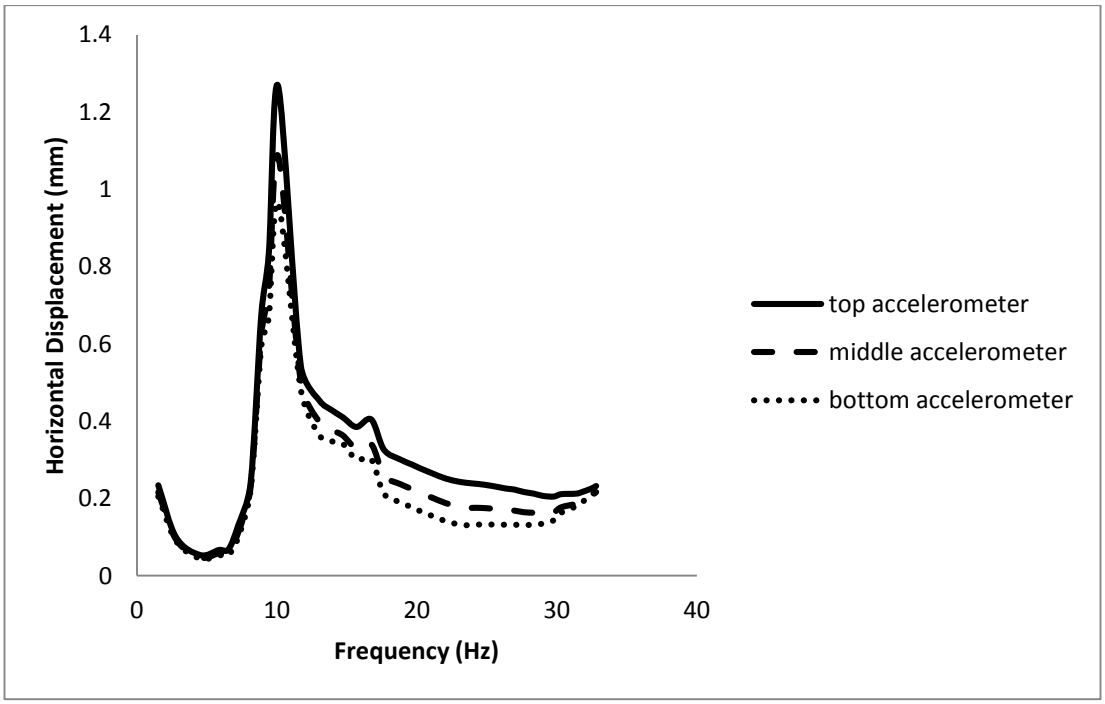

Figure-16: Horizontal displacement v/s Frequency curve for pile diameter 30cm at e= 50°

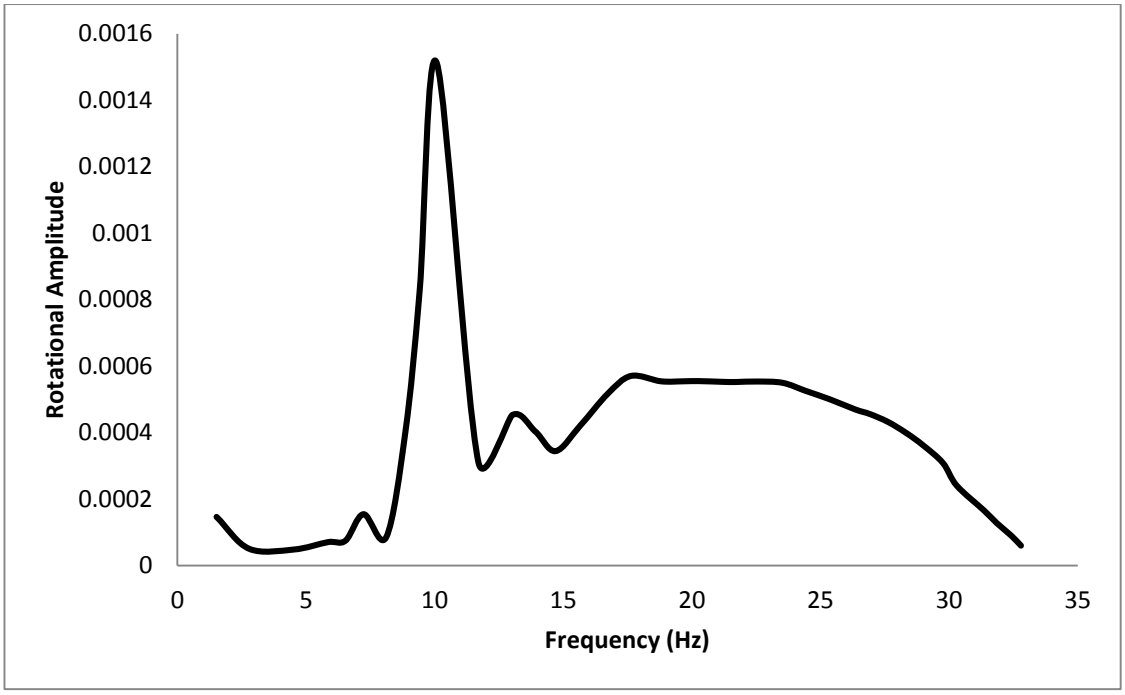

Figure-17: Rotational Amplitude v/s Frequency curve for pile diameter 30cm at e= 50°

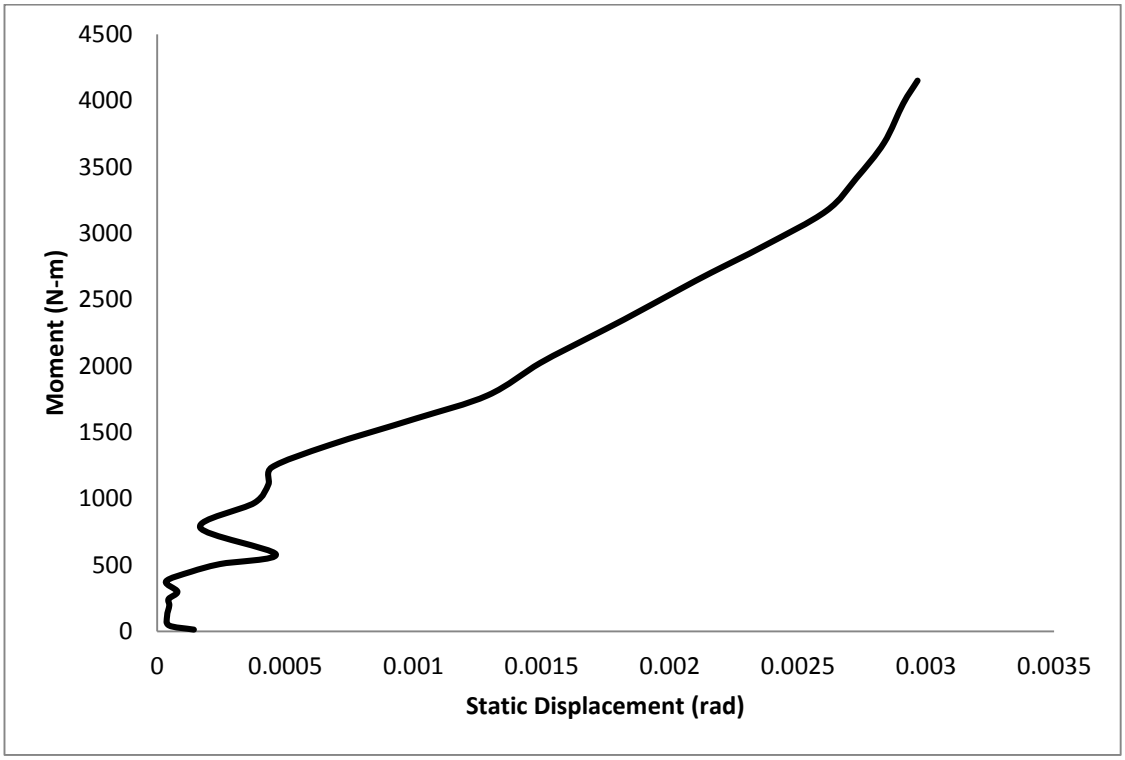

Figure-18: Moment v/s Static Displacement curve for pile diameter 30cm at e= 50°

C) Pile diameter = 40cm

For e=20°

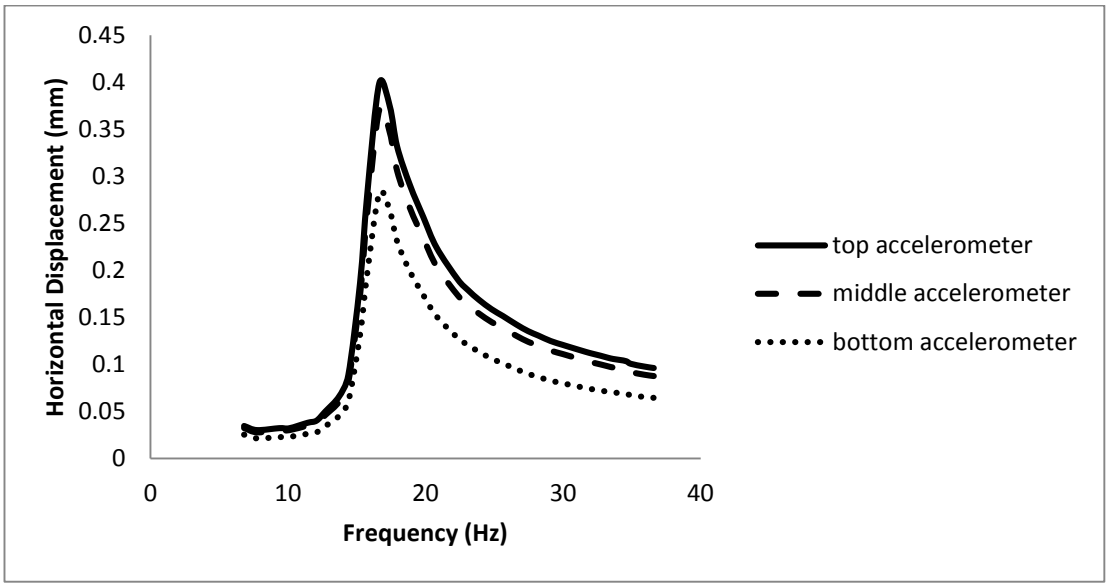

Figure-19: Horizontal displacement v/s Frequency curve for pile diameter 40cm at e= 20°

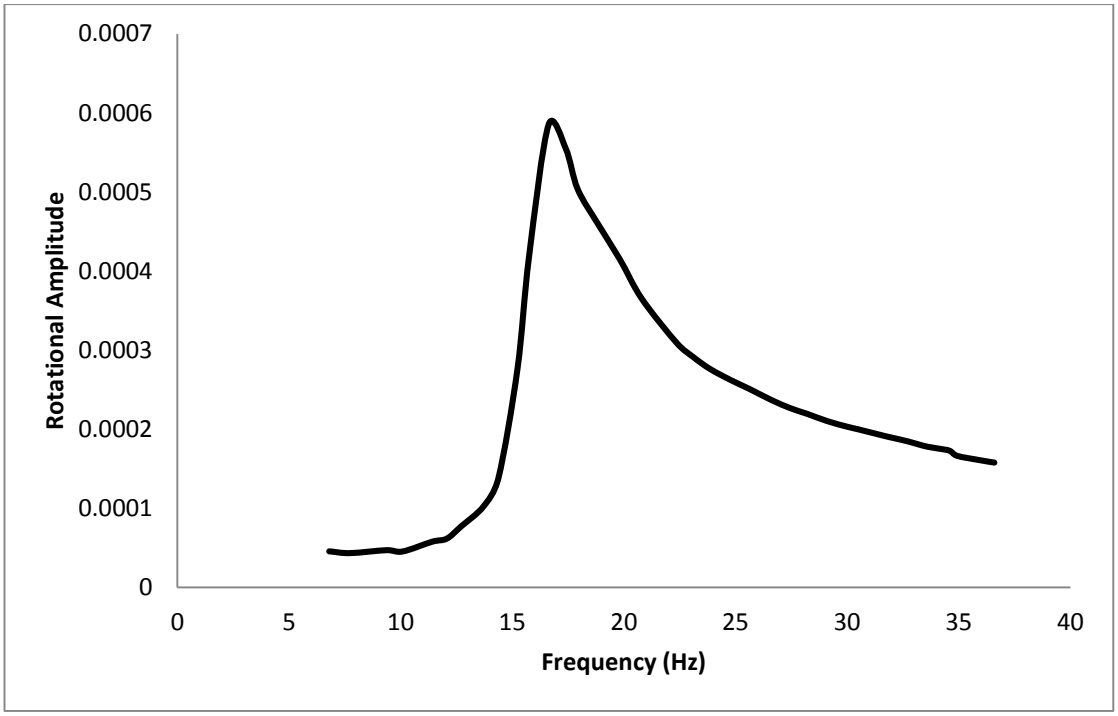

Figure-20: Rotational Amplitude v/s Frequency curve for pile diameter 40cm at e= 20°

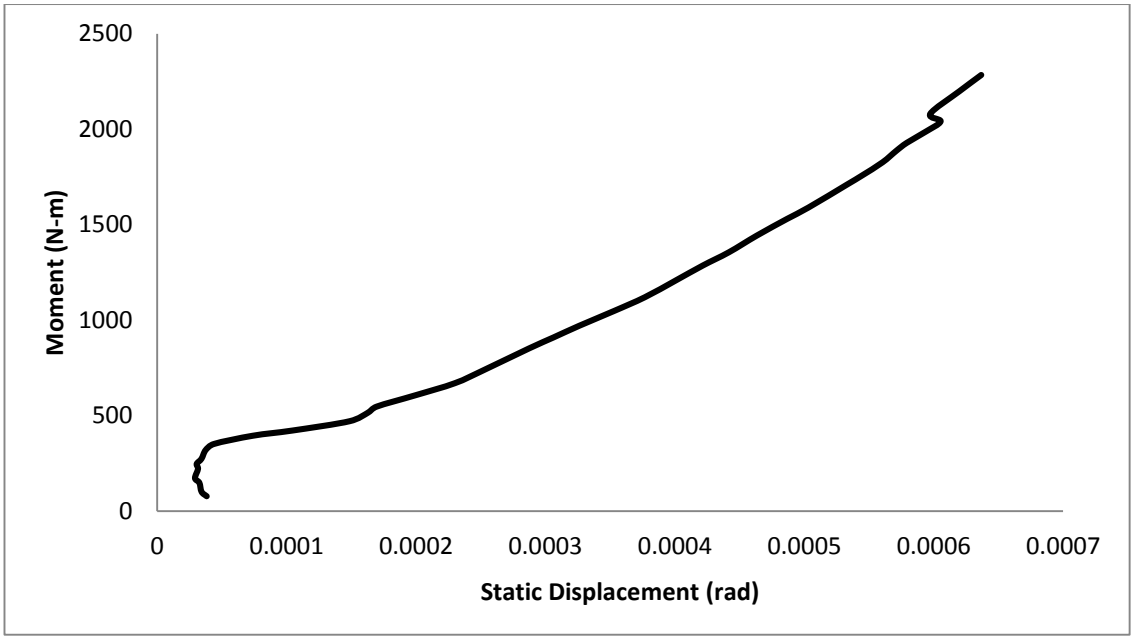

Figure-21: Moment v/s Static Displacement curve for pile diameter 40cm at e= 20°

For e=40°

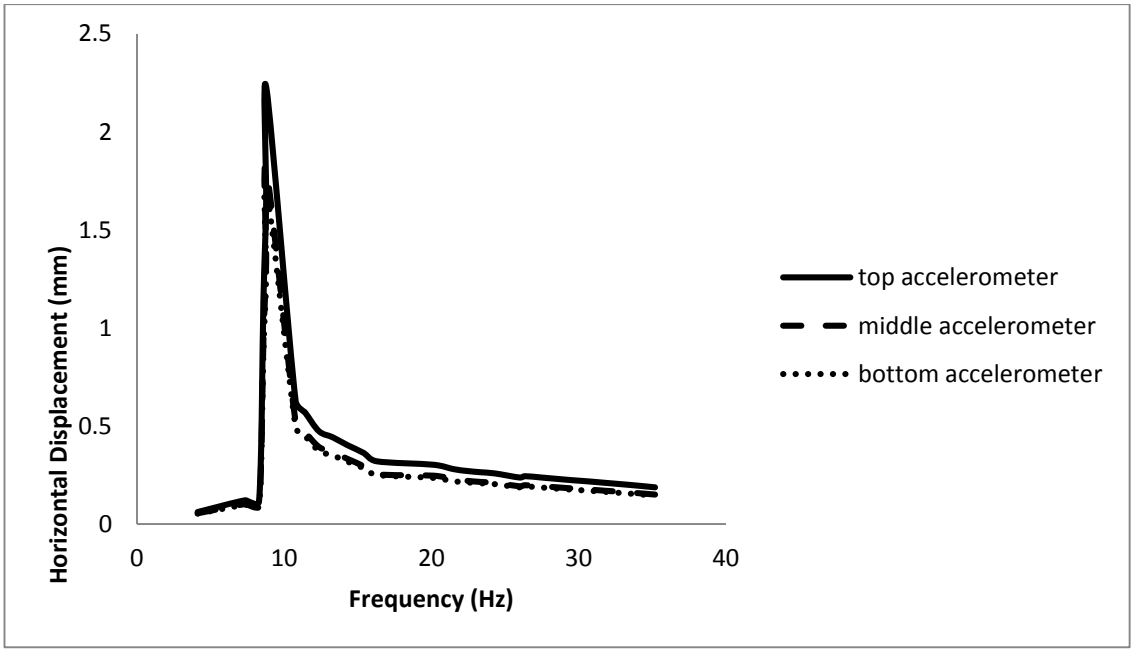

Figure-22: Horizontal displacement v/s Frequency curve for pile diameter 40cm at e= 40°

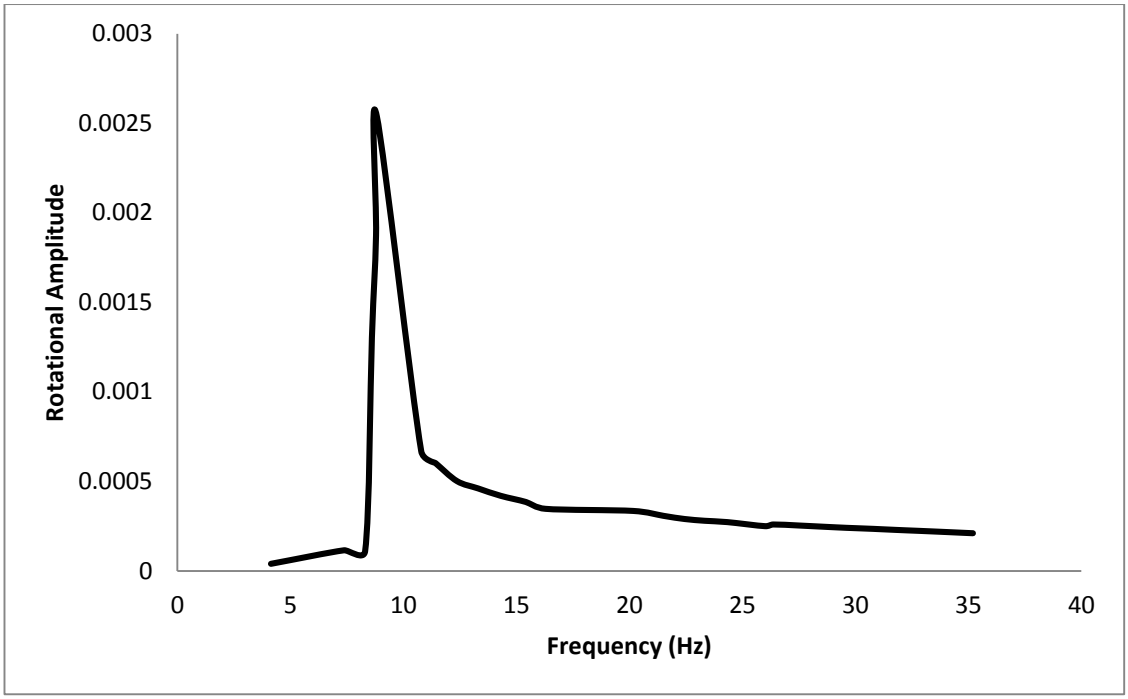

Figure-23: Rotational Amplitude v/s Frequency curve for pile diameter 40cm at e= 40°

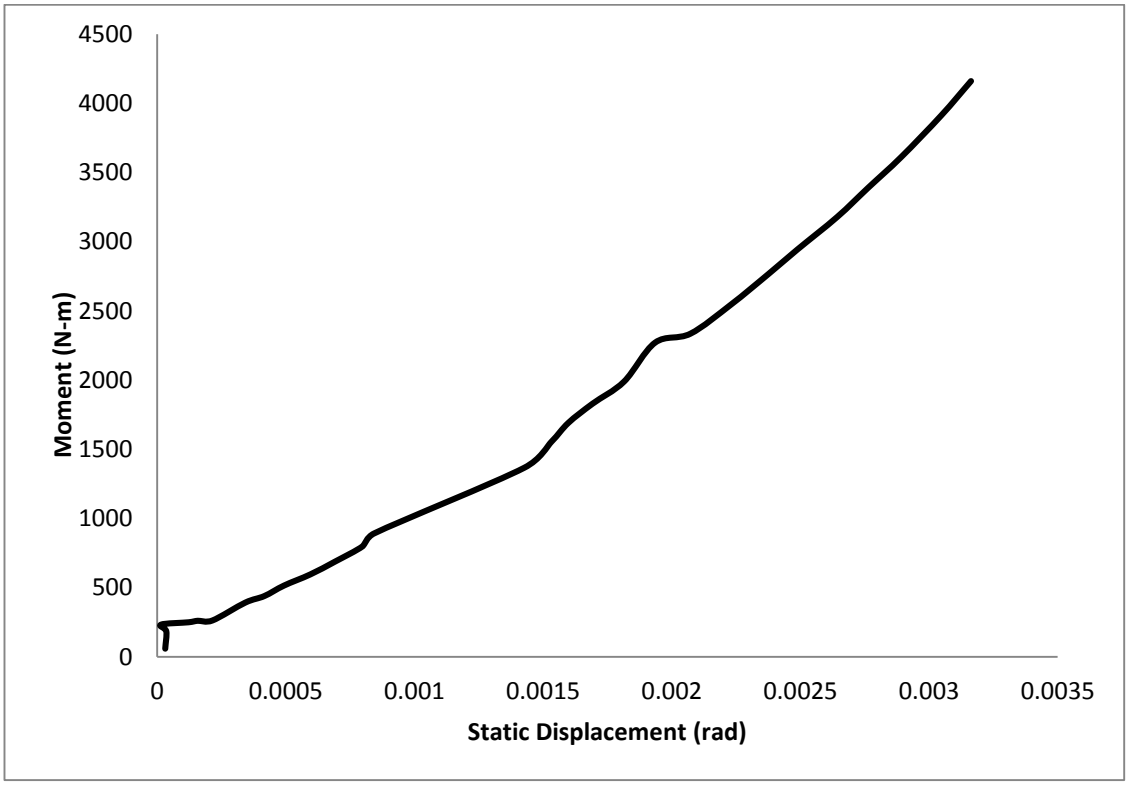

Figure-24: Moment v/s Static Displacement curve for pile diameter 40cm at e= 40°

For e=50°

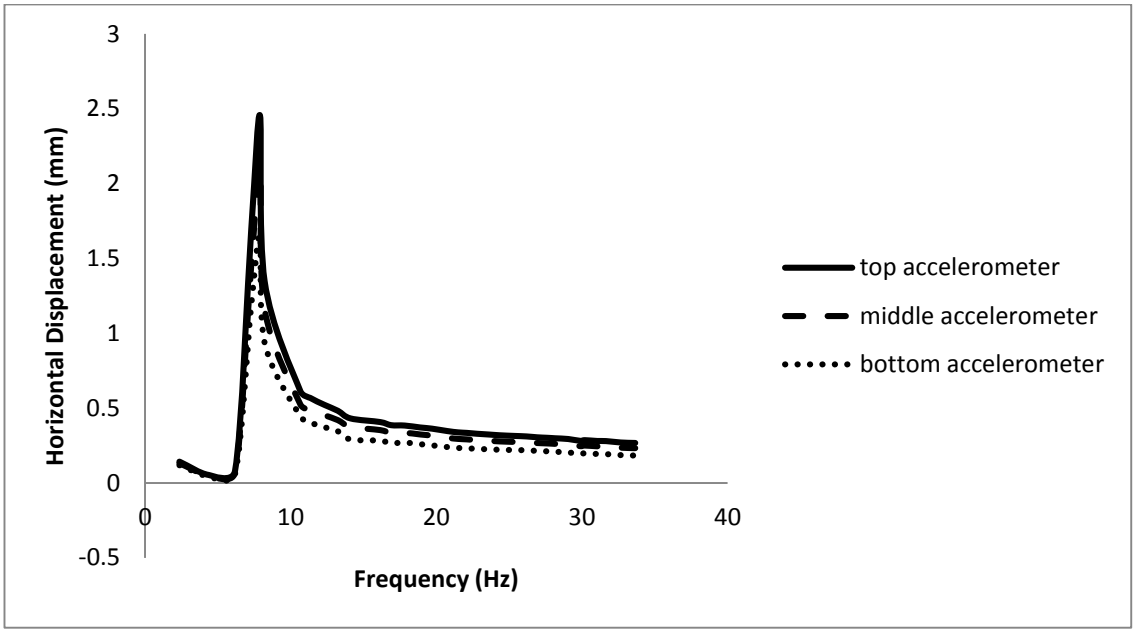

Figure-25: Horizontal displacement v/s Frequency curve for pile diameter 40cm at e= 50°

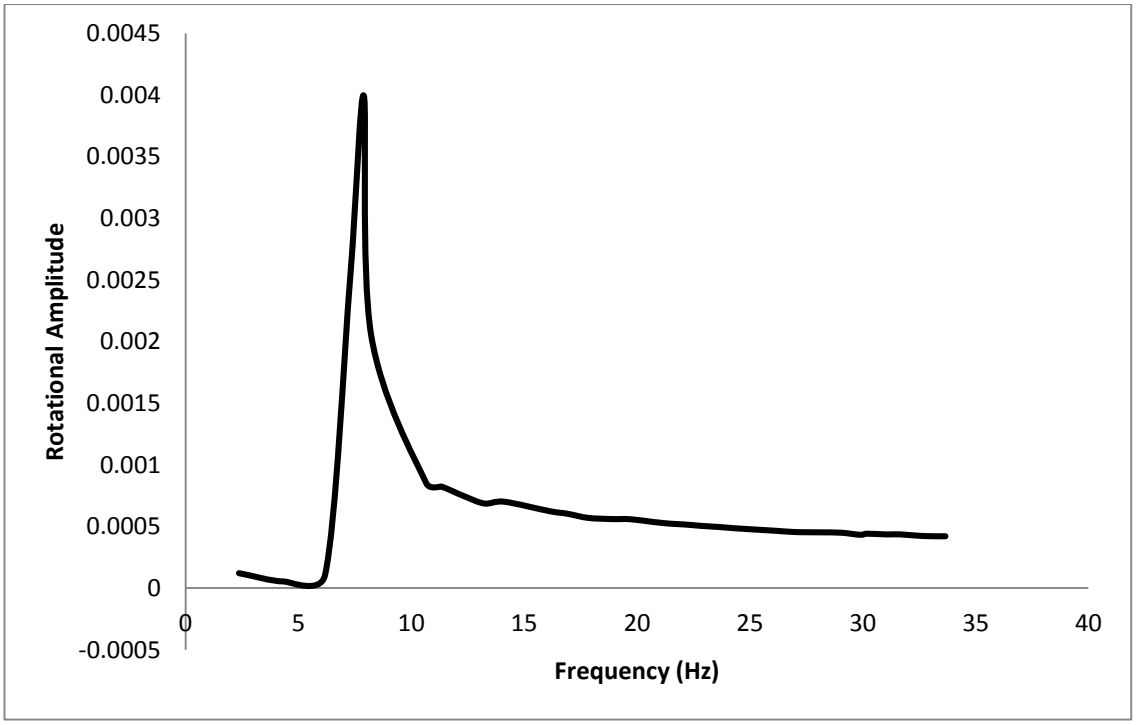

Figure-26: Rotational Amplitude v/s Frequency curve for pile diameter 40cm at e= 50°

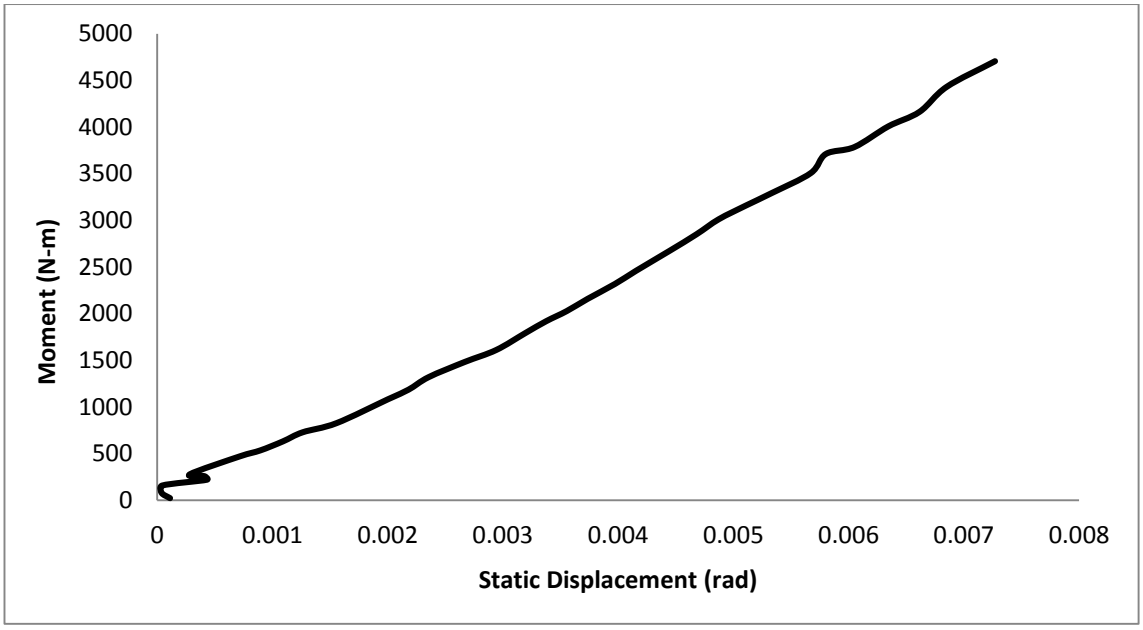

Figure-27: Moment v/s Static Displacement curve for pile diameter 40cm at e= 50°

D) Pile diameter = 50cm

For e=30°

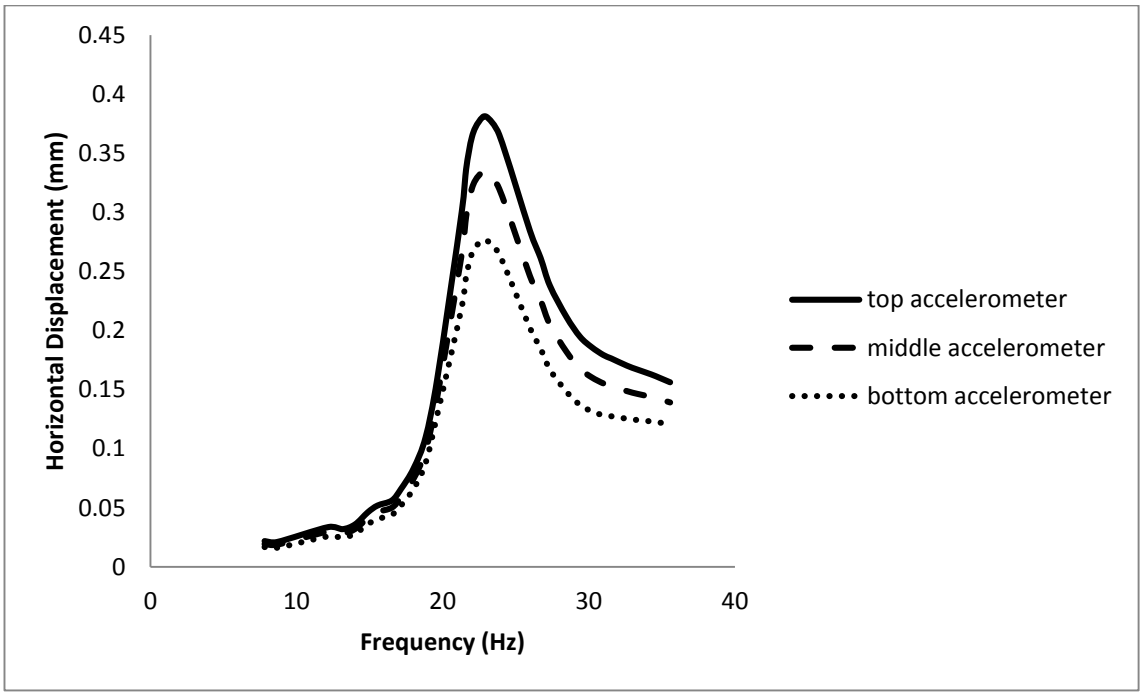

Figure-28: Horizontal displacement v/s Frequency curve for pile diameter 50cm at e= 30°

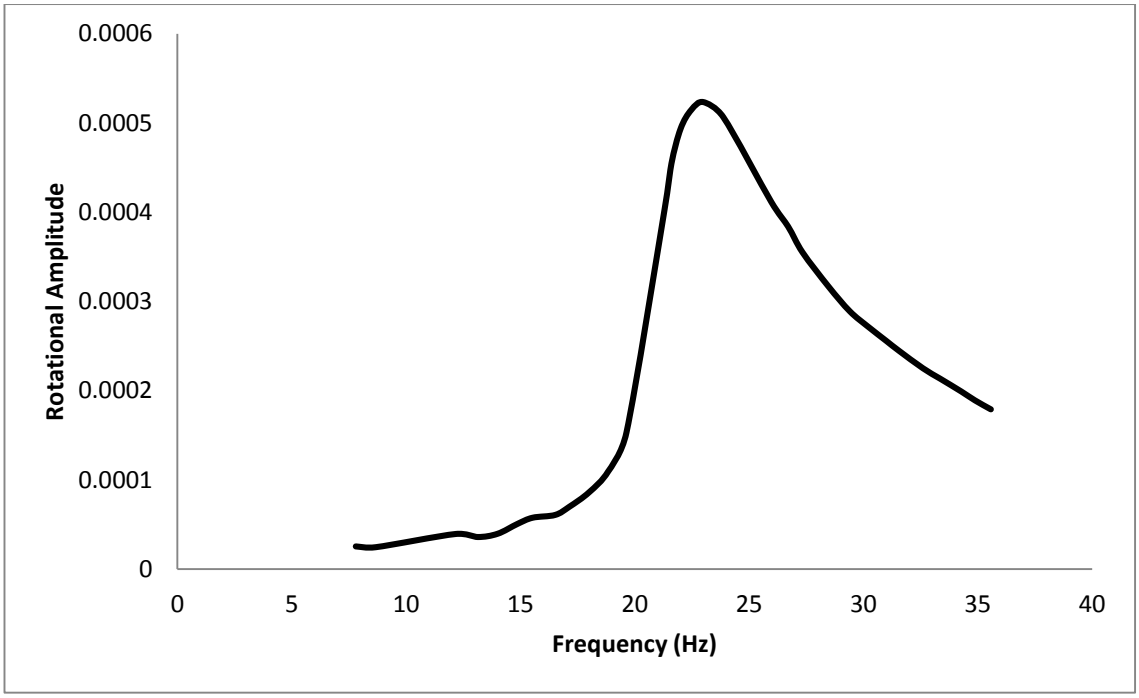

Figure-29: Rotational Amplitude v/s Frequency curve for pile diameter 50cm at e= 30°

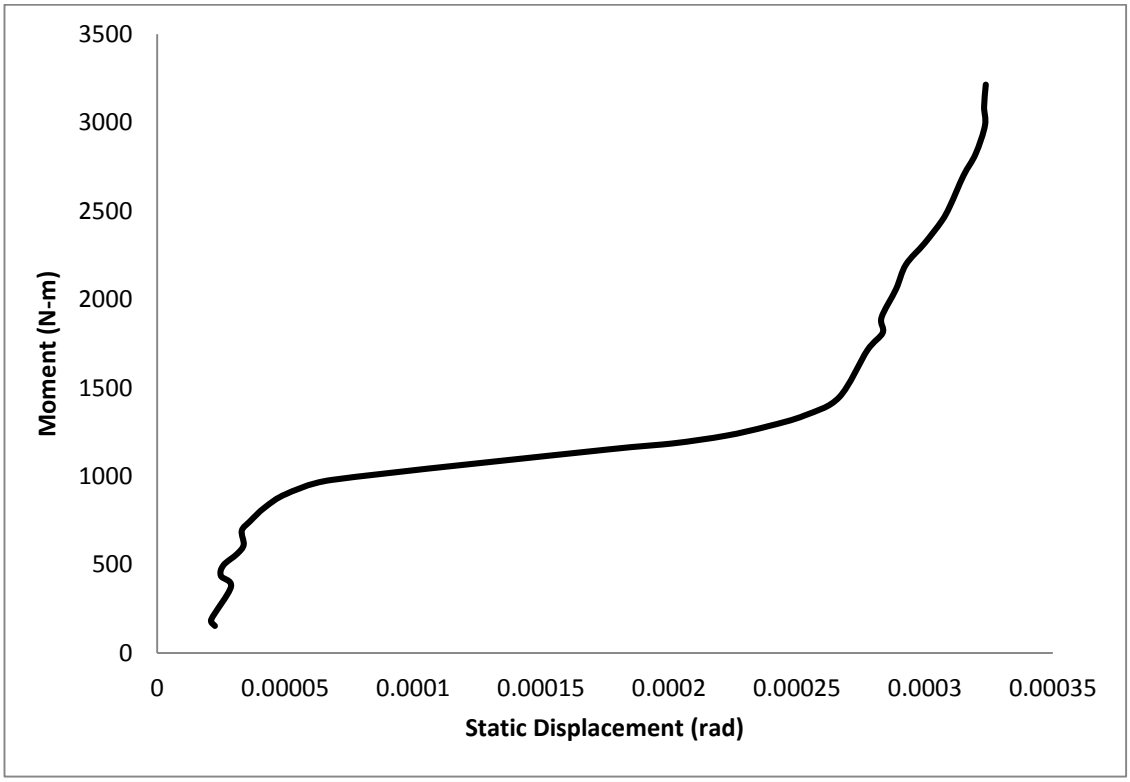

Figure-30: Moment v/s Static Displacement curve for pile diameter 50cm at e= 30°

For e=40°

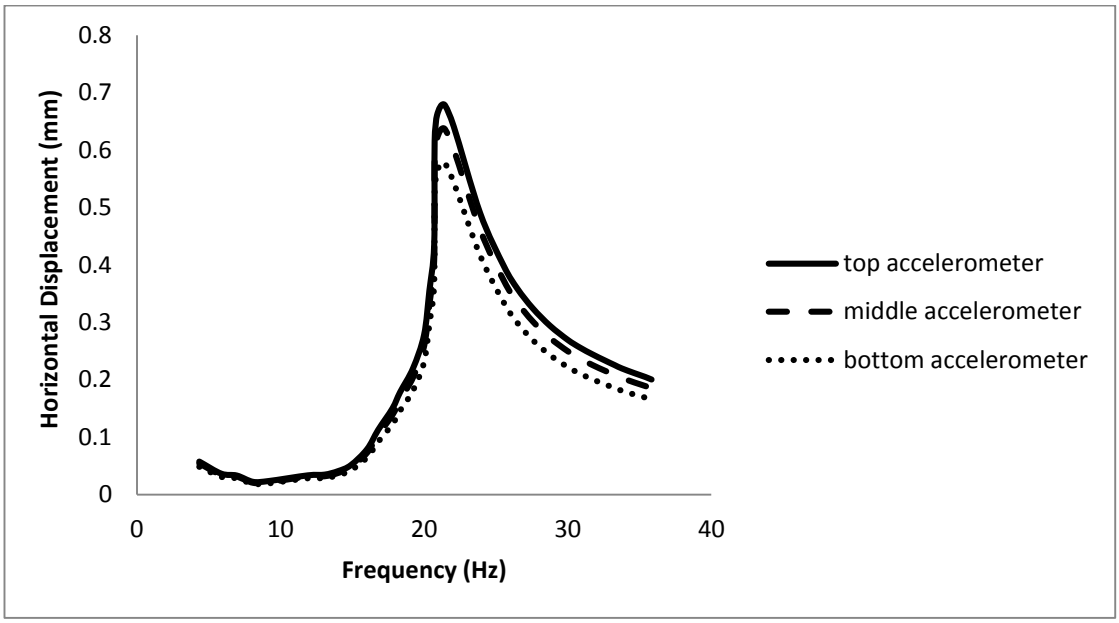

Figure-31: Horizontal displacement v/s Frequency curve for pile diameter 50cm at e= 40°

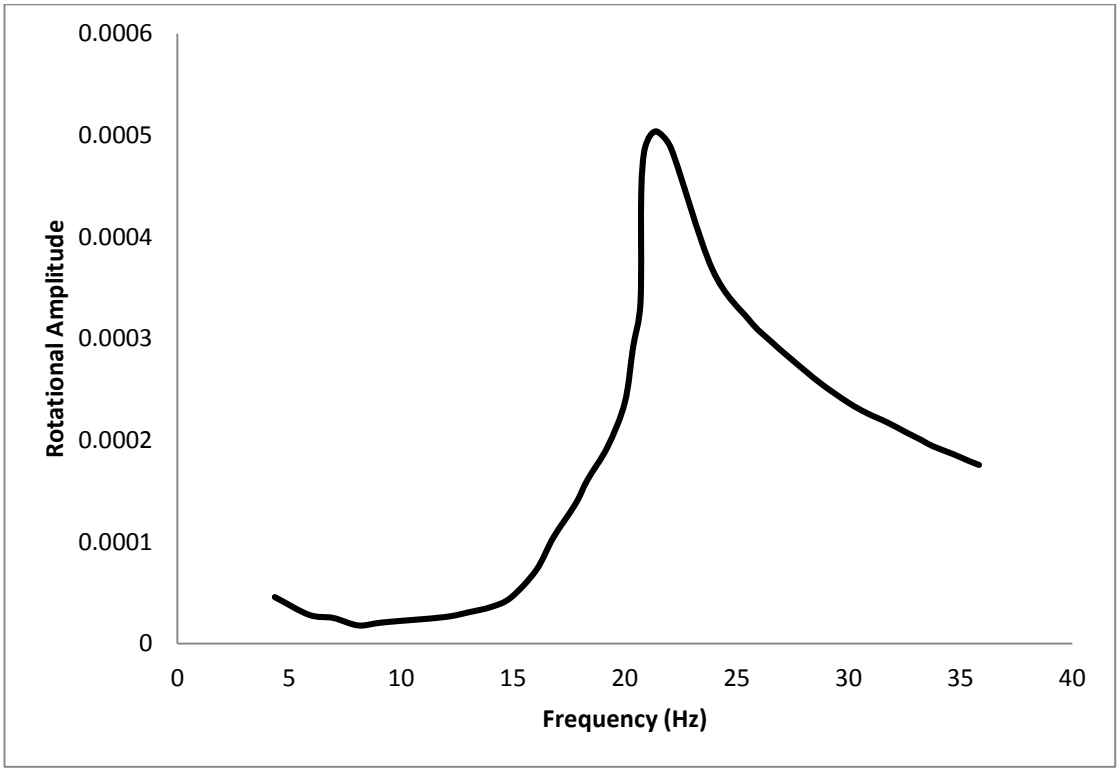

Figure-32: Rotational Amplitude v/s Frequency curve for pile diameter 50cm at e= 40°

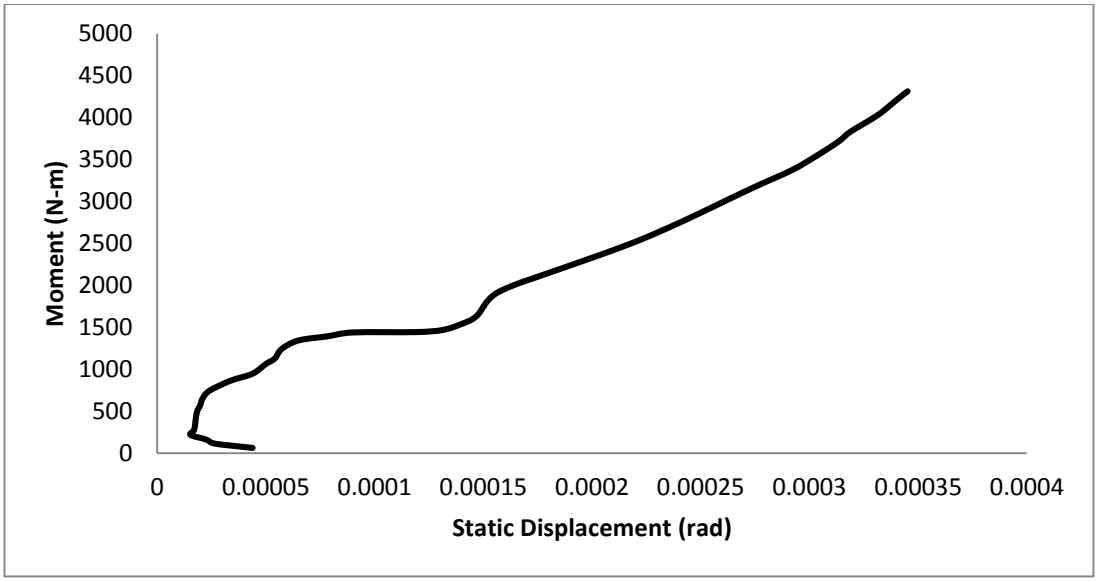

Figure-33:. Moment v/s Static Displacement curve for pile diameter 50cm at e= 40°

For e=50°

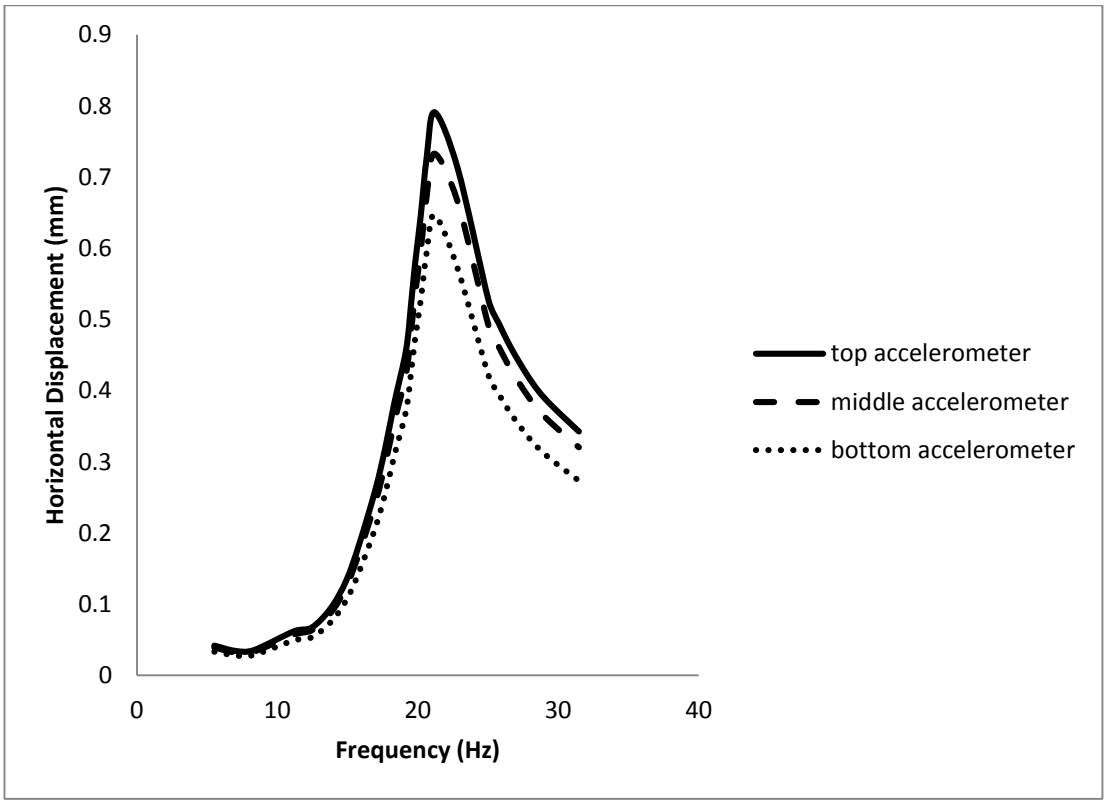

Figure-34: Horizontal displacement v/s Frequency curve for pile diameter 50cm at e= 50°

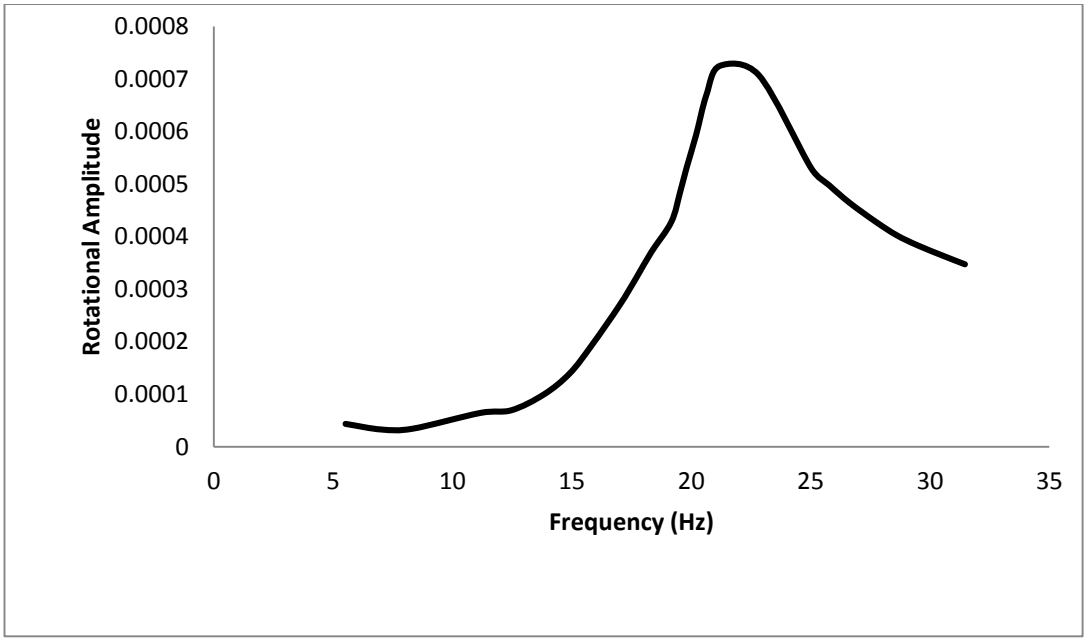

Figure-35: Rotational Amplitude v/s Frequency curve for pile diameter 50cm at e= 50°

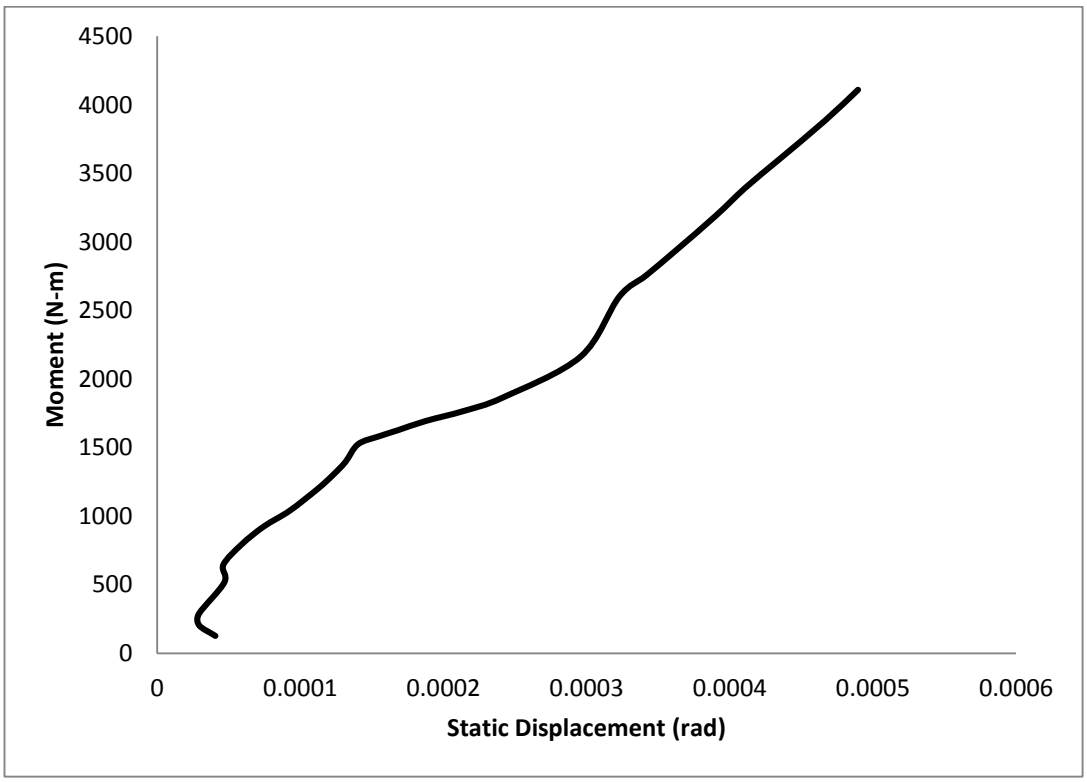

Figure-36: Moment v/s Static Displacement curve for pile diameter 50cm at e= 50°

For e=60°

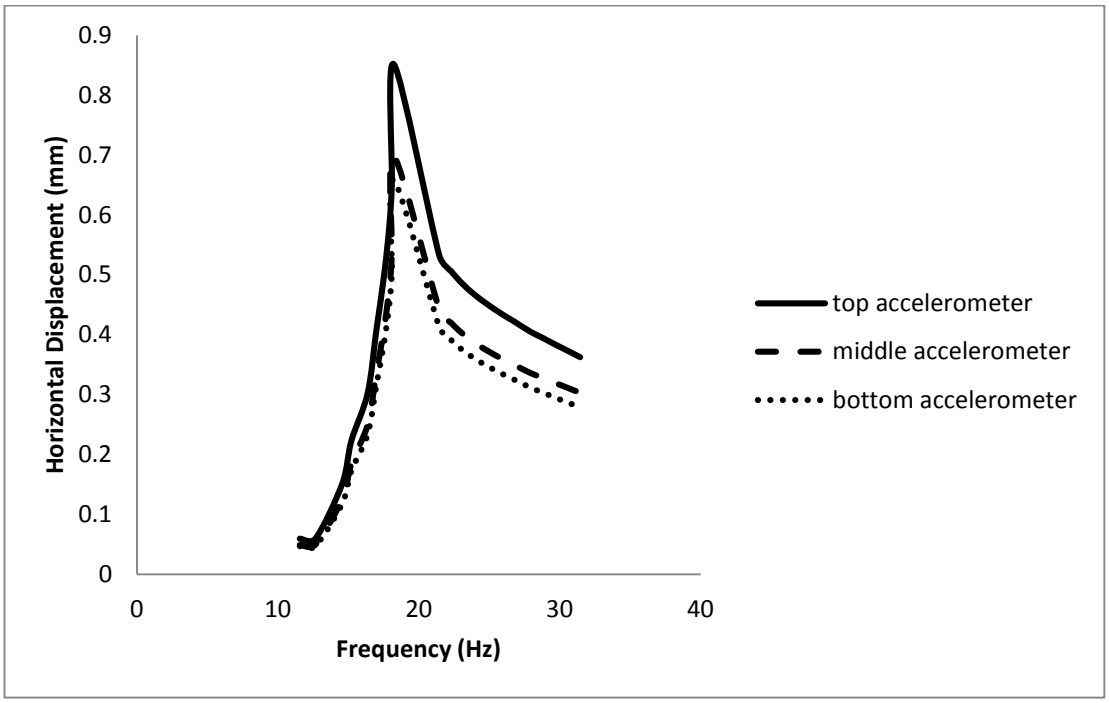

Figure-37: Horizontal displacement v/s Frequency curve for pile diameter 50cm at e= 60°

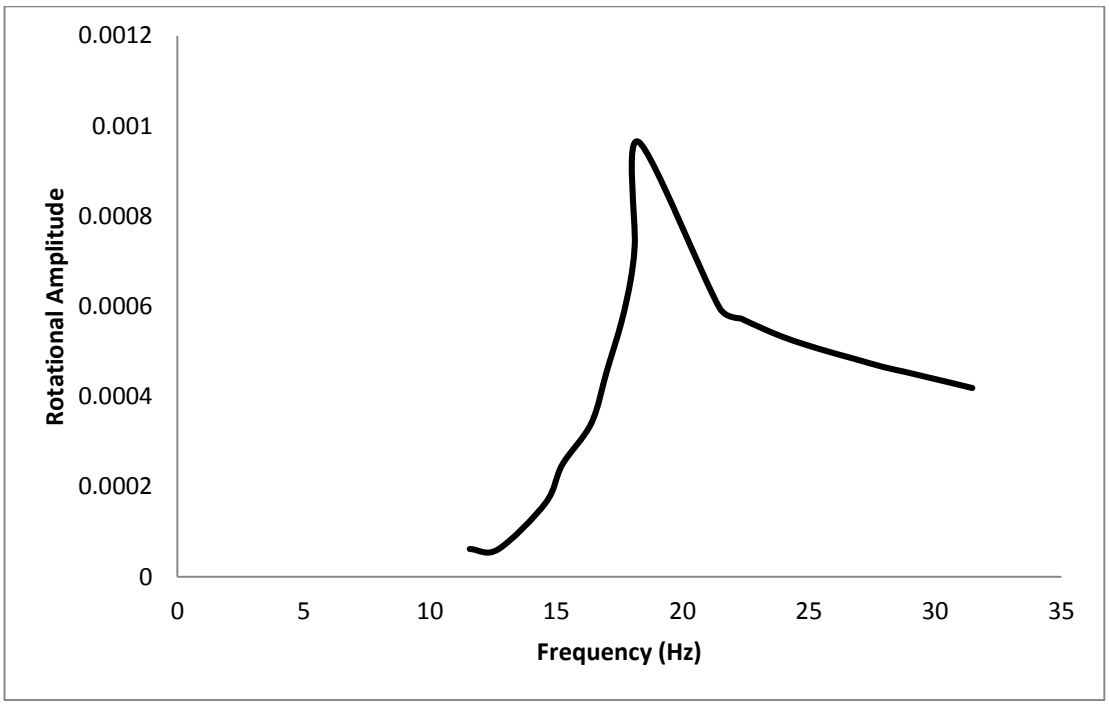

Figure-38: Rotational Amplitude v/s Frequency curve for pile diameter 50cm at e= 60°

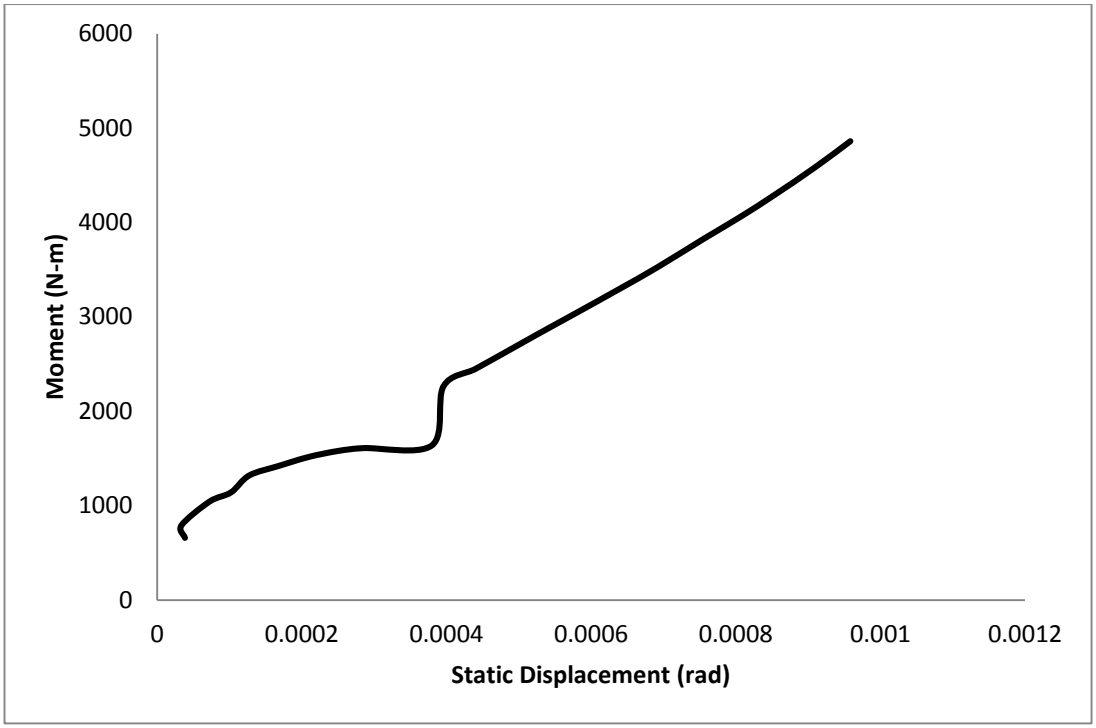

Figure-39: Moment v/s Static Displacement curve for pile diameter 50cm at e= 60°